Ammonia Removal from Mining Wastewater by Ion-Exchange Regenerated by Chlorine Solutions

By: Tianguang Zhang

A thesis submitted to the University of Ottawa
in partial fulfillment of the requirements for the
Master of Applied Science in Environmental Engineering*,
under the joint supervision of
Dr. Roberto M Narbaitz and Dr. Majid Sartaj

*The Masters in Applied Sciences in Environmental Engineering is a Joint Program with Carleton University, administrated by the Ottawa-Carleton Institute for Environmental Engineering

Department of Civil Engineering

University of Ottawa

Ottawa, Ontario, Canada

Abstract

The mining industry is a significant contributor to the Canadian economy. However, the mining activities can be detrimental to the environment due to the release of pollutants. Ammonia is one of the noxious and toxic contaminants associated with mining, ammonia contamination is created by the oxidizing agent in explosives. The explosives impacted mining wastewater (EIMWW) usually contains ammonia and other metal ions. The ammonia in EIMWW could harm the aquatic environment by the depletion of oxygen and its lethal toxicity to aquatic organisms. Before release to environment, EIMWW needs to be treated with an easy-to-operate method for ammonia removal at the remote mining sites. Ion-exchange (IE) with zeolite is an effective method for ammonia removal that is easy-to-operate, is not significantly impacted by cold temperature or toxicity effects. However, the traditional IE regeneration approach of using high concentration NaCl solutions creates a secondary polluting stream. Chlorine regeneration of ammonia-loaded zeolite appears to be a promising option, an evaluation of this option is the main topic of this thesis.

This thesis includes three initiatives. The first is a set of multi-cycle batch loading-regeneration tests to assess the viability of ammonia removal with a commercial zeolite (SIR-600) for the treatment of a synthetic EIMWW (containing total ammonia nitrogen (TAN), K, and Ca) and to examine the performance of different ion-exchange regeneration solutions. The long-term TAN uptake of SIR-600 regenerated using a NaOCl (100 mg free Cl_2/L) solution was 0.24 meq/g, which was approximately 20% lower than that after a NaCl regeneration. However, chlorine regeneration is promising because the selectivity of SIR-600 for TAN over Ca and K increased after the chlorine regeneration. To simulate recycling of the NaOCl regenerants, K and Ca were added to the NaOCl solution, it did not substantially affect the subsequent SIR-600's ion uptake. This initiative represents a significant contribution since the earlier studies into chlorine regeneration did not investigate the impact of competing ions.

The second initiative addressed concerns regarding the long-term integrity of SIR-600 arising from its exposure to high chlorine concentrations during the regeneration. The five-week long chlorine batch exposure tests with solutions of up to 1000 mg free Cl_2/L showed that chlorine exposure did not significantly affect the SIR-600's characteristics in terms of particle size distribution, surface area, FTIR spectra and ion uptake. Thus, SIR-600 has the potential for long-term use in field applications.

The final initiative evaluated the feasibility of chlorine regeneration for continuous flow IE column systems used for ammonia removal from a synthetic EIMWW. Continuous flow column systems are important because these are the standard IE units used in full-scale applications. Multi-cycle column loading-regeneration tests were performed to compare the zeolite performance using a NaOCl (1000 ppm as free Cl_2) solution with that using a 5% NaCl regeneration. The influence of loading duration was also assessed. The use of 6-hr loading cycles were shown to be preferable to 23-hr loading cycles because it had lower effluent concentrations and they could achieve higher overall TAN mass removals per unit

time. After three operational cycles, the SIR-600 had similar TAN uptake performances (0.21 meq/g Vs. 0.21 meq/g) after NaOCl regeneration and after salt (NaCl) regeneration. This is in contrast to the lower TAN uptakes for the NaOCl regeneration in the batch tests, this indicates that batch tests are not always representative of full-scale applications. Compared to NaCl regenerated SIR-600, SIR-600 after NaOCl regeneration had a higher preference for TAN over Ca and K, which makes this type of regeneration very promising. Its only apparent limitation is that the NaOCl regeneration required a longer duration. During the NaOCl regeneration, the main mechanism appears to be the oxidation of ammonia to nitrogen gas and hydrogen ions, however the Na in the NaOCl solution also seems to have a role in the regeneration.

Acknowledgement

For this thesis, I need to thank some people who gave me tremendous helps and supports.

First, I want to express sincere gratitude to my supervisors: Dr. Roberto M Narbaitz and Dr. Majid Sartaj who professionally offered me valuable suggestions and instructions during the research. Moreover, they made research fundings from Natural Sciences Engineering Research Council of Canada's Engage program, Ontario Centre of Innovation's VIP program and our partners Milestone Environmental Inc. and Dowclear Inc. available to support this work.

Second, I want to thank Jason Downey who is from Milestone Environmental Inc. and Dowclear Inc. Jason helped initiate this research and he provided many important information which boosted my research activities.

Third, I want to thank all uOttawa staffs who always provided me the brilliant technical support.

Finally, I want to thank my family: Yueshuang Qiu, Donghui Zhang, and Yuting Liu. They are always there to support me mentally and financially.

Table of Contents

List of Figures

List of Tables

List of abbreviation

AAS: Atomic Absorption Spectrometer

ACS: American Chemical Society

BET: Brunauer-Emmett-Teller

BV: Bed volume

CLL: Chlorine long loading

CSL: Chlorine short loading

DO: Dissolved oxygen

EIMWW: Explosive impacted mining wastewater

EZ: Exchange zone

FTIR: Fourier-transform infrared spectroscopy

IE: Ion-exchange

Rpm: Revolution per minute

SAC: Strong-acid cation

SBA: Strong-base anion

SEM: Scanning Electron Microscopy

SLL: Salt long loading

SSL: Salt short loading

STP: Standard temperature and pressure

TAN: Total ammonia nitrogen

VSS: Volatile suspended solids

WAC: Weak-acid cation

WBA: Weak-base anion

List of nomenclature

K_A^B: Selectivity coefficient for ion A and ion B

α_B^A: Separation factor for ion A and ion B

℃: Celsius Degree

$C_{breakthrough}$: Breakthrough concentration

C_{eff}: Effluent concentration

C_{feed}: Feeding water concentration

C_i: Initial liquid-phase concentration of ion

C_{inf}: Influent concentration

C_k: liquid-phase concentration of ion k

M: Mass of ion-exchange material

pKa: Acid disassociation constant

Q_{eq}: Solid-phase concentration of ion at the equilibrium state

Q_i: Initial solid concentration of ion

q_i: solid-phase concentration of ion i

q_T: Sum of solid-phase ion concentrations of all the ions

Q_{uptake}: Ion uptake by each gram of IE material

R^2: R-squared value

V: Volume

Chapter 1 Introduction

1.1 Mining Industry Impacted Environment

Canada is regarded as one of the most important mining countries in the world (Government of Canada, 2021). Canada is the world's leading producer of potash, as well as cadmium, cobalt, diamonds, gemstones, gold, graphite, indium, nickel, niobium, platinum group metals, salt, titanium concentrate, aluminum, and uranium (Government of Canada, 2021). In 2019, the total value of Canada's mineral production was $48.2 billion (Government of Canada, 2021).

However, the mining industry can negatively impact the environment by discharging toxic substances including heavy metals, arsenic, and ammonia (Forsyth et al., 1995; Razo et al., 2004). Ammonia contamination can be produced by explosives that have extensively been used in mining activities as the oxidizing agent in commercial explosives is generally NH_4NO_3 (Forsyth et al., 1995). Thus, generated explosives impacted mining wastewater (EIMWW) is an environmental concern. The released ammonia will negatively affect the aquatic environment, primarily due to the following facts: the nitrification of ammonia may deplete dissolved oxygen in the water; the toxicity of unionized ammonia can threaten aquatic organisms; and may lead to eutrophication; (Halling-Sørensen and Jørgensen, 1993; Khan and Mohammad, 2014; Souza-Bastos et al., 2017; Conley et al., 2009).

Biological nitrification and denitrification is the most commonly applied method for ammonia removal (Metcalf and Eddy, 2014). Air stripping, ion-exchange, and breakpoint

chlorination are other alternative methods for ammonia removal (United States Environmental Protection Agency, 2000; Stone, 1978; Jorgensen et al., 1976). Considering the fact that most Canadian mining sites are located in remote areas and experience very cold winters, often complicated large-scale wastewater treatment units can not be installed and supported. Thus, an easy-to-operate and cost-effective treatment method that is not impacted by cold temperatures is required for ammonia removal from EIMWWs. Multiple loading/regeneration cycles with SIR-600 (a commercial zeolite) with 5% NaCl regeneration have proven that ion-exchange is an efficient process for the removal of ammonia from an EIMWW (Chartrand, 2018). Considering the high salt concentration and the significant amount of NH_4-N in the regeneration effluent, more sustainable alternative regeneration approaches are desired. Chlorine regeneration for ammonia-loaded zeolite seems to be a suitable alternative (Huang et al., 2015) and is the focus of this thesis.

1.2 Objectives

As the most conventional ion-exchange regeneration method is to use salt regeneration solution, the major objective of this study was to assess the performance of SIR-600 (a commercially available zeolite) ion-exchange system in conjunction with chlorine regeneration for the treatment of a synthetic EIMWW containing calcium, potassium, and ammonia. The specific objectives are as follows. First, to evaluate effectiveness of salt and chlorine regenerants on Ca, K, and TAN loaded SIR-600 using multiple batch loading/regeneration cycles. Batch tests were used because they are good screening technique in that they can be completed more rapidly than continuous flow column

systems that are normally utilized in full-scale applications. Second, to evaluate the impact of long-term chlorine exposure on the characteristics of SIR-600. Third, to perform continuous flow column tests to evaluate the feasibility of chlorine regeneration in SIR-600 column applications.

1.3 Thesis layout

This thesis consists of six chapters. The first chapter is referred to as the introduction chapter, it introduces the environmental issues and proposes a method to address these, then it outlines the research objectives. The following chapter is a literature review that discusses the current ammonia removal methods, probes into the ammonia removal by ion exchange material, and then it discusses different ion exchange regeneration options. This second chapter concludes with a discussion of a research gap of the proposed research. The third chapter introduces the material, general procedures, and analytical methods used in the experiments conducted to address the objectives.

Chapter four is in the format of an academic paper. The title of this paper is "Batch Application of Ion-exchange and Chlorine Regeneration Process for Ammonia Removal in Mining Wastewater". In this paper, the performances of chlorine and salt regenerated SIR-600 were compared in multiple batch loading-regeneration cycles. The durability of the ion-exchange material in chlorine exposure was also evaluated (i.e., the second objective) in this chapter. The results generated in Chapter four provided confidence basis for the continuous flow column experiments in Chapter five. Chapter five is also in the format of an academic paper, it is titled "Assessing the Feasibility and Performance of

Chlorine Regeneration of Bench-scale Zeolite Column for Ammonia Removal from Explosives Impacted Mining Wastewater". This paper investigated the feasibility of the SIR-600 column applications in ammonia removal of the synthetic EIMWW with salt and chlorine regeneration. The last chapter summarizes the conclusions of the research and points out the possible direction for future work.

References:

Chartrand, Z. (2018). *The Selective Ion-Exchange Removal of Ammonia from Mining Wastewater*. [MASc dissertation]. Department of Civil Engineering, University of Ottawa, Ottawa, Canada.

Conley, D. J., Paerl, H. W., Howarth, R. W., Boesch, D. F., Seitzinger, S. P., Havens, K. E., Lancelot, C., and Likens, G. E. (2009). "Controlling eutrophication: nitrogen and phosphorus." *Science*, 323, 1014–1015.

Forsyth, B., Cameron A., and Miller, S. (1995). "Explosives and water quality." In T.P. Hynes, and M.C. Blanchette (Ed.), *Proceedings of Sudbury '95: Mining and the Environment, Volume II* (pp. 795-803). CANMET, Ottawa, Canada.

Government of Canada. (2021). "Minerals and the economy." Retrieved on June 3, 2021, from https://www.nrcan.gc.ca/our-natural-resources/minerals-mining/minerals-metals-facts/minerals-and-the-economy/20529.

Halling-Sørensen, B., and Jørgensen, S. E. (1993). The *Removal of Nitrogen Compounds from Wastewater*. Elsevier, Amsterdam, Netherlands.

Huang, H., Yang, L., Xue, Q., Liu, J., Hou, L., and Ding, L. (2015). "Removal of ammonium from swine wastewater by zeolite combined with chlorination for regeneration." *Journal of Environmental Management*, 160, 333–341.

Jorgensen, S. E., Libor, O., Lea Graber, K., and Barkacs, K. (1976). "Ammonia removal by use of clinoptilolite." *Water Research*, 10, 213–224.

Khan, M., and Mohammad, F. (2014). “Eutrophication: Challenges and solutions.” Chapter 1 in A. A. Ansari and S. S. Gill (Ed.), *Eutrophication: Causes, Consequences and Control. Volume 2* (pp. 1-15). Springer, Dordrecht, Netherlands.

Metcalf and Eddy. (2014). *Wastewater Engineering: Treatment and Resource Recovery (5th ed.).* McGraw-Hill Education, New York, NY.

Razo, I., Carrizales, L., Castro, J., Díaz-Barriga, F., and Monroy, M. (2004). “Arsenic and heavy metal pollution of soil, water and sediments in a semi-arid climate mining area in Mexico.” *Water, Air, and Soil Pollution*, 152, 129–152.

Souza-Bastos, L. R., Val, A. L., and Wood, C. M. (2017). “Are Amazonian fish more sensitive to ammonia? Toxicity of ammonia to eleven native species.” *Hydrobiologia*, 789, 143– 155.

Stone, R. W. (1978). “Full-Scale demonstration of nitrogen removal by breakpoint chlorination.” Environmental Protection Agency, Office of Research and Development, Municipal Environmental Research Laboratory, Ohio. Access by the National Technical Information Service. https://nepis.epa.gov/Exe/ZyPURL.cgi?Dockey=9101XG1X.txt.

United States Environmental Protection Agency. (2000). *Wastewater Technology Fact Sheet Ammonia Stripping, USEPA 832-F-00-019.* Washington, D.C.

Chapter 2 Literature Review

This literature review describes ammonia and its impact in the environment, wastewater treatment methods for its removal, and then focuses on ion-exchange process. The latter includes a discussion of ion-exchange fundamentals, the process operation characteristics, the various ion-exchange materials, the selectivity of zeolite ion exchangers in multicomponent wastewaters, its application for ammonia removal, and the regeneration methods available for reusing the saturated ion-exchanger after the ammonia removal.

2.1 Ammonia

Ammonia, which is made of nitrogen and hydrogen, can be synthesized in industry or generated in nature (Appl, 1999). It is reported that the pK_a of ammonia is equal to 9.25 at 25 ℃ (Emerson et al., 1975). Unionized ammonia (NH_3) and ammonium (NH_4^+) are two different natural forms of ammonia. The allocation between the two forms is related to the temperature and pH of the aqueous environment (Emerson et al., 1975). The equations describing two forms are:

$$\mathrm{N}H_4^+ \leftrightarrow NH_3 + H^+ \qquad \text{(eq. 2.1)}$$

$$pK_a = 9.25 \text{ at } 25°C$$

$$K_a = \frac{[NH_3] \cdot [H^+]}{[\mathrm{N}H_4^+]} = 10^{-9.25} = 5.6 \times 10^{-10} \qquad \text{(eq. 2.2)}$$

Because of the difficulty to analytically quantify NH_3 and NH_4^+ separately, total ammonia nitrogen (TAN) is normally used to express the sum of the two forms of ammonia. Figure

2-1 shows the changing ratio of NH_3 and NH_4^+ with respect to the pH at 25°C and STP. Below pH 7, NH_4^+ is the dominant species, and the NH_4^+ concentration decreases as pH increases. The proportions of the two components are equal when the pH equals 9.25.

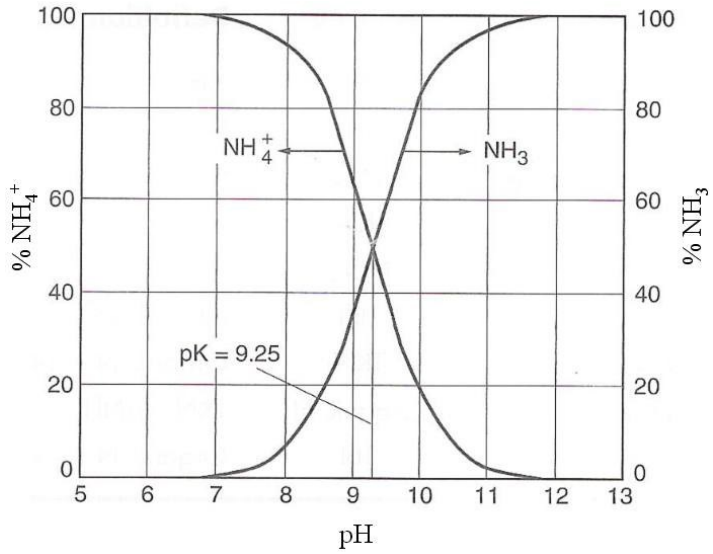

Figure 2-1 Ammonia and ammonium proportions with respect to pH (Source: Kunz and Mukhtar, 2016)

Nitrogen is regarded as a key nutrient for plant growth. Thus, chemical fertilizers that contain nitrogen are significant for agriculture, and in many of them, the nitrogen is in the form of ammonia (Appl, 1999). Consequently, the fertilizer industry releases approximately 12,000 tonnes ammonia/year which is the largest industrial ammonia release in Canada (Environment Canada and Health Canada, 2001). The effluent generated from municipal wastewater treatment plants also contributes considerably to the ammonia pollution in aquatic ecosystems. Canadian municipal wastewater treatment

facilities release approximately 62,000 tonnes ammonia per year (Environment Canada and Health Canada, 2001). Mines, food processing, and agriculture are other sources of ammonia release into aquatic ecosystems (Environment Canada and Health Canada, 2001).

2.1.1 Ammonia in the Aquatic Environment

The discharged ammonia will exert several negative impacts on the aquatic ecosystem (Halling-Sørensen and Jørgensen, 1993). First, the oxidation of ammonia to nitrate by nitrifying bacteria consumes significant amount of dissolved oxygen (DO), and a depletion of DO is detrimental or even fatal to many aquatic organisms (Halling-Sørensen and Jørgensen, 1993; Suter et al., 2021). This bacteria-mediated ammonia oxidation is known as nitrification which consumes 4.6 mg of DO to convert each mg of ammonium nitrogen into nitrate (Halling-Sørensen and Jørgensen, 1993). Nitrifying bacteria are ubiquitous, so the problem is widespread. The second principal detrimental impact of ammonia discharges is that NH_3 (the unionized form of ammonia) is very toxic to aquatic organisms (Randall and Tsui, 2002; Canadian Council of Ministers of the Environment, 2010; Souza-Bastos et al., 2017; Kleinhenz et al., 2018). Many studies on the influence of ammonia on fish have been reported (Environment Canada and Health Canada, 2001). Their results are reported in terms of the acute lethality values (LC_{50}), i.e., the un-ionized ammonia concentration causing 50% death rate for a specific species in a period of time (Environment Canada and Health Canada, 2001). Green sunfish is the most tolerant fish species, they have the highest mean LC_{50} value (i.e., 1.86 mg NH_3/L); white perch is the least NH_3 tolerant species, its mean LC_{50} is 0.28 mg NH_3/L after 48-96 hour (U.S.

Environmental Protection Agency (USEPA), 1985; Environment Canada and Health Canada, 2001).

Furthermore, as an important nutrient, excessive nitrogen can cause eutrophication in aquatic systems which may boost algal and cyanobacterial growth (Khan and Mohammad, 2014; Conley et al., 2009). The algal bloom can hinder the light penetration thereby reducing the photosynthesis by underwater aquatic plants and the related oxygen production at lower layers of water (Salameh and Harahsheh, 2011; Ansari et al., 2011; Chartrand, 2018). This whole process may lead to a high-density aquatic biomass and eventually a hypoxic aquatic environment (Salameh and Harahsheh, 2011; Ansari et al., 2011; Conley et al. 2009). In addition, agricultural and municipal effluents rich in nitrate can contaminate groundwater. The intake of nitrate-contaminated water can lead to the mortality of infants as it interferes the transport of oxygen by blood, the specific illness is called methemoglobinemia (Fan et al., 1987; Fewtrell, 2004). Therefore, ammonia is a significant pollutant in the aquatic system, and it needs to be removed from treated wastewaters before its release into the environment.

Mining wastewaters are a significant source of ammonia pollution. Large quantities of ammonia can be generated in mining activities since the commercial explosives usually use NH_4NO_3 as the oxidizing agent (Forsyth et al., 1995). The TAN concentration of explosive impacted mining wastewater (EIMWW) has been widely investigated. The TAN concentration in mining and mineral wastewater ranges from 0.3 to 80 mg as N/L (Pommen, 1983). Due to the toxicity of unionized ammonia, different jurisdictions have

set different wastewater discharge limits. The Canadian Council of Ministers of Environment (CCME) recommended that the unionized ammonia concentration of freshwater bodies should be lower than 0.019 mg/L (Canadian Council of Ministers of the Environment, 2010). The acute lethality is also a parameter to limit the ammonia level in the water. The acute lethal concentration of ammonia refers to a level of ammonia in an effluent at 100 percent concentration that causes the death of 50% of the rainbow trout in a period of 96-hour when tested complying to the acute lethality test stated in Reference Method EPS 1/RM/13 (Environment Canada, 2004; Environmental Technology Center of Canada and Environmental Canada, 2000). In the pH range from 7 to 9.5, the upper limit of wastewater effluent's TAN level ranges from 1 to 188 mg TAN as N /L ensuring that the effluent doesn't contain acute lethal level of ammonia (Environment Canada, 2004). The Canadian Metal and Diamond Mining Effluent Regulations (SOR/2002-222) requires that under the Fisheries Act mining wastewater effluents should not be acute lethal, so it indirectly limits the ammonia level in them (Minister of Fisheries and Oceans of Canada, 2012a). The Canadian Municipal Wastewater Systems Effluent Regulations (SOR/2012-139) under the Canadian Fisheries Act set 1.25 mg N-NH_3/L as the upper limit for wastewater effluents at 15 ± 1 ^oC (Minister of Fisheries and Oceans Canada, 2012b). Furthermore, in terms of provincial regulations, the Ministry of Environment and Energy of Ontario (MOEE) sets 0.02 mg NH_3/L as the upper limit of unionized ammonia concentration in water bodies receiving effluents (MOEE, 1994). Thus, the degree of instream dilution will impact the maximum allowable ammonia effluent discharge concentrations.

2.2 Treatment of Ammonia

Ammonia can be removed from wastewaters by several different types of processes including biological and physicochemical methods. Some of these will be discussed below, ion-exchange, the focus of this thesis, will be discussed in more details in Section 2.3.

2.2.1 Biological Treatment

Biological treatment is the most commonly used treatment method for municipal wastewaters, although not all biological wastewater treatment processes incorporate ammonia removal, many do. A well designed and operated biological treatment system can achieve more than 90% ammonia removal rate (McCarty, 2018). Well-designed activated sludge systems need to: a) have sufficient retention times to accommodate for the slower growth rate of nitrifying bacteria (Davis, 2020); b) provide higher oxygen levels to satisfy the need of nitrifying bacteria (Gerardi, 2002); and c) provide enough carbonate alkalinity to compensate for H^+ produced by the nitrification reaction (Gerardi, 2002).

Some conditions may limit the application range of biological methods. First, bacterial toxicity caused by heavy metals, organic compound, and high ammonia concentrations (Loveless and Painter, 1968; Stensel et al., 1976, Luther, 2015). Second, because of the relatively slow growth rates of nitrifying bacteria they require long start-up times, and their performance is susceptible to flowrate fluctuations or fluctuations of ammonia concentrations (Kruner and Rosenthal, 1983; Jeavons et al., 1998 as cited by Judd and Judd, 2011; Judd and Judd, 2011; Liu, 2012). Third, biological nitrification rates are greatly impacted by temperature since low temperatures, water temperatures (below 10 ^oC) may

cause difficulties in suspended growth nitrification systems (Jorgensen and Weatherley, 2003; Wang et al., 2006; Widiastuti et al., 2011, Chartrand, 2018). Due to local weather conditions many treatment systems at Canadian mining projects operate at low temperatures and makes biological nitrification more difficult. However, moving bed biological reactors (MBBRs), which are attached growth systems, have been found to nitrify municipal wastewaters at low temperature (1^{o}C) (Young et al., 2017). For the biological treatment of EIWWW at low temperature (~5 ^{o}C), fixed-bed biofilm reactors were also studied in the lab scale (Zaitsev et al., 2008). The complexity of the flow rate and the content of mining wastewater could significantly impact the efficiency of biological systems and thus may not be the most appropriate option for onsite operation. Considering the small size of many mines, physicochemical treatment methods may be preferred due to the great reliability and their lower operator dependence.

2.2.2 Air Stripping

The United States Environmental Protection Agency (USEPA) sponsored ammonia stripping in the 1970's and this process was presented as an alternative ammonia removal technology in Metcalf and Eddy (2014), the standard wastewater treatment design textbook. However, there does not seem to be many full-scale applications. Air stripping is a physicochemical water treatment method for dissolved volatile substances removal which is accomplished by transferring the substances from water to the contacted air (Crittenden et al., 2012a). Henry's Law Constant, i.e., the gas-liquid equilibrium constant, is used to quantify the target substance's volatility which is crucial for a successful air stripping process (Crittenden et al., 2012a; Chartrand, 2018). In an aquatic environment,

ammonia is more volatile at higher pH values (Dasgupta and Dong, 1986; Kinidi et al., 2018). Packed tower is the major type of air stripping system (Crittenden et al., 2012a). Research has shown that air stripping of ammonia has an ideal performance when pH ranges from 10.8 to 11.5 (United States Environmental Protection Agency, 2000). It is claimed that 90% of ammonia removal rate could be achieved by this method, but the performance could be affected by low temperature since Henry's law constant is significantly influenced by temperature (O'Farrell et al., 1972; O'Farrell et al., 1973; Crittenden et al., 2012a; Chartrand, 2018). The ammonia removal decreased from 90-95% to 75% when the air temperature decreased from 20 ℃ to 10 ℃ (United States Environmental Protection Agency, 2000). In addition, packed tower air stripping is not feasible in the low temperatures encountered in Northern Canada due to the icing issues and lower efficiency, and heating is not cost-effective (Crittenden et al., 2012a; Chartrand, 2018).

2.2.3 Chlorination

As an efficient oxidant, chlorine is widely utilized for drinking water disinfection. Chlorine can be incorporated into water in a variety of ways, including as a chlorine gas, a liquid (NaOCl solution, i.e., bleach), or as a solid ($Ca(OCl)_2$ powder). In water, the free chlorine exists as hypochloric acid (HOCl) and hypochlorous ion (OCl^-), and free chlorine is the sum of the HOCl and OCl^- concentrations (Crittenden et al., 2012c). Owing to its strong oxidizing power, the free chlorine reacts with ammonia to generate monochloramine (NH_2Cl) and dichloramine ($NHCl_2$) by the following reactions (Metcalf and Eddy, 2014):

$$NH_3 + HOCl \rightarrow NH_2Cl + H_2O \quad \text{(eq. 2.3)}$$

$$NH_2Cl + HOCl \rightarrow NHCl_2 + H_2O \quad \text{(eq. 2.4)}$$

Monochloramine and dichloramine are generated if the chlorine to ammonia nitrogen ratio is up to 1:1 based on mole or 5:1 based on mass ratio (Davis, 2020).

If there is additional chlorine introduced, trichloramine (NCl_3) is generated by the reaction below (Metcalf and Eddy, 2014):

$$NHCl_2 + HOCl \rightarrow NCl_3 + H_2O \quad \text{(eq. 2.5)}$$

The chloramine can be oxidized into nitrogen gas with further chlorine additions, the overall reaction is as follows (Metcalf and Eddy, 2014):

$$2NH_4^+ + 3\text{HOCl} \rightarrow N_2 + 3H_2O + 3HCl + 2H^+ \quad \text{(eq. 2.6)}$$

NH_2Cl, $NHCl_2$, and NCl_3 are also known as combined chlorine (Metcalf and Eddy, 2014). The process of the chlorination is demonstrated by Fig. 2-2. The reactions and the products are largely determined by the chlorine to nitrogen ratio as illustrated in this figure. Before the point when the chlorine (Cl_2) to nitrogen mass ratio reaches 5:1, the ammonia nitrogen is oxidized into chloramine. The majority of the chloramine will be oxidized when weight ratio of chlorine to ammonia nitrogen approaches to 7.6 : 1 (a small portion of combined chlorine residual is still left behind in reality as shown in Fig.2-2); the depletion of chloramine could be explained by eq. 2.6 (Metcalf and Eddy, 2014). The

point when chlorine to nitrogen ratio reaches 7.6:1 is called the chlorination breakpoint, additional chlorine will lead to increasing free chlorine (Metcalf and Eddy, 2014).

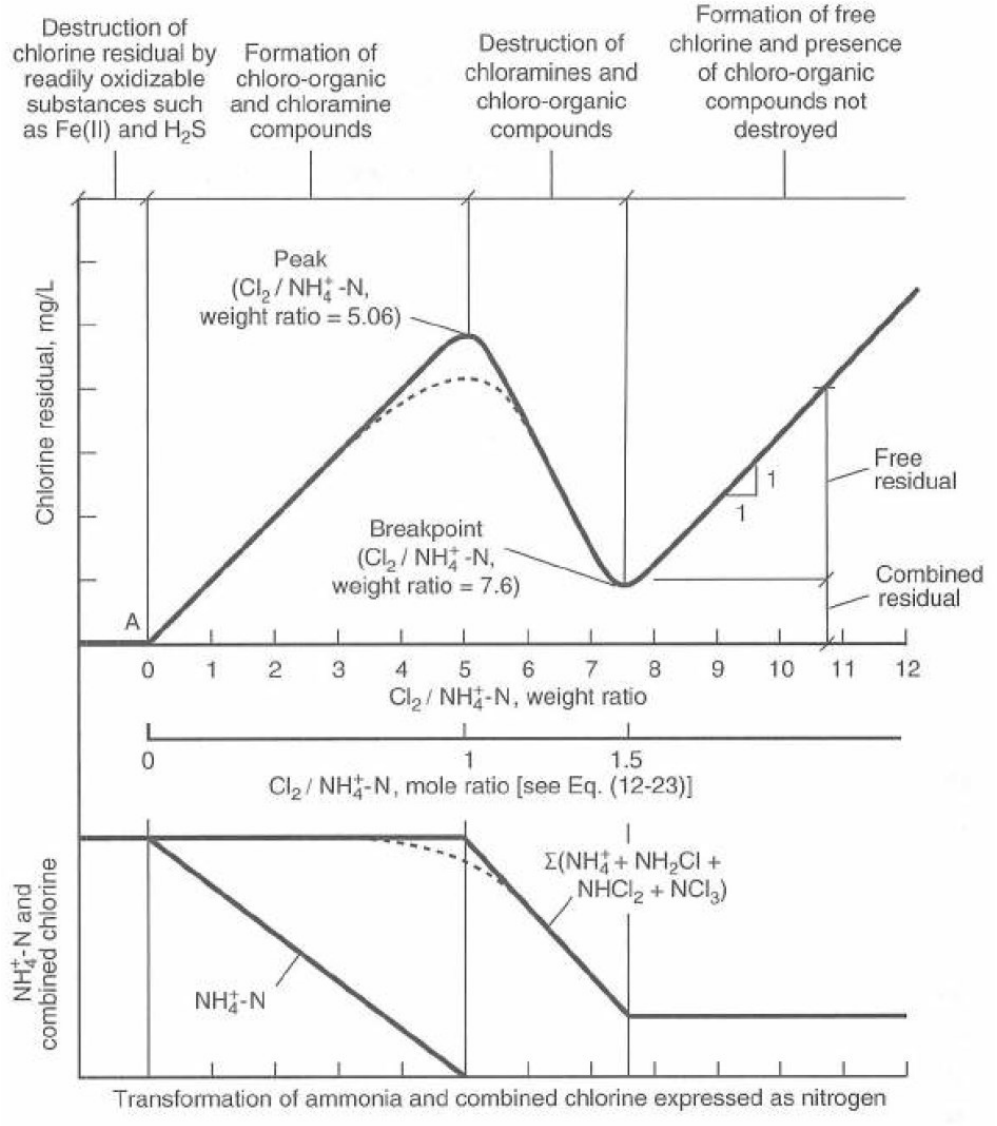

Figure 2-2 Breakpoint chlorination curves (Source: Metcalf and Eddy, 2014).

Breakpoint chlorination followed by the treatment of excess free chlorine (i.e., a molar ratio of $Cl_2/NH_3 > 1.5$) is a method of treating ammonia in wastewater that has been applied in practice (Stone, 1978). Due to the toxicity of free chlorine to fish, it is important to reduce the total residual chlorine levels before discharge to below 0.02 mg/L which is the required level within the Canadian Municipal Wastewater Effluent (Minister of Fisheries and Oceans Canada, 2012b).

Breakpoint chlorination had been reported to be applied in full-scale municipal and industrial wastewater treatment (Stone, 1978). However, this method is currently not considered as the best process if the water to be treated contains stronger reducing agents, such as ferrous iron, that cause a high chlorine demand. This method is only appropriate when the concentration of stronger reducing agents' level is low (Woodard, 2001; Metcalf and Eddy, 2014; Moran, 2018).

According to Metcalf and Eddy (2014), disinfecting activated sludge effluents requires chlorine doses ranging from 5.5 to 7.5 mg Cl_2/L to meet the effluent coliform standard of 1000 MPN/100 ml. Thus, at such plants the ammonia is converted to chloramines (Metcalf and Eddy, 2014). To meet the chlorine effluent regulations, most plants add a dechlorination agent, such as sodium sulfite, in this type of application to reduce the chlorine to chloride (Davis, 2020). However, few applications with this method for mining wastewater were reported.

2.2.4 Other physicochemical treatment methods.

Several other physicochemical treatment methods have been studied and applied for the removal of ammonia from wastewater, such as ion-exchange (Svetich, 1993), microwave radiation (Dong and Sartaj, 2016), and chemical precipitation (Khai and Trang, 2012). As ion-exchange is the focus of this thesis, the following section focuses on ion exchange process, its characteristics, effectiveness, and limitations.

2.3 Ion-Exchange

Ion-exchange (IE) is a process where the liquid-phase charged ions transfer and bind to an insoluble and immobile solid and replace other like-charged ions (Helfferich, 1995; Davis, 2020). This technology is not regarded as a conventional process in municipal water treatment due to the limited number of full-scale applications (Crittenden et al., 2012b). However, full-scale ion-exchange are still applied in water treatment in some industries including boiler water treatment, pharmaceutical and semiconductor manufacturing. (Crittenden et al., 2012b). In addition, millions of rural North American homes use IE-based water softening units.

IE materials consist of a framework of fixed coions with positive or negative charge and that are used to neutralize and remove target ions with the opposite charge (counterions) from the water being treated (SenGupta, 2017; Chartrand, 2018). The target counterions diffuse to the ion exchange material and form bonds removing them from solution. Prior to use, the IE materials are usually preloaded with presaturant counter ions (Crittenden et al., 2012b). When the ion-exchange material contacts a water containing target ion,

the IE material will exchange the preloaded ions (i.e., attached to the fixed ions) for the like-charged ions within the water, and the target contaminant ions are moved from the liquid phase to the solid phase whereas the preloaded counter ions are transferred from the solid phase to the liquid phase (Chartrand, 2018). The ion exchange process can be described by eq. 2.7 (Harland, 1994):

$$z_B R_{zA} A^{z_A} + z_A B^{z_B} \leftrightarrow z_A R_{zB} B^{z_B} + z_B A^{z_A} \qquad \text{(eq. 2.7)}$$

In the formula above, *R* represents the fixed coion of the IE material, z is the ionic charge, *A* is the preloaded ion attached to the fixed coion, and *B* is the contaminant counterion exchanged from solution. So, for example, for a sodium strong acid cation type resin, *R* may be $-SO_3^-$; A^{Z_A} is Na^+; and B^{Z_B} could be any exchangeable cation (e.g., NH_4^+). This process is referred to as a loading phase. Eventually, all of the available pre-loaded counter ions are removed, so the target ions in the solution can no longer be exchanged onto the IE material, and the ion exchange material is considered to be exhausted. Due to the reversibility of the ion exchange process, the target ions on the exhausted IE material can then be desorbed and the IE material can be reused (SenGupta, 2017). This process is called regeneration (SenGupta, 2017). In the regeneration phase, the ion-exchange is usually exposed to high concentration salt, acid, or base solutions so that their ions become the attached counterions and the contaminant that was attached to the IE material now desorbs (Crittenden et al., 2012b). Thus, a loading step and a regeneration step basically constitute a cycle in ion-exchanger application (SenGupta, 2017). In most

cases, the feasible ion-exchangers should be capable to be used for hundreds of cycles (SenGupta, 2017).

2.3.1 Ion Exchange Materials

The two main groups of ion-exchange materials applied in water treatment are synthetic IE resins and inorganic ion exchange materials, such as zeolites (Crittenden et al., 2012b)

The synthetic resins consist of a crosslinked backbone matrix which usually consists of vinyl polymers connected using divinylbenzene (DVB) (Crittenden et al., 2012b). The synthetic ion-exchange resins matrixs are elastic and can swell and shrink according to the counter ion (Helfferich, 1995; Crittenden et al., 2012b). The cross-linking degree of the resin determines its flexibility and elasticity (Helfferich, 1995).

According to functional groups, there are four main categories of synthetic resins (Davis, 2020; Clifford et al., 2012; Crittenden et al., 2012b): Strong-acid cation (SAC), Weak-acid cation (WAC), Strong-base anion (SBA), and Weak-base anion (WBA). The acid cation exchanger has negative fixed ion as a functional group and target the uptake of positively charged counter-ions; the basic anion exchanger has positive fixed ion as a functional group and target the removal of negative charged counter-ions (Davis, 2020; Chartrand, 2018). To remove NH_4^+ which is a cation, an acid cation resin is required (Imchuen et al., 2016). The ammonia removal of synthetic IE resin will be discussed in a later section.

Natural zeolites (crystalline aluminosilicate minerals) were the first IE materials, and they were used for full-scale water softening (Clifford et al., 2012). Zeolites can be naturally

occurring or synthesized (SenGupta, 2017). Due to their high abundance and their high stability in some conditions, zeolites are preferred in some special industrial ion exchange applications including treatment of high temperature waters and those containing ionized nuclear radiation (Harland, 1994). The porous 3-dimentional structure of zeolite is due to the corner-sharing TO_4 tetrahedra (basic building unit) where T is any cation can have tetrahedral coordination (McCusker and Baerlocher, 2007). SiO_4 and AlO_4 are two types of basic building units of zeolites (MIntova and Čejka, 2007). AlO_4 provides the fixed negative charge and cation-exchange capacity to these zeolites (SenGupta, 2017). The common formula of zeolite is $M_{2/n}O{\cdot}Al_2O_3{\cdot}xSiO_2{\cdot}yH_2O$ where M denotes a cation with valence of n (commonly n = 1 or 2) (Harland 1994). Sodium, potassium, and calcium have been used as the ions to pre-saturate zeolites, they are the ions that are exchanged in the ion exchange of the target ion. Ion-exchange properties of zeolites were first studied on naturally mined zeolitic materials including chabazite and natrolite (Dyer, 2007). Compared to naturally occurring mined zeolites, synthetic zeolites have the advantage that the Si:Al ratio can be modified to control the ion exchange properties (Harland, 1994). Zeolites have been extensively studied for ammonia removal (Li et al., 2010; Montégut et al., 2016) and heavy metals removal (Jamil et al., 2010; Taamneh and Sharadqah, 2017) from wastewaters.

Compared to natural aluminosilicate materials (i.e., natural zeolites), synthetic ion-exchange resins possess the following advantages: a) higher chemical stability; b) higher physical stability; c) consistent particle size; and d) can be selected either for cation or

anion exchange (Harland, 1994). Thus, synthetic IE resins are much more widely used over natural ion exchange media in full-scale water treatment.

Synthetic IE resins are usually used for large-scale chemical waste stream treatment to remove or recover target cations (e.g., ammonia and copper) and anions (e.g., chromate) (Harland, 1994). Hydrophobic type zeolites with high Si/Al ratios are better for the removal of organic compounds from water due to their appropriate pore size (Ellis and Korth, 1993; Kawai et al., 1994; Rossner and Knappe, 2008; Summers et al., 2012).

Ding and Sartaj (2016) reported that in batch tests using single solute ammonia solutions, a strong acid synthetic IE material showed high TAN uptake capacity. They reported that Amberlite IR120 H (a strong acid cation resin) had ammonia uptake of 0.6 meq/g of total ammonia nitrogen in single-solute ammonia solution when the equilibrium liquid concentration reached 11.2 meq TAN/L (Ding and Sartaj, 2016). Chartrand (2018) also reported that two strong acid cation exchangers (Purolite SSTC60 and Amberlite IR 120 Na) both had high ammonia uptakes (i.e., 1.8 meq TAN/g in the same single-component ammonia solution at equilibrium concentration of 3.6 meq TAN/L). However, their ammonia uptake from a multi-component EIMWW solution was significantly lower. They decreased to 0.24 and 0.25 meq TAN/L at the equilibrium concentrations (~4.0 and ~3.4 meq TAN/L). Thus, the K in the EIMWW greatly decreased the TAN uptake capacity (i.e., an 86% decrease). The significant reduction of synthetic resins' TAN uptake capacity in competition was also reported by Malovanyy et al. (2013).

Hydrophilic zeolites with relatively low Si/Al ratios are regarded as cation (e.g., NH_4^+) exchangers in water treatment (Dyer, 1984; Townsend, 1984, Summers et al., 2012). This material has been applied or extensively studied for ammonia removal (SenGupta, 2017; Chartrand et al., 2020; Koon and Kaufman, 1975; Svetich, 1993). The removal of ammonia using zeolite will be discussed in a later section.

2.3.2 Process Operation

Ion-exchange processes are conducted in a batch or continuous flow column systems. The batch system is operated with IE media and the contacting water in a sealed reactor with adequate contacting time to ensure the ion-exchange occurs (Chartrand, 2018). Batch tests are widely applied in IE research because they only require simple equipment and multiple tests can be conducted simultaneously. The other main type of IE systems are continuous flow columns packed with IE material; in full-scale applications, this is the most common type of IE systems used.

In order to incorporate the dynamic nature of the IE columns into full-scale designs, designers generally perform small laboratory column tests (Wachinski, 2017; Crittenden et al., 2012b). Within downflow columns, the ion exchange process can be described by an exchange zone (EZ) which gradually moves down the column as the IE material gets saturated (Davis, 2020). The target ions concentration in the liquid within the EZ ranges from zero at downstream end of the EZ to that in the feed water at the beginning of the EZ. This ion transfer is often called a moving front which moves along column as the preloaded ions are released and are substituted by the target ions in the feeding water

(Chartrand, 2018). Figure 2-3 (a) shows a downflow IE column and the EZ moving down during four different phases (∀). The zone ahead of the EZ, shown in white, contains IE without the target ions. As the column slowly gets saturated ($\forall_2$), the EZ starts to move down in the same direction as the liquid flow. The zone upstream of the EZ is called the saturated zone and it is denoted by closely spaced horizontal lines. At time, $\forall_1$ the saturated zone is very small, with time and it expands and at time $\forall_4$ it comprises almost all of the entire column (Treybal, 1981; Davis, 2020).

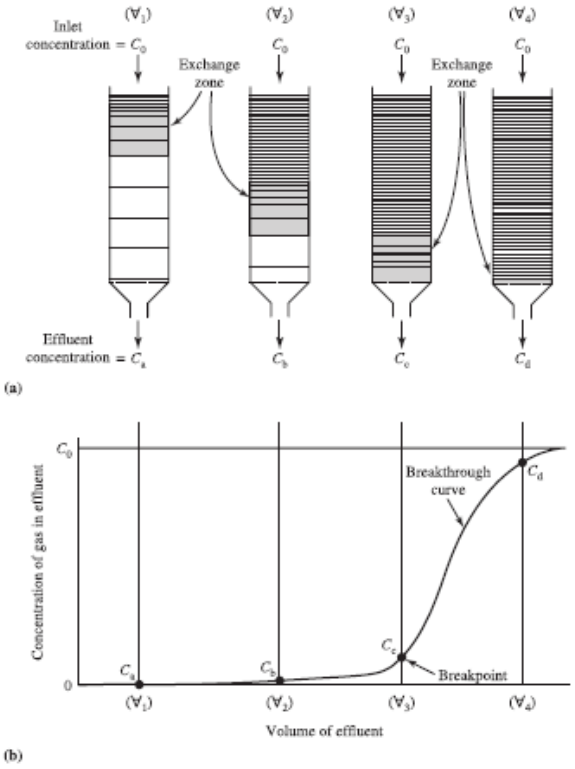

Figure 2-3 Ion exchange process in column (a) and breakthrough (b). (Source: Treybal, 1968 as cited by Davis, 2020)

Figure 2-3 (b) shows the target ion concentration in the IE column's effluent, the curve in the figure is the breakthrough curve. In the early stages of operation, before the EZ reaches the bottom of the column (i.e., $\forall_1$ and $\forall_2$), the column's effluent contains no target ion. Once EZ reaches the bottom of the column, the target ion starts appearing in the column's effluent, this is the start of the breakthrough. With time the EZ moves down the column and the effluent target ion concentration increases with time. Eventually the end of the EZ reaches the bottom of the column and effluent concentration of the target compound approaches that of the influent (i.e., $\forall_4$). At this point, the IE material is nearly fully saturated (Wachinski, 2017; Treybal, 1981; Davis, 2020).

IE column systems generally incorporate at least two columns, one treating feed water at a time. The effluent regulations or design criteria will define the breakthrough concentration, i.e., the effluent concentration until which the column will normally be operated prior to regeneration (Harland 1994; Davis, 2020; Chartrand, 2018). If one continued to operate the lead column, the effluent concentration will increase until it eventually approaches the concentration in the feed water (Wachinski, 2017). It should be noted that the kinetics of ion exchange are relatively rapid and the breakthrough concentration in IE columns is generally reached in less than a day. In some cases, it is as low as few hours.

2.3.3 Selectivity, Selectivity Coefficients and Separation Factors

The selectivity is one of the most important properties of an IE material, it is defined as the affinity or preference for one type of ion over another type of ion (Crittenden et al.,

2012b). Resin selectivity is determined by the physical and chemical properties of the exchanging ion and those of the ion-exchanger media (Crittenden et al., 2012b). The key chemical properties include the valence and the number of atoms of the ion; the key physical characteristics of the IE material include the pore size and the functional group(s) (Crittenden et al., 2012b).

In column tests, the length of the time before the breakthrough of the target ion depends primarily on the selectivity and the target ions concentration in the feed relative to the concentration of the competing ions. If the ion-exchange media has higher selectivity on one type of ion, the longer is the length of the run. In a batch-mode binary exchanging process, the selectivity can be quantified using a separation factor α_B^A or a selectivity coefficient K_A^B (Clifford et al., 2012).

Considering the ion exchange equation (eq. 2.7) for a bi-solute system involving ions A and B, the equilibrium constant or selectivity coefficient, K_A^B, is (Davis, 2020; Harland, 1994):

$$K_A^B = \frac{[A]^{Z_B}[RB]^{Z_A}}{[RA]^{Z_B}[B]^{Z_A}} \qquad \text{(eq. 2.8)}$$

In the equation above, [A] and [B] represent the concentration of ion A and ion B in the liquid; [RA] and [RB] stand for the solid phase concentrations (or activities) of two types of ions, respectively; and Z_A and Z_B denote the valence of two different ions respectively (Davis, 2020; Harland, 1994).

Separation factor (α_B^A), which takes the valence of the ions into consideration, is another way to express an ion exchange material's preference on a type of ion over another type (Crittenden et al., 2012b). For a bi-solute system containing ion A and B, the separation factor is calculated as (Crittenden et al., 2012b):

$$\alpha_B^A = \frac{Y_A X_B}{X_A Y_B} \qquad \text{(eq. 2.9)}$$

where X_A is the fraction of ion "A" (in equivalents) in the total equivalents of like-charged ions in the liquid phase, and Y_A represents the fraction of ion "A" (in equivalents) in the total equivalents of like-charged ions in the solid phase; A represents the ion to be removed from the solution; *B* is the ion preloaded on IE material (i.e., that introduced by the pre-saturated solution or regeneration solution). Similarly, X_B represents the equilibrium equivalent fraction of B in the liquid phase, while Y_B represents the equilibrium equivalent fraction of ion *B* on the IE material (Crittenden et al. 2012b). At the same liquid phase concentrations of the target ion (A and B), the IE material prefers to exchange ion *A* over ion *B* if the value of separation factor α_B^A is larger than 1, and this preference is positively related to the value of separation factor α_B^A (Crittenden et al. 2012b).

In the practical applications, the wastewaters which need to be treated usually contain numerous various ions, but the available sites on the resin are limited. As a result, the competition between different ions exists in such a multi-component environment. At the

equilibrium state, the solid-phase concentration of a specific ion could be calculated by the following equation (Crittenden et al., 2012b):

$$q_i = \frac{q_T C_i}{\sum_{k=1}^{N} \alpha_i^k C_k} \qquad \text{(eq. 2.10)}$$

Where q_i represents the solid-phase concentration of ion i, eq/g of IE material; q_T is the sum of solid-phase ion concentrations of all the ions, eq/g of IE material; C_i is the liquid-phase concentration of ion i, eq/L; C_k is the liquid-phase concentration of ion k, eq/L; and α_i^k represents separation factor for ion i over ion k (Crittenden et al., 2012b).

It should be noted that separation factors are reported in the literature, however these factors not only vary somewhat with the various IE materials properties but also vary with the ion concentrations (Crittenden et al., 2012b; Davis, 2020). Accordingly, rather than predicting the values of q_i using equation 2.10 the more common approach is to conduct multicomponent experiments to determine q_T, summation of all of the q_i values, all the C_k values and using them regress the values of α_i^k (Crittenden et al., 2012b).

2.3.4 Ammonia Removal by Zeolite

Metcalf and Eddy (2014) describes several zeolite-based ammonia removal treatment systems. Although this book does not explicitly cite actual applications, it implies that there are some full-scale applications. It is also reported in other sources that a large-scale ammonia removal system using clinoptilolite was operated in California in the 1980s (Svetich, 1993).

In contrast, there has been a great deal of research on the removal of ammonia using zeolites. Most of this research involved single-component batch systems, i.e., ammonium as the only contaminant ion existing in the wastewater. Table 2-1 presents the ammonia uptake reported by a number of selected studies, the first seven entries pertain to single component experiments. It needs to be mentioned that the presented studies did not utilize the same experimental conditions including the ammonium/ammonia level in the test solution, pH or temperature of the solution. In addition, the IE materials of these studies came from various places and presumably had somewhat different characteristics. From the data in Table 2-1, it can be observed that the NH_3/NH_4^+ equilibrium uptakes of selected clinoptilolite vary from 0.19 to 1.3 meq/g with various aquatic NH_3/NH_4^+ concentration at the equilibrium states for single-component solutions. In this scenario, the presaturant ions on the virgin IE material can be only replaced by NH_4^+ ions in the wastewater without competition for sites from other counterions (Jorgensen et al., 1976; Leyva-Ramos et al., 2004; Weatherley and Miladinovic, 2004; Chartrand, 2018).

Table 2-1 TAN capacities of selected clinoptilolite in batch tests.

Clinoptiloite origins	NH_3/NH_4^+ uptake	Aquatic ammonia equilibrium Level	Water type	Competitive ion in the feeding water	Reference
Hungary	0.36 meq NH_4^+/g	1.54 meq NH_3/L	single-component	/	(Jorgensen et al., 1976)
Mexico	~1.3 meq NH_3/g*	~42 meq NH_3/L*	single-component	/	(Leyva-Ramos et al., 2004)
New Zealand	0.42 meq NH_4^+/g	0.8 meq NH_4^+/L*	single-component	/	(Weatherley and Miladinovic, 2004)
Turkey	~0.57 meq NH_4^+/g	~1.29 meq NH_4^+/L*	single-component	/	(Tosun, 2012)
U.S.	1.0 meq TAN/g	3.5 meq TAN/L	single-component	/	(Chartrand, 2018)
U.S.	0.57* meq TAN/g	4 meq TAN/L	single-component	/	(Chartrand, 2018)
Unknown	0.19* meq NH_4^+/g	0.06 meq NH_4^+/L	single-component	/	(Vocciante et al., 2018)
U.S.	0.42 meqTAN/g	~3.5 meq TAN/L	multi-component	K, Ca, Fe, Al, Mg, Si, B, Sr, Na	(Chartrand, 2018)
New Zealand	0.38 meq NH_4^+/g	1.2 meq NH_4^+/L*	multi-component	Ca	(Weatherley and Miladinovic, 2004)
New Zealand	0.40 meqNH_4^+/g	1.0 meq NH_4^+/L*	multi-component	K	(Weatherley and Miladinovic, 2004)
Unknown	0.16* meq NH_4^+/g	0.19 meq NH_4^+/L	multi-component	K	(Vocciante et al., 2018)
Unknown	0.035 meq NH_4^+/L*	0.25 meq NH_4^+/L	multi-component	Na, Ca, Mg, K, Sr, Fe,Ni	(Vocciante et al., 2018)

* was not directly found in the literatures, so they were calculated or estimated according to the given results

However, in practical applications of IE material, it's inevitable to deal with wastewater with multi-components. In such a system, NH_4^+ is no longer the only counter ion in the wastewater. Many studies reported ammonia removal process from multi-component solutions using IE, including natural zeolites (Montégut et al., 2016; Vocciante et al., 2018; Chartrand, 2018). Ames (1960) studied ammonium as one of the exchangeable cations existing in solution (Hedström, 2001; Sarioglu, 2005). By comparing the effect of the competitive ions on the Cs^+ uptake capacity of clinoptilolite, which is the most used natural zeolite, these studies observed the following cation preference sequence:

$$Cs^+ > Rb^+ > K^+ > NH_4^+ > Ba^{2+} > Na^+ > Ca^{2+} > Fe^{2+} > Al^{3+} > Mg^{2+} > Li^+ \qquad \text{(eq. 2.11)}$$

Several subsequent studies have also basically agreed the position of NH_4^+ in the preference sequence shown in eq. 2.11 (Jama and Yücel, 1989; Rahmani et al., 2004; Leyva-Ramos et al., 2004; Guo et al., 2008). Thus, it should be noted that potassium is slightly preferred by this IE material over ammonium in accordance to the cation preference sequence (Chartrand, 2018).

Some researchers have studied the ammonia removal performance of zeolites in wastewaters containing multiple competitive ions (Weatherley and Miladinovic, 2004; Vocciante et al., 2018). Furthermore, some of these multi-competitive ion studies (Chartrand, 2020; Vocciante et al., 2018) used real wastewater and some of them (Weatherley and Miladinovic, 2004; Vocciante et al., 2018) used synthetic solutions. As observed in Table 2-1, the NH_3/NH_4^+ equilibrium uptakes of selected different zeolites in multi-component solution varies from 0.04 to 0.42 meq/g at different equilibrium liquid

phase NH_3/NH_4^+ concentrations (0.19 to 3.5 meq/L). Weatherly and Miladinovic (2004) found that the presence of Ca decreased the TAN uptake from 0.42 meq/g to 0.38 meq/g, while the presence of K decreased the TAN uptake to 0.40 meq/g. The greater competitive impact of Ca was surprising given the cation preference observed by Ames (1960). Based on the results of Vocciante et al. (2018) it appears that the presence of K decreased the TAN uptake from 0.19 meq/g to 0.16 meq/g, while the presence of K plus other ions decreased significantly more.

Chartrand (2018) conducted batch equilibrium tests with a natural zeolite (clinoptilolite) and a commercial zeolite (Resintech SIR-600) using a single component TAN solution and a multi-component EIMWW containing Ca, K, TAN, and other competitive cations. He had several interesting findings. First, as expected he found that IE materials had lower TAN capacities for the multi-component solution and that potassium was the main competing ion (Chartrand, 2018). The TAN uptake of clinoptilolite in EIMWW in the batch tests were 68% lower than that in single component (TAN) solution due to the competitive cations (Chartrand, 2018). In treating the EIMWW using an IE dose of 12 g/L, the $\alpha_{K^+}^{TAN}$ for the natural clinoptilolite was 0.8 which was much lower than that of Resintech SIR-600 (2.95). However, this result implies SIR-600 had higher preference of TAN over K comparing to the natural clinoptilolite and is a promising IE material for further ammonia removal research (Chartrand, 2018). Second, although some of the synthetic IE resin (e.g., Purolite SSTC60 and Amberlite IR 120 Na) had higher TAN uptake for the single component TAN solution, the clinoptilolite and the SIR-600 had higher uptakes for the multicomponent EIMWW (Chartrand, 2018).

There are a number of points related to the selectivity in continuous flow IE column operations that need to be discussed. First, for column operations, one cannot calculate the selectivity factor (α), so one must rely on the ratio of the TAN uptake (i.e., loading) to the K uptake instead. Second, TAN and K uptakes in batch tests will likely be different from those achieved in columns because of the differences in the experiments. For example, in a batch test the liquid phase concentration of the ions decreases with time reducing the ion exchange driving force, while in a column the feed solution continuously replenishes the ions. This is particularly significant because the feed maintains the concentration of the highest selectivity ion and may impact the uptakes of the lower selectivity ions. Third, the TAN and K uptakes achieved are a function of the column's operating conditions, such as the breakthrough concentration.

Some of these points were illustrated by Chartrand et al. (2020) who performed batch and column tests using a EIMWW (~3.85 meq TAN/L, 2.85 meq K/L and 4 meq Ca/L) and a synthetic (single-solute) TAN solution. Their column test with EIMWW used 0.55 meq/L as TAN breakthrough concentration ($C_{breakthrough}/C_{feed}$ = 0.14), which was reached after treating approximately 50 bed volumes (BV) of water. The lower effluent K concentration than that for TAN indicated that the column was more effective at removing K and presumably IE material had a preference for K. Surprisingly, the TAN capacity for the EIMWW was nearly identical to that for the synthetic TAN solution over the first 50 BV and K effluent concentration remained at a low level (~0.1 meq K/L). Given the IE media (Resintech SIR-600) has a higher preference for K this suggests the TAN uptake front within the column was proceeding without competition from the K during the first 50 BVs.

These K preference results were consistent with the batch test results. At the time of the breakthrough, the TAN to K uptake ratio was 0.24 meq/g to 0.21 meq/g or 1.14, so this ratio shows a slight preference for TAN for this breakthrough level. In comparison, the batch tests using the same regeneration solution yielded a q_{TAN}/q_K ratio of 0.885. Thus, for the breakthrough concentration in question the column was able to achieve a higher TAN preference than predicted by the batch tests. This also indicates that for such competitive ion exchange applications batch test may not provide a good indicator of the selectivity that will be achieved in column runs.

To recover the zeolite's TAN capacity for the next cycle, the regeneration process needs to be conducted. In the next section, some potentially effective regeneration methods will be introduced.

2.3.5 Ion-Exchange Material Regeneration

The process of IE capacity restoration is referred as regeneration. The regeneration process is important for the feasibility and efficiency of IE application (Crittenden et al., 2012b; SenGupta, 2017). High concentration NaCl solutions (e.g., 3 to 14% NaCl or 30,000 to 140,000 mg NaCl/L) are the most common regenerants for IE material regeneration (Crittenden et al., 2012b). The following section will discuss NaCl regeneration, some alternative regeneration solutions, and sustainable regeneration solution management.

2.3.5.1 NaCl Regeneration

NaCl regeneration is accomplished using a highly concentrated NaCl regenerant which immerses or passes through IE material to release most of loaded ions (Crittenden et al.,

2012b; Chartrand, 2018). Although as shown in eq. 2.11, zeolites have a lower preference for Na^+ than NH_4^+ (and other cations), much higher (> 100-fold greater) concentrations of the pre-saturation ion (i.e., A^{z_A} in eq. 2.7) reverses preference order and cause the equation 2.7 to shift to the left (Crittenden et al., 2012b). The results are that more pre-saturation ions loaded on the IE material (i.e., $R_{zA}A^{z_A}$) and relocate the NH_4^+ from the IE material into the regeneration solution (Crittenden et al., 2012b). The regenerated IE material can then be applied in the subsequent loading phase. In column applications, the NaCl regeneration effect can be controlled by three factors: the regeneration concentration, the regenerant flow rate, and the regenerant mass applied divided per unit IE volume (Crittenden et al., 2012b). The effectiveness of NaCl regeneration has been proven by many studies: NaCl solution can effectively desorb NH_4-N from zeolite (Rahmani et al., 2004; Chartrand, 2018), and basic conditions improved the regeneration performance (Koon and Kaufman, 1975; Chartrand, 2018). Also, the regeneration efficiency is positively related to the salt concentration of the NaCl regenerant, however the improvement is relatively small when the NaCl concentration increased from 5% to 10% (Chartrand, 2018). Nonetheless, this regeneration method produces a solution with a high NaCl concentration solution, which also contains significant concentrations of NH_4^+-N (Koon and Kaufman, 1975; Miladinovic and Weatherley, 2008; Huang et al., 2015). Thus, the regeneration solution cannot be reused without first removing the NH_4^+-N. Accordingly, the management of the used regeneration solution is considered as another environmental issue. These environmental concerns are motivations to find alternative regeneration methods.

2.3.5.2 Acid and Alkali Regeneration

Regeneration of the used IE materials can also be achieved by using concentrated acid and alkali. HCl regenerant can be applied in the regeneration process of strong- and weak-acid cation exchangers which are usually synthetic IE resins (Clifford et al., 2012; Crittenden et al., 2012b). 0.5-3 M HCl is usually applied as a regenerant in the regeneration of spent SAC resins; the WAC resins do not need highly concentrated acid regenerant due to the high H^+ ion affinity of WAC functional groups (e.g., carboxylate) (Clifford et al., 2012; Crittenden et al., 2012b). Conversely, NaOH solution is used to accomplish SBA resins and WBA resins regeneration (Clifford et al., 2012; Crittenden et al., 2012b).

Jorgensen et al. (1976) applied 1M (4%) NaOH solution for the regeneration of NH_4^+ loaded zeolite. This regeneration effect could be explained by the facts that the excessive amount of Na^+ ions drive off the loaded cations on the IE material and the basic condition helps the conversion of NH_4^+ to its unionized form (NH_3). However, zeolite is not very chemically stable in solutions with high or low pH (Harland, 1994). This instability suggests the application of acid and alkali regenerant may not be appropriate for zeolite regeneration in practice.

2.3.5.3 Sustainable Regeneration Solution Management

Preferably, the regeneration solution can be reused after removing the desorbed ammonia. Considering the properties of ammonia, the ammonia could be removed from the used regenerant by a high pH air stripping unit which is shown in Figure 2-4 (11-71

from Metcalf and Eddy, 2014). Although this combined IE-air stripping system is presented in this design book, it is unclear if this approach is being used in full-scale applications. Complexity of operation in remote mining site locations is a drawback for such applications. Various other approaches have been researched for the regeneration of NH_4^+–loaded zeolite. These methods, including bio-regeneration, electrochemical regeneration, and chlorination regeneration, will be discussed below.

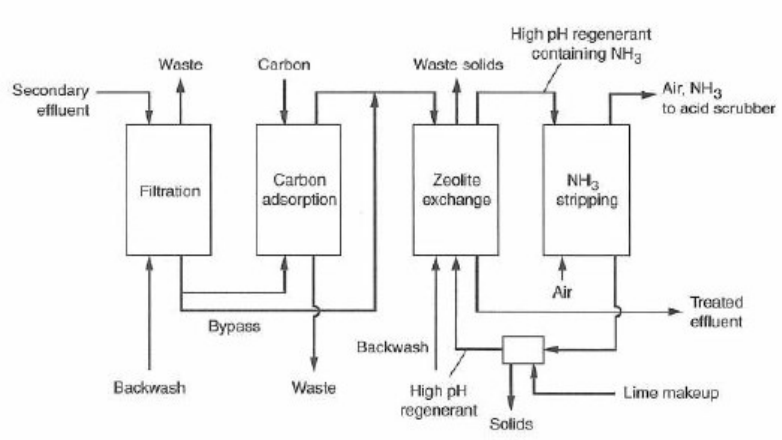

Figure 2-4 Flow diagram for the ammonium removal by zeolite combined with air stripping regeneration (Source: Metcalf and Eddy, 2014).

Previous research results indicated that ammonium saturated zeolite can be regenerated by biological methods (Lahav and Green, 1998; Wu et al., 2008). In the research of Lahav and Green (1998), the ammonium-loaded zeolite in the column was regenerated in a batch-like mode after the loading phase. This regeneration process was accomplished by nitrifying bacterial attached to the zeolite (Lahav and Green, 1998). This biological regeneration is promising since this technology consumes less energy and generates less wastewater than high salt concentration regeneration (Lahav and Green, 1998). In Lahav and Green's research (Lahav and Green, 1998), the rate of bio-regeneration can reach

0.21 g NH_4-N/L*h where a 9-liter reactor contained 2000g zeolite with 9-10g VSS /L nitrifying biomass. However, constant monitoring is required, since the biological regeneration method may be affected by several conditions including pH, carbon source level, temperature, the removal of by-products, and fouling of the IE material (Li et al., 2010). Furthermore, considering the potential metal toxicity of the mining wastewater, toxic organic compound, and the sensitivity of bacteria to ammonia, biological regeneration may not be the best choice for recovering used zeolite in the mining wastewater system (Loveless and Painter, 1968; Stensel et al., 1976, Luther, 2015).

The electrochemical method has also been studied for the regeneration of NH_4^+ loaded zeolites (Li et al., 2010). It is reported that the ammonia adsorbed by zeolite can be converted to nitrogen gas using electrified anode and cathode which can oxidize Cl^- ion into Cl_2 (Li et al., 2010). They found that electrochemical regeneration is very effective in oxidizing and removing the ammonia loaded on the zeolite avoiding secondary pollution in the used regenerant (Li et al., 2010). However, there are still some drawbacks to this regeneration method including the complexities of the equipment and high-energy consumption (4-6 g NH_4^+-N/KWh) (Huang et al., 2015; Lei et al., 2009). Consequently, the operating cost of wastewater treatment might be high (Huang et al., 2015).

Another approach to improve the sustainability of the IE system is to use an alternative regeneration solution, this approach will be discussed below.

2.3.5.3.1 Chlorine Regeneration Solution

For the purpose of removing ammonia loaded on the zeolite, hypochlorite solution was studied as an alternative regeneration solution (Zhang et al., 2017; Huang et al., 2015). Hypochlorite was used to oxidize adsorbed NH_4^+ to N_2. Consequently, the ion-exchanger which was saturated with ammonium was regenerated (Huang et al., 2015).

Huang et al. (2015) conducted bench-scale batch tests using a Chinese zeolite loaded with a synthetic swine wastewater containing 320-1120 mg/L NH_4-N. The loading experiments used large zeolite doses, many of them used 160 g/L. In the experiments, the capacity of the IE material was approximately 2 mg NH_4-N/g (0.11 meqTAN/g), which is relatively low. They claim that 99% of the NH_4^+ exchanged by zeolite can be removed by chlorination and the ammonium was oxidized into nitrogen gas. Furthermore, multiple-cycle chlorine regenerations did not significantly affect the zeolite's NH_4^+ removal efficiency (Huang et al. 2015). According to Huang et al. (2015) the reaction can be described by the following equation:

$$2NH_4^+ + 3HClO \rightarrow N_2 + 3H_2O + 5H^+ + 3Cl^- \qquad \text{(eq. 2.12)}$$

This is the breakpoint chlorination equation described in section 2.2.3, and for it to be completed the Cl_2:N molar ratio needs to at least a 1.5 (or 7.5 Cl:N mass ratio). To make sure the reaction goes to completion, Huang et al. (2015) recommended an 8:1 mass Cl:N ratio at the neutral pH level. This process can achieve effective and rapid (less than 10 minutes in their batch tests) zeolites regeneration without secondary pollution if the

residual chlorine is removed (Huang et al., 2015). It is not clear whether the same levels of regeneration efficiency could be achieved for the more common IE column operation.

Zhang et al. (2017) studied the use of a combined NaClO-NaCl-for regeneration and compared it to NaCl alone regeneration and NaClO alone regeneration. Their bench-scale batch tests used a Chinese clinoptilolite loaded with a 25 mg/L NH_4-N ammonium solution and a 40 g/L clinoptilolite dose. The NaClO-NaCl regeneration outperformed the regenerations using the NaCl or the NaOCl only solutions since the zeolite regeneration efficiency of NaOCl-NaCl regenerant was respectively ~19% and ~7% higher than that of NaCl and that of NaOCl regenerant. The optimum regeneration conditions were ClO^-/N ratio of 1.75, 20 g NaCl/L and pH=10 (Zhang et al., 2017). It should be noted that this paper uses a very large clinoptilolite dose, it does not state the loading time or present the NH_4-N loadings achieved during the loading. This study evaluates the regeneration efficiency using two parameters determined via a single-loading cycle in batch mode, it did not determine the regeneration efficiency based on the actual NH_4^+-N loading that could be achieved after multiple reloading cycles.

2.4 Research Summary and Knowledge Gap

Ion-exchange using zeolites appears to be an appropriate technology for the removal of ammonia from explosive impacted wastewaters produced at remote northern mines. This is because its operation can be automated, it does not appear to be significantly impacted by low temperature. The IE ammonia removals are significantly impacted by competing ions such as potassium in the wastewater and the type of regeneration method used.

Conventional NaCl regeneration generates a solution that can only be reused if the ammonia is first removed from it. Thus, there is a need for more research on the impact of the different regeneration methods and in particular the possibility of using chlorine solutions for the regeneration. And it must be recognized that although regeneration solutions may be recycled numerous times, because of the built-up of other ions it will have to be eventually discarded.

Many northern mines are relatively small and thus do not have sufficient infrastructure. The use of a combined NaClO-NaCl, like the one proposed by Zhang et al. (2017) is not practical because the eventual discharge of the used regeneration solution is problematic. Thus, for this type of application regeneration using chlorine only solution seems more promising. To the candidate's knowledge only Huang et al. (2015) have looked at this approach, but the study was limited and only used batch tests. Thus, there are many questions about the feasibility of this approach, some of the topics that need to be studied are as follows. First, the feasibility of Cl_2 regeneration needs to be confirmed for an EIMWW containing competing cations. This should be examined initially through batch tests to perform a preliminary optimization. Second, how well does the Cl_2 regeneration approach work when the more common IE columns are used. Given the 8:1 mass Cl:N ratio required for regeneration and the much larger IE mass in IE columns, the regeneration solution will have to have concentration of possibly 1000 mg Cl_2 /L. So thirdly, what will be the long-term impact of the high Cl_2 solutions on the integrity of the IE material and its IE uptake capacity? Fourth, theoretically the Cl_2 regeneration will remove NH_4^+ from the IE but to what extent does it remove the competing cations?

References

Ames, L. L. (1960). “The cation sieve properties of clinoptilolite.” *The American Mineralogist*, 45, 689–700.

Ansari, A. A., Gill, S. S., and Khan, F. A. (2011). “Eutrophication: Threat to Aquatic Ecosystems.” Chapter 7 in A. A. Ansari., S. S. Gill., G. R. Lanzan., and W. Rast (Ed.), *Eutrophication: Causes, Consequences and Control* (pp. 143-170). Springer, Dordrecht, Netherland.

Appl, M. (1999). *Ammonia: principles and industrial practice*. Wiley-VCH, Weinheim, Germany.

Canadian Council of Ministers of the Environment. (2010). “Canadian water quality guidelines for the protection of aquatic life: Ammonia.” In *Canadian environmental quality guidelines, 1999*. Canadian Council of Ministers of the Environment, Winnipeg, MB, Canada.

Chartrand, Z. (2018). *The Selective Ion-Exchange Removal of Ammonia from Mining Wastewater.* [MASc dissertation]. Department of Civil Engineering, University of Ottawa, Ottawa, Canada.

Chartrand, Z.G., Narbaitz, R.M., Sartaj, M., and Downey J. (2020) Ammonia-Ca-K competitive ion-exchange on zeolites in mining wastewater treatment: batch regeneration and column performance. J. of Sustainable Mining, 19, 59-71.

Clifford, D., Sorg, T. J., and Ghurye, G.L. (2012). “Ion exchange and adsorption of inorganic contaminants.” Chapter 12 in J. K. Edzwald (Ed.), *Water quality & treatment: a handbook on drinking* water (6th ed., pp. 12.1-12.97). McGraw-Hill, New York, NY.

Conley, D. J., Paerl, H. W., Howarth, R. W., Boesch, D. F., Seitzinger, S. P., Havens, K. E., Lancelot, C., and Likens, G. E. (2009). “Controlling eutrophication: nitrogen and phosphorus.” *Science*, 323, 1014–1015.

Crittenden, J. C., Trussell, R. R., Hand, D. W., Howe, K. J., and Tchobanoglous, G. (2012a). “Air Stripping and Aeration.” *Chapter 14 in MWH’s Water Treatment: Principles and Design (3*rd *ed.*, pp.1033–1115). John Wiley and Sons, Inc., Hoboken, NJ.

Crittenden, J. C., Trussell, R. R., Hand, D. W., Howe, K. J., and Tchobanoglous, G. (2012b). “Ion Exchange.” *Chapter 16 in MWH’s Water Treatment: Principles and Design, (3*rd *ed.*, pp. 1263–1334). John Wiley and Sons, Inc., Hoboken, NJ.

Crittenden, J. C., Trussell, R. R., Hand, D. W., Howe, K. J., and Tchobanoglous, G. (2012c). “Disinfection with Free and Combined Chlorine.” *Chapter 13 in MWH’s Water reatment: Principles and Design* (*3rd ed.*, pp.903–1032). John Wiley and Sons, Inc., Hoboken, NJ.

Dasgupta, P., and Dong, S. (1986). “Solubility of ammonia in liquid water and generation of trace levels of standard gaseous ammonia.” *Atmospheric Environment*, 20, 565–570.

Davis, M. L. (2020). *Water and wastewater engineering: design principles and practice*. 2nd ed. McGraw-Hill, New York, NY.

Ding, Y., and Sartaj, M. (2016). “Optimization of ammonia removal by ion-exchange resin using response surface methodology.” *International Journal of Environmental Science and Technology,* 13**,** 985–994.

Dong, S., and Sartaj, M. (2016). “Statistical analysis of thermal and nonthermal effects of sequential microwave/aeration process for the removal of ammonia from aqueous solution.” *Desalination and Water Treatment*, 57, 20005–20015.

Dyer, A. (1984). “Uses of natural zeolites”. *Chemistry and Industry,* 7, 241–245.

Dyer, A. (2007). “Ion-exchange properties of zeolites and related materials.” Chapter 16 in J. Čejka (Ed.), *Introduction to zeolite science and practice (3rd rev. ed., pp 525-553).* Elsevier, Amsterdam, Netherlands.

Ellis, J., and Korth, W. (1993). “Removal of geosmin and methylisoborneol from drinking water by adsorption on ultrastable zeolite-Y”. *Water Research,* 27, 535–539.

Emerson, K., R. Lund, R. Thurston and R. Russo. (1975). “Aqueous ammonia equilibrium calculations: effect of pH and temperature.” *Journal of the Fisheries Research Board of Canada,* 32, 2379–2383.

Environment Canada and Health Canada. (2001). *Ammonia in the aquatic environment.* Environment Canada and Health Canada, https://www.canada.ca/en/health-canada/services/environmental-workplace-health/reports-publications/environmental-contaminants/canadian-environmental-protection-act-1999-priority-substances-list-assessment-report-ammonia-aquatic-environment.html

Environment Canada. (2004). *Guideline for the Release of Ammonia Dissolved in Water Found in Wastewater Effluents. Canada Gazette, December 4th, Part I.*

Environmental Technology Center of Canada and Environmental Canada. (2000). Biological test method: Reference method for determining acute lethality of effluents to rainbow trout (2nd ed.). Environmental Canada, Ottawa.

Fan, A.M., Willhite, C.C., and Book, S.A. (1987). "Evaluation of the nitrate drinking water standard with reference to infant methemoglobinemia and potential reproductive toxicology." *Regulatory Toxicology and Pharmacology*, 7, 135–148.

Fewtrell, L. (2004). "Drinking-water nitrate, methemoglobinemia, and global burden of disease: A discussion." *Environmental Health Perspectives*, National Institute of Environmental Health Sciences, 112, 1371–1374.

Forsyth, B., Cameron A. and Miller, S. (1995). "Explosives and Water Quality". In T.P. Hynes, and M.C. Blanchette (Ed.), *Proceedings of Sudbury '95: Mining and the Environment, Volume II, Ground and Surface water (pp. 795-803)*. CANMET, Ottawa, Canada.

Gerardi, M. H. (2002). *Nitrification and denitrification in the activated sludge process*. John Wiley and Sons, Inc., New York, NY.

Guo, X., Zeng, L., Li, X., and Park, H.-S. (2008). "Ammonium and potassium removal for anaerobically digested wastewater using natural clinoptilolite followed by membrane pretreatment." *Journal of Hazardous Materials*, 151, 125–133.

Halling-Sørensen, B., and Jørgensen, S. E. (1993). The *Removal of Nitrogen Compounds from Wastewater*. Elsevier, Amsterdam, Netherlands.

Harland, C. E. (1994). *Ion Exchange: Theory and Practice*. 2nd ed. Royal Society of Chemistry, Cambridge, UK.

Hedström, A. (2001). "Ion exchange of ammonium in zeolites: a literature review." *Journal of Environmental Engineering*, 127, 673–681.

Helfferich, F. (1995). *Ion exchange.* Dover Publications, INC., New York, NY.

Huang, H., Yang, L., Xue, Q., Liu, J., Hou, L., and Ding, L. (2015). "Removal of ammonium from swine wastewater by zeolite combined with chlorination for regeneration." *Journal of Environmental Management*, 160, 333–341.

Imchuen, N., Lubphoo, Y., Chyan, J.M., Padungthon, S., and Liao, C.-H. (2016). "Using cation exchange resin for ammonium removal as part of sequential process for nitrate reduction by nanoiron." *Sustainable Environment Research*, 26, 156–160.

Jama, M. A., and Yücel, H. (1989). "Equilibrium studies of sodium-ammonium, potassium-ammonium, and calcium-ammonium exchanges on clinoptilolite zeolite." *Separation Science and Technology*, 24, 1393–1416.

Jamil, T. S., Ibrahim, H. S., Abd El-Maksoud, I. H., and El-Wakeel, S. T. (2010). "Application of zeolite prepared from Egyptian kaolin for removal of heavy metals: I. Optimum conditions." *Desalination*, 258, 34–40.

Jeavons, J., Stokes, L., Upton, J., and Bingley, M. (1998). “Successful sidestream nitrification of digested sludge liquors”. *Water Science and Technology*, 38, 111-118.

Jorgensen, S. E., Libor, O., Lea Graber, K., and Barkacs, K. (1976). “Ammonia removal by use of clinoptilolite.” *Water Research*, 10, 213–224.

Jorgensen, T. C., and Weatherley, L. R. (2003). “Ammonia removal from wastewater by ion exchange in the presence of organic contaminants.” *Water Research*, 37, 1723–1728.

Judd, S., and Judd, C. (Eds.). (2011). *The MBR Book: Principles and Applications of Membrane Bioreactors for Water and Wastewater Treatment*. Elsevier Science & Technology, Amsterdam, Netherlands.

Kawai, T., Yanagihara, T., and Tsutsumi, K. (1994). “Adsorption characteristics of chloroform on modified zeolites from gaseous phase as well as its aqueous solution.” *Colloid & Polymer Science,* 272, 1620–1626.

Khai, N. M., and Trang, H. T. (2012). “Chemical precipitation of ammonia and phosphate from Nam Son landfill leachate, Hanoi.” Iranica Journal of Energy & Environment 3 (Special Issue on Environmental Technology), 32-36.

Khan, M., and Mohammad, F. (2014). “Eutrophication: Challenges and solutions.” Chapter 1 in A. A. Ansari and S. S. Gill (Ed.), *Eutrophication: Causes, Consequences and Control. Volume 2* (pp. 1-15). Springer, Dordrecht, Netherlands.

Kinidi, L., Tan, I., Abdul Wahab, N., Tamrin, K., Hipolito, C., and Salleh, S. (2018). “Recent development in ammonia stripping process for industrial wastewater treatment.” *International Journal of Chemical Engineering*,2018, 1–14.

Koon, J. H., and Kaufman, W. J. (1975). “Ammonia removal from municipal wastewaters by ion exchange.” *Journal-Water Pollution Control Federation*, 47, 448–465.

Kruner, G., and Rosenthal, H. (1983). “Efficiency of nitrification in trickling filters using different substrates.” *Aquacultural Engineering*, 2, 49-67.

Kunz, A., and Mukhtar, S. (2016). “Hydrophobic membrane technology for ammonia extraction from wastewaters.” *Engenharia Agrícola*, 36, 377–386.

Lahav, O., and Green, M. (1998). “Ammonium removal using ion exchange and biological regeneration.” *Water Research*, 32, 2019–2028.

Lei, X., Li, M., Zhang, Z., Feng, C., Bai, W., and Sugiura, N. (2009). “Electrochemical regeneration of zeolites and the removal of ammonia.” *Journal of Hazardous Materials*, 169, 746–750.

Leyva-Ramos, R., Aguilar-Armenta, G., Gonzalez-Gutierrez, L. V., Guerrero-Coronado, R. M., and Mendoza-Barron, J. (2004). “Ammonia exchange on clinoptilolite from mineral deposits located in Mexico.” *Journal of Chemical Technology and Biotechnology*, 79, 651–657.

Li, M., Feng, C., Zhang, Z., Lei, X., Chen, N., & Sugiura, N. (2010). "Simultaneous regeneration of zeolites and removal of ammonia using an electrochemical method." *Microporous and Mesoporous Materials*, 127, 161–166.

Liu, G. (2012). *Nitrification performance of activated sludge under low dissolved oxygen conditions (Order No. 3553136).* [Doctoral dissertation, Missouri University of Science and Technology]. ProQuest Dissertations & Theses Global.

Loveless, J. E., and Painter, H. A. (1968). "The influence of metal ion concentrations and pH value on the growth of a Nitrosomonas strain isolated from activated sludge." *The Journal of General Microbiology,* 52, 1-14

Luther, A. K. (2015). *Ammonia toxicity in bacteria and its implications for treatment of and resource recovery from highly nitrogenous organic wastes* (Order No. 10019315). [Doctoral dissertation, The State University of New Jersey]. ProQuest Dissertations and Theses Global.

Malovanyy, A., Sakalova, H., Yatchyshyn, Y., Plaza, E., and Malovanyy, M. (2013). "Concentration of ammonium from municipal wastewater using ion exchange process." *Desalination, 329, 93–102.*

McCarty, P.L., (2018). **"**What is the best biological process for nitrogen removal: When and why?" *Environmental Science & Technology,* 52, 3835-3841.

McCusker, L. B., and Baerlocher, C. (2007). “Zeolite structure.” Chapter 2 in J. Čejka (Ed.), *Introduction to zeolite science and practice* (3rd rev. ed., pp. 13-38). Elsevier, Amsterdam, Netherlands.

Metcalf and Eddy. (2014). *Wastewater Engineering: Treatment and Resource Recovery (5th ed.).* McGraw-Hill Education, New York, NY.

Miladinovic, N., and Weatherley, L. R. (2008). “Intensification of ammonia removal in a combined ion-exchange and nitrification column.” *Chemical Engineering Journal*, 135, 15– 24.

Minister of Fisheries and Oceans of Canada. (2012a). *Metal and Diamond Mining Effluent Regulations (SOR/2002-222)*. https://laws-lois.justice.gc.ca/eng/Regulations/SOR-2002-222/index.html

Minister of Fisheries and Oceans of Canada. (2012b). *Wastewater Systems Effluent Regulations (SOR/2012-139)*. https://laws-lois.justice.gc.ca/eng/regulations/sor-2012-139/index.html

Ministry of Environment and Energy of Ontario (MOEE). (1994). *Water management: policies, guidelines, provincial water quality objectives.*

https://www.ontario.ca/page/water-management-policies-guidelines-provincial-water-quality-objectives

Mintova, S., and Čejka, J. (2007). "Micro/mesoporous composites." Chapter 9 in J. Čejka (Ed.), *Introduction to zeolite science and practice* (3rd rev. ed., pp. 301-326). Elsevier, Amsterdam, Netherlands.

Montégut, G., Michelin, L., Brendlé, J., Lebeau, B., and Patarin, J. (2016). "Ammonium and potassium removal from swine liquid manure using clinoptilolite, chabazite and faujasite zeolites." *Journal of Environmental Management*, 167, 147–155.

Moran, S. (2018). "Dirty water unit operation design: Chemical processes." Chapter 13 in S. Moran (Ed.), *An Applied Guide to Water and Effluent Treatment Plant Design (*pp.165-169). Elsevier, Amsterdam, Netherlands.

O'Farrell, T. P., Bishop, D. F., and Cassel, A. F. (1973). *Nitrogen removal by ammonia stripping, USEPA-670/2-73-040*. U.S. Environmental Protection Agency. Washington, D.C.

O'Farrell, T. P., Frauson, F. P., Cassel, A. F., and Bishop, D. F. (1972). "Nitrogen removal by ammonia stripping." *Journal-Water Pollution Control Federation*, 44, 1527–1535.

Pommen, L.W. (1983). *The Effect on Water Quality of Explosives Use in Surface Mining. Volume 1: Nitrogen Sources, Water Quality, and Prediction and Management of Impacts.* Ministry of Environment Technical Report 4. Ministry of Environment, Water Management Branch, Victoria: B.C..

Rahmani, A., Mahvi, A., Mesdaghinia, A., and Nasseri, S. (2004). "Investigation of ammonia removal from polluted waters by Clinoptilolite zeolite." *International Journal of Environmental Science and Technology (Tehran)*, 1*,* 125–133.

Randall, D. J., and Tsui, T. K. N. (2002). "Ammonia toxicity in fish." *Marine Pollution Bulletin*, 45, 17–23.

Rossner, A., and Knappe, D. R. U. (2008). "MTBE adsorption kinetics on alternative adsorbents and packed bed adsorber performance." *Water Research,* 42, 2287–2299.

Salameh, E., and Harahsheh, S. (2011). "Eutrophication Processes in Arid Climates." Chapter 3 in A. A. Ansari., S. S. Gill., G. R. Lanzan., and W. Rast (Ed.), Eutrophication: Causes, Consequences and Control (pp. 69-90). Springer, Dordrecht, Netherland.

Sarioglu, M. (2005). "Removal of ammonium from municipal wastewater using natural Turkish (Dogantepe) zeolite." *Separation and Purification Technology*, 41, 1–11.

SenGupta, A. (2017). *Ion exchange in environmental processes: fundamentals, applications and sustainable technology*. John Wiley and Sons, Inc., Hoboken, NJ.

Souza-Bastos, L. R., Val, A. L., and Wood, C. M. (2017). "Are Amazonian fish more sensitive to ammonia? Toxicity of ammonia to eleven native species." *Hydrobiologia*, 789, 143–155.

Stensel, H., McDowell, C., and Ritter, E. (1976). "An automated biological nitrification toxicity test." *Journal of Water Pollution Control Federation*, 48, 2343-2350.

Stone, R. W. (1978). *Full-Scale Demonstration of Nitrogen Removal by Breakpoint Chlorination*. Environmental Protection Agency, Office of Research and Development, Municipal Environmental Research Laboratory, Ohio. Access by the National Technical Information Service. https://nepis.epa.gov/Exe/ZyPURL.cgi?Dockey=9101XG1X.txt.

Summers, R. S., Knappe, D. R. U., and Snoeyink, V.L. (2012). "Adsorption of organic compounds by activated carbon." Chapter 14 in J. K. Edzwald (Ed.), *Water quality & treatment: a handbook on drinking water* (6th ed., pp. 14.1-14.105). McGraw-Hill, New York, NY.

Suter, G., II, Latimer, H., Bowersox, M., Schofield, K., and Cormier, S. (2021). *Ammonia.* Retrieved on April 13, 2021, from https://www.epa.gov/caddis-vol2/ammonia#:~:text=Ammonia%20also%20exerts%20a%20biochemical,ammonia%20into%20nitrite%20and%20nitrate.

Svetich, R. (1993, June 20-28). "Long-term use of clinoptilolite in the treatment of sewage at Tahoe-Truckee Sanitation Agency, Truckee, California." *Zeolite '93, 4th International Conference on the Occurrence, Properties and Utilization of Natural Zeolites Program and Abstracts* (pp. 197-199). Red Lion Hotel-Riverside, Boise, ID.

Taamneh, Y., and Sharadqah, S. (2017). "The removal of heavy metals from aqueous solution using natural Jordanian zeolite." *Applied Water Science*, 7, 2021–2028.

Kleinhenz, L. S., Trenfield, M. A., Mooney, T. J., Humphrey, C. L., van Dam, R. A., Nugegoda, D., and Harford, A. J. (2018). "Acute ammonia toxicity to the larvae (glochidia) of the

tropical Australian freshwater mussel Velesunio spp. Using a modified toxicity test protocol." *Environmental Toxicology and Chemistry*, 37, 2175–2187.

Tosun, I. (2012). "Ammonium removal from aqueous solutions by clinoptilolite: determination of isotherm and thermodynamic parameters and comparison of kinetics by the double exponential model and conventional kinetic models." *International Journal of Environmental Research and Public Health*, 9, 970–984.

Townsend, R. P. (1984). "Ion exchange in zeolites: Basic principles." *Chemistry and Industry,* 7, 246–251.

Treybal, R. E. (1968). *Mass Transfer Operations.2nd ed.* McGraw-Hill, New York, NY.

Treybal, R. E. (1981). *Mass Transfer Operations. 3rd ed.* McGraw-Hill, New York, NY.

U.S. Environmental Protection Agency. (1985). *Ambient water quality criteria for ·ammonia — 1984*. Office of Water Regulations and Standards Criteria and Standards Division, Washington, D.C.

United States Environmental Protection Agency. (2000). *Wastewater Technology Fact Sheet Ammonia Stripping, USEPA 832-F-00-019*. Washington, D.C.

Vocciante, M., De Folly D'Auris, A., Finocchi, A., Tagliabue, M., Bellettato, M., Ferrucci, A., Reverberi, A.P., and Ferro, S. (2018). "Adsorption of ammonium on clinoptilolite in presence of competing cations: Investigation on groundwater remediation." *Journal of Cleaner Production*, 198, 480-487

Wachinski, A. M. (2017). E*nvironmental ion exchange principles and design* (*second edition).* CRC press, Boca Raton, FL.

Wang, Y., Liu, S., Xu, Z., Han, T., Chuan, S., and Zhu, T. (2006). "Ammonia removal from leachate solution using natural Chinese clinoptilolite." *Journal of Hazardous Materials*, 136, 735–740.

Weatherley, L. R., and Miladinovic, N. D. (2004). "Comparison of the ion exchange uptake of ammonium ion onto New Zealand clinoptilolite and mordenite." *Water Research*, 38, 4305– 4312.

Widiastuti, N., Wu, H., Ang, H. M., and Zhang, D. (2011). "Removal of ammonium from greywater using natural zeolite." *Desalination*, 277, 15–23.

Woodard, F. (2001). *Industrial Waste Treatment Handbook.* Butterworth–Heinemann, Woburn, MA.

Wu, Z., An, Y., Wang, Z., Yang, S., Chen, H., Zhou, Z., and Mai, S. (2008). "Study on zeolite enhanced contact–adsorption regeneration–stabilization process for nitrogen removal." *Journal of Hazardous Materials*, 156,317–326.

Young, B., Delatolla, R., Kennedy, K., Laflamme, E., and Stintzi, A. (2017). "Low temperature MBBR nitrification: Microbiome analysis." *Water Research*, 111, 224–233.

Zaitsev, G., Mettänen, T., and Langwaldt, J. (2008). "Removal of ammonium and nitrate from cold inorganic mine water by fixed-bed biofilm reactors." *Minerals Engineering*, 21, 10–15.

Zhang, W., Zhou, Z., An, Y., Du, S., Ruan, D., Zhao, C., Ren, N., and Tian, X. (2017). "Optimization for zeolite regeneration and nitrogen removal performance of a hypochlorite-chloride regenerant." *Chemosphere*, 178, 565–572.

Chapter 3 Experimental Materials & Methods

Sustainable use of ion exchange materials requires one to assess both its removal of the target contaminant (i.e., loading phase) as well as its regeneration. This thesis consists of three experimental initiatives dealing with the ion exchange treatment of a synthetic EIMWW for ammonia removal using a commercial zeolite coupled with regeneration using chlorine solutions as a novel alternative regeneration approach.

The first initiative used batch tests to compare the performance of a commercial zeolite (SIR-600) using conventional salt solution regeneration and chlorine solution regeneration. The batch experiments consisted of multiple-cycles of loading SIR-600 with synthetic EIMWW wastewater followed by regeneration using different regenerants. The batch experiments were designed to compare the impact of different regenerants on the loaded commercial zeolite. The performance of each regenerant was evaluated by the equilibrium ion uptake of zeolite in the next cycle.

As the most common of ion exchange systems are column systems, the second initiative consisted of continuous flow column runs comparing the two modes of regeneration. The first initiative's batch test results were used to design the column tests. Column tests were conducted to evaluate the multiple-cycle performances of salt and chlorine regenerants on Ca, K and TAN loaded commercial zeolite. And each cycle of operation included a loading phase followed by a regeneration phase.

Effective chlorine regeneration of the SIR-600 within the column required very high chlorine concentration solutions. Although the column's regeneration phase may only be

two to four hours, the IE material is likely regenerated two to four times per day and it is expected to last for at least a year. The Resintech SIR-600 data sheet suggests this IE material has limited resistance to chlorine exposure. Due to concerns about the impact of these high chlorine concentrations on the long-term durability of SIR-600, the third initiative consisted of several longer-term batch tests to evaluate the impact of exposure to high chlorine concentrations on the characteristics of the ion exchange material used. Then virgin SIR-600 and chlorine-exposed SIR-600 were characterized in terms of SEM (Scanning Electron Microscopy) images, BET (Brunauer, Emmett and Teller) surface area tests, pore size distribution analysis, FTIR (Fourier-transform infrared spectroscopy) analysis, particle size distribution analysis, and ion uptake tests. This chapter provides information on the materials used, the analytical methods as well as the experimental procedures.

3.1 Materials

3.1.1 Ion-Exchange Material

The ion-exchange material evaluated in this thesis is a type of commercial zeolite (SIR-600, ResinTech Inc., Candem, NJ). This product was selected because Chartrand (2018) demonstrated that it was superior to several other ion-exchange media for the ammonia removal from an EIMWW. According to the information from the manufacturer, SIR-600 possesses a high selectivity for ammonium and cesium (ResinTech Inc., 2020). SIR-600 is presumed to be a clinoptilolite given its selectivity sequence is close to that of clinoptilolite (Ames, 1960; ResinTech Inc., 2020). Before use, the zeolite was rinsed with

deionized water and dried in the oven. After drying, the zeolite was put in a desiccator until used. Table 3-1 presents some basic information about SIR-600.

Table 3-1 Physical Properties of SIR-600 (Modified from source: ResinTech Inc., 2020)

Material Structure	Zeolite
Material Type	Crystalline
Functional Group	Aluminosilicate
Physical Form	Granules
Ionic Form (as shipped)	Na/K form
Total Capacity	>0.6 meq/ml
~Shipping Weight	60 lbs/ft^3

3.1.2 Chemicals

The synthetic EIMWW wastewater was prepared using ammonium chloride, potassium chloride and calcium chloride hexahydrate (ACS grade, Fisher Scientific, Waltham, MA). The chlorine regeneration solutions were prepared with a commercial bleach (No Name). The salt regeneration solutions were prepared with NaCl (ACS grade, Fisher Scientific, Waltham, MA).

3.1.3 Synthetic EIMWW

In this thesis, a synthetic EIMWW was used for all the loading tests. To prepare this synthetic wastewater, American Chemical Society (ACS) grade ammonium chloride, potassium chloride and calcium chloride dihydrate were dissolved and mixed well in distilled water. The prepared synthetic wastewater contained 21 ppm total ammonia nitrogen (TAN), 30 ppm K, and 80 ppm Ca as the initial concentrations of three exchangeable species. The composition of the synthetic wastewater was recommended by Jason Downey (2018) who is the research partner from Dowclear Inc. This synthetic

wastewater was chosen as a simulation of an EIMWW with lower TAN concentrations than that studied by Chartrand (2018). It should be noted that these concentrations of the synthetic wastewater are similar to the those reported as typical for underground mine water (i.e., 87 ppm Ca, 14 ppm K and 20 ppm TAN) by Schoeman (1986).

3.2 Analytical methods

3.2.1 Ammonia Analysis

The Nessler method was used for the determination of the TAN concentrations. This method was adapted from Standard Method 4500-NH_3 C (American Public Health Association, 1992). This Nessler method needs the addition of Rochelle salt stabilizer and Nessler reagent for each measurement. The Nessler reagent contains HgI_2, KI, and NaOH (American Public Health Association, 1992). The addition of Nessler reagent (Hach, Loveland, CO) changes the solution color to yellow if TAN is present in the solution. The Rochelle salt stabilizer (Potassium Sodium Tartrate solution) (RICCA, Arlington, TX) was added to prevent precipitations in the solution (American Public Health Association, 1992). The detailed procedure consisted of adding 0.125 ml of Rochelle salt stabilizer to each 10 ml sample and mixed well, after 5 minutes, 0.1 ml of the Nessler reagent was added and mixed well with. After 10-minute sitting, the concentration of TAN in the solution is proportional to the yellow colour which is quantified by the absorbance of light at a wavelength of 425 nm. The absorbance was measured using a spectrophotometer (DR6000, Hach, Loveland, CO). Before analyzing a real sample, a calibration curve was

established. In this thesis, TAN concentration range of 1-5 ppm was used to build the calibration curve. To ensure the reliability of the calibration curve, it was based on triplicate analysis of 5 different standards. As shown in Figure 3-1 the response was not linear over the entire range of concentration.

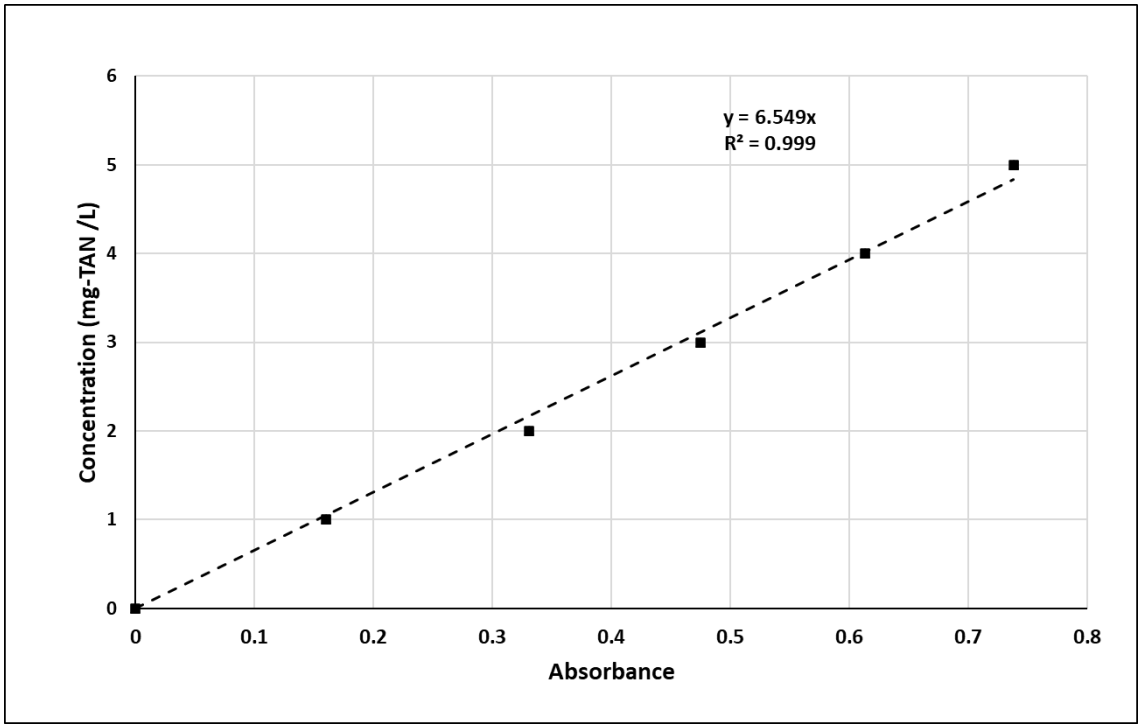

Figure 3-1 Calibration curve of Nesslerization

Before measuring real samples, a 10-ml distilled water (blank) was analyzed following the above procedure to zero the spectrophotometer. This was followed by the analysis of a standard to assure that calibration curve was valid.

3.2.2 pH

pH values were measured with VER Symphony B10P pH meter (VER Symphony B10P, VWR, Radnor, PA) with a pH probe (VWR 89231-580, VWR, Radnor, PA). Before use, the pH meter was calibrated with three pH buffer solutions (4, 7, and 10).

3.2.3 Temperature

All experiments were conducted at room temperature. The solution temperature was measured with Sartorius pHBasic meter (Sartorius, Goettingen, Germany) with a temperature sensor-integrated probe (PY-P11-2S, Sartorius, Goettingen, Germany)

3.2.4 Chlorine Measurements

Free and total chlorine levels were analyzed following Hach method 8021 and 8167 (equivalent to Standard Method 4500-Cl G for drinking water) (American Public Health Association, 2017). The DPD free/total chlorine reagent pillows (Hach, Loveland, CO) were used for measuring total/free chlorine. The measurements were conducted using spectrophotometer (DR6000, Hach, Loveland, CO) with built-in calibrations.

3.2.5 Metal Analysis

Two types of metal ions were quantified in this research: calcium (Ca) and potassium (K). The Ca and K ion concentrations were both measured using a flame atomic absorption spectrometer (AAS) (PinAAcle 500, PerkinElmer, Waltham, MA, United States) at the Department of Civil Engineering of the University of Ottawa. The instrument uses an air-acetylene flame to vaporize the sample solution, then the generated atomic vapor could absorb the light from hollow cathode lamp. The absorbance of this light is used to quantify

the concentration of the metal in the sample. The metals concentrations were quantified following a procedure adapted from Standard Method 3111B. (American Public Health Association, 2017).

0.1% La and 0.1% HNO_3 were added to standards, samples, and reagent blank. 0.1% Lanthanum solution was added to the sample, standards, and blank the avoid the possible ionization and chemical interference; 0.1% HNO_3 solution was added to insure the dissolution of the metals. The blank sample was prepared with deionized water. Before using the AA spectrometer, the burner head of this instrument was adjusted to assure optimal alignment. Then, the flame was turned on and a dilute nitric acid solution was sipped up the analyzer's capillary sampling tube for cleaning purposes. A blank sample (deionized water) was used to zero the instrument. The reagent blank was also tested to eliminate the error from the La and HNO_3 additions. A calibration curve was established by analyzing the absorbance of standard solution. Subsequently, the samples with unknown concentrations were tested. The calibration curve was checked with one standard after the curves was built. To assure that the calibration didn't drift, the standard was also checked after 10 samples were tested.

To avoid clogging of the capillary tube of the AA instrument by particles, the samples were pre-filtered through 0.45 µm filter membranes (GN-6, Pall, Port Washington, NY) when necessary. For accurate and stable measurements, the samples and standards were pre-sipped by the instrument for more than 10 seconds before the readings. To prevent cross-contaminations, the capillary tube was inserted into deionized water to run for a few seconds and wiped between samples, standards, or blanks.

Three standards (usually 2 ppm, 6 ppm, and 10 ppm) were used to build calibration curves for the calcium and potassium measurements. The option of “nonlinear through zero” was chosen for the instrument’s automatically generated calibration curves. To fit the range of the calibration curve, the samples were diluted to be in the 0-10 mg/L range.

3.2.5.1 Potassium Analysis

The potassium was measured using a potassium Lumina™ hollow cathode lamp (PerkinElmer, Waltham, MA, United States) installed in the AAS for this analysis. The operation conditions selected were wavelength = 769.90nm, slit width 0.7 nm, acetylene flow rate = 2.5L/min and air flow rate = 10 L/min.

3.2.5.2 Calcium Analysis

For the calcium analysis, a calcium Lumina™ hollow cathode lamp (PerkinElmer, Waltham, MA, United States) was installed in the AAS. The key operating conditions were wavelength = 422.67 nm, slit width = 0.7 nm, acetylene flow rate = 2.7 L/min and air flowrate = 10 L/min.

3.3 Ion-Exchange Experimental Methods

3.3.1 EIMWW Batch Loading Experiments

The loading phase is the first step of a batch loading-regeneration cycle. In each test, 0.24 g of SIR-600 was added to a 120 ml glass bottle and filled with the synthetic EIMWW. This dose was selected to match the doses used by Chartrand (2018), who also studied TAN removal using SIR-600. To prevent the loss of ammonia due to volatilization, the bottles were filled with the solution to the top without headspace. The threaded necks of the

bottles were covered with Teflon tape so that the screw-on caps provided a good seal. The sealed bottles were fastened in an end-over-end tumbler (Figure 3-2) and rotated at approximately 10 revolutions per minute (rpm) to provide effective and sufficient contact between solid and liquid. Chartrand (2018) showed that for an EIMWW-SIR-600 the required equilibration time was less than two hours. In this study, the rotation was maintained for 24 hrs for completed equilibriums. Then, the bottles were removed from the tumbler, and the particles and the liquid were separated using vacuum filtration through 0.45 µm membrane filters. The equilibrium NH_3-N, K^+ and Ca^{2+} aqueous concentrations can be found by analyzing the liquid. After being rinsed with distilled water, the loaded SIR-600 particles were kept for the following regeneration phase. The batch tests were conducted at room temperature (~ 22 ^oC). The experiments were conducted in duplicate, and the average results were reported. The steps in batch loading phase are shown in Figure 3-3.

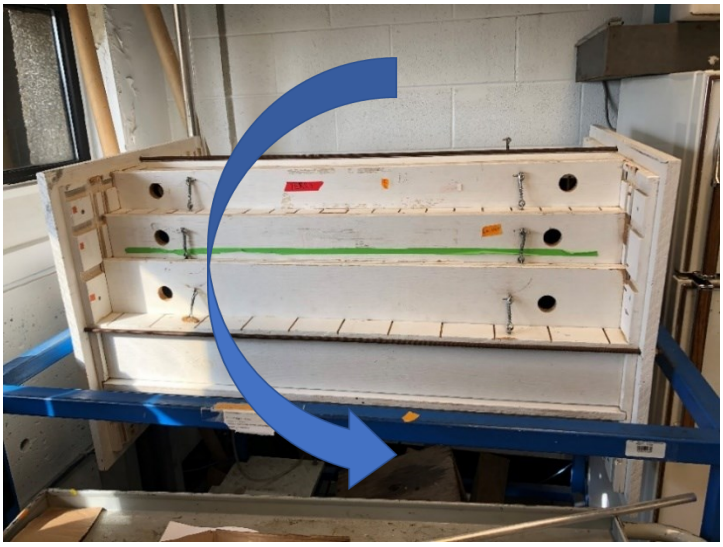

Figure 3-2 Tumbler for mixing in the loading phases and regeneration phases of batch tests.

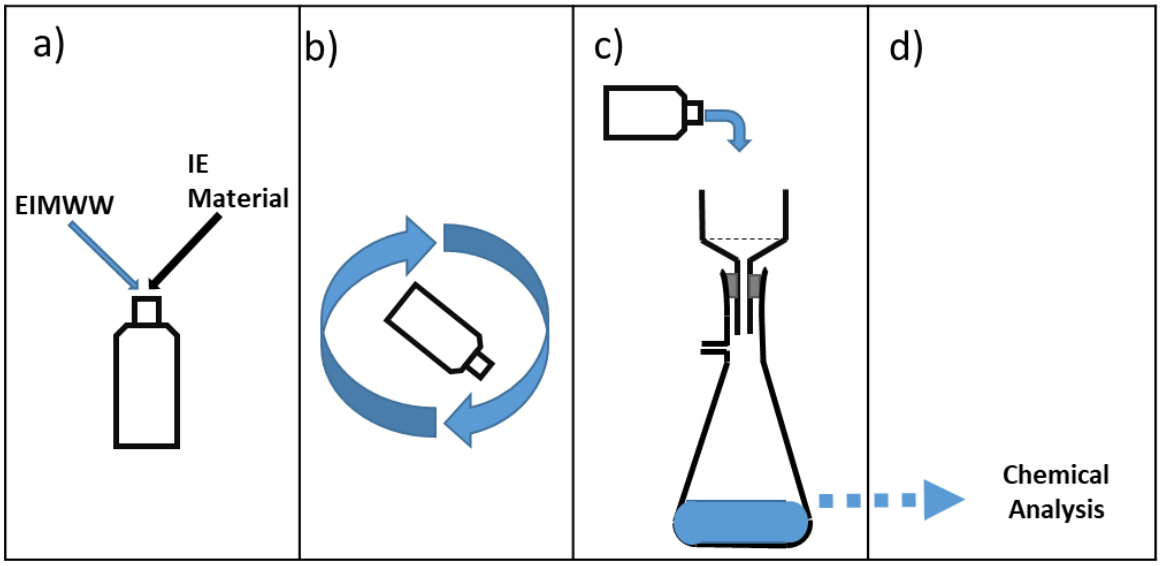

Figure 3-3 The schematic of batch loading phase. a) Prepare EIMWW and SIR-600 in bottles; b) Mixing in tumbler; c) Filtration; d) Chemical analysis. (Source: adapted from Chartrand et al., 2020)

The target ion concentration in the filtrate is considered as the equilibrium liquid phase concentration, C_{eq}. One can find the solid phase concentration at equilibrium (Q_{eq}) by using a mass balance equation with the known initial and final solid-phase and liquid-phase concentrations of this target ion.

$$M * Q_i + V * C_i \leftrightarrow M * Q_{eq} + V * C_{eq} \qquad \text{(eq. 3.1)}$$

Where, M is the mass of SIR-600 (g); Q_i is the initial solid concentration of this target ion (meq/g IE material); V is the volume of the liquid (L); C_i is the initial liquid-phase concentration (meq/L); C_{eq} is the liquid-phase concentration of this target ion at the equilibrium state (meq/L); Q_{eq} is the solid-phase concentration of this target ion at the equilibrium state (meq/g of IE material).

As frequently Q_i is not known, especially when chlorine oxidizes the ammonia into nitrogen gas, one generally uses the ion uptake by each gram of IE material (Q_{uptake}) in

each cycle, it is calculated by assuming Q_i is equal to 0. This is particularly the case for the chlorine regeneration where the ammonia is oxidized to oxygen, which was not quantified, so it was impossible to determine Q_i via a mass balance of the regeneration cycle. Q_{uptake} is also know as the variation of Q_{eq} before and after the loading phase. This Q_{uptake} can also be demoted as ΔQ_{eq}. Thus, Q_{uptake} can be found by the following equation:

$$Q_{uptake} = (C_{eq} - C_i) * \frac{V}{M} \qquad \text{(eq. 3.2)}$$

3.3.2 Batch Regeneration Tests

Different regenerants, including the hypochlorite regenerant, sodium chloride regenerant, and their combinations, were tested in the regeneration phases. A 5% NaCl solution, prepared by dissolving ACS-grade NaCl particles (Fisher Scientific, Waltham, MA) into distilled water, was used as the conventional regeneration approach. The proposed novel hypochlorite regenerant used in the batch tests consisted of a 100 ppm as Cl_2 free chlorine, it was obtained by diluting commercial bleach with distilled water. The necessary quantity of bleach was determined through preliminary tests that evaluated the free Cl_2 concentrations resulting from various bleach doses. A third regenerant evaluate was a combination of 100 ppm as Cl_2 free chlorine and 5% NaCl. The pH of the regenerants was increased to pH 10 by 4 M NaOH solution additions. The pH was increased to 10 because it benefits the regeneration. As pH increases, an increasing fraction of TAN is converted ammonium ion to unionized ammonia, thus increasing pH reduces the ion exchange uptake of TAN. During the regeneration of TAN loaded ion exchange media, increasing pH

can potentially facilitate the TAN elution by converting the aquatic ammonium ion into unionized ammonia. Koon and Kaufman (1975)'s experiment has verified this effect for pHs up to 12.5. The previous studies also indicated that pH 10 condition could optimize the chlorine regeneration performance on TAN loaded zeolite (Zhang et al., 2017). A pH 10 was used in this current study, which is also the maximum pH recommended by SIR-600's manufacturer (ResinTech Inc., 2020).

During the regeneration phase, the loaded SIR-600 was added to a clean 120 ml clear glass bottle, then filled with the regeneration solution (without leaving headspace) and sealed as above. Then the bottle was placed into the end-over-end tumbler and rotated for 48 hours to insure re-equilibration. Then the contents of the bottle were vacuum filtered through a 0.45 um filter to recover the regenerated SIR-600. After a rinse with deionized water, the regenerated SIR-600 materials were collected for the loading phase of the next cycle. The steps in batch regeneration phase are shown in Figure 3-4.

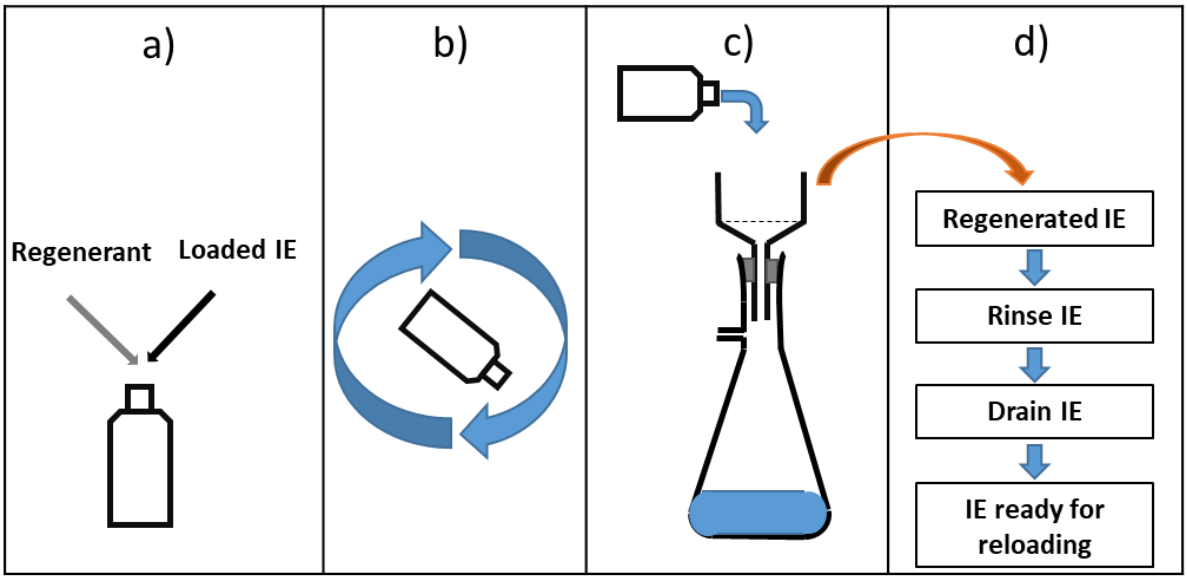

Figure 3-4 The schematic of batch regeneration phase. a) Prepare regenerant and SIR-600 in bottles; b) Mixing in tumbler; c) Filtration; d) Prepare SIR-600 for reuse (Source: adapted from Chartrand et al., 2020).

3.3.3 IE Material Durability Tests with Chlorine Exposure

Due to the possible deteriorative effect of chlorine exposure on IE material, SIR-600 durability tests were conducted by characterizing the IE material before and after the different long-term chlorine exposure levels. Two free chlorine concentration levels (100 ppm and 1000 ppm as Cl_2) were selected to conduct these tests.

Approximately 50 g SIR-600 was added to several 1L glass bottles and filled with hypochlorite solutions. The bottles were placed in the end-over-end tumbler for mixing. After 5 weeks chlorine exposure in hypochlorite solution, the IE materials were separated, rinsed, and dried. The SEM (Scanning Electron Microscopy) images, BET (Brunauer, Emmett and Teller) surface area tests, FTIR (Fourier-transform infrared spectroscopy) analysis, and particle size distribution were conducted on these materials to characterize

fresh (without chlorine exposure) and chlorine exposed SIR-600. Two replicates measurements/analysis were performed.

The BET surface area tests were performed in the Chemistry and Biomolecular Science Department of the University of Ottawa using N_2 adsorption-based surface area analyzer (ASAP 2020, Micromeritics, Norcross, GA). The samples were analyzed at 77K. The FTIR tests and SEM tests were performed with field emission SEM (JMS7500F, JEOL Ltd, Tokyo, Japan) and a FT-IR spectrometer (Nicolet 6700FT-IR, ThermoFisher Scientific, Waltham, MA), respectively. These instruments are part of the Centre for Advanced Material Research of the University of Ottawa.

The particle size distribution tests were performed by sieve tests conducted at the Geotechnical Laboratories of the Civil Engineering Department of the University of Ottawa. After 5-week chlorine exposure, approximate 50g dried SIR-600 were loaded on top of a stacked series of pre-weighed sieves (12, 16 20, 30, 40, 45, 50 US mesh). The sieves were shaken for about 10 minutes with a sieve shaker (SS-8R, Gilson company, Lewis Center, OH). Each sieve was re-weighed to obtain the mass of SIR-600 retained in it. This procedure was adapted from a standard method ASTM D6913/D6913M – 17 (2017).

To evaluate the impact of chlorine exposure on the ion exchange uptake ability of SIR-600, long-term loading-regeneration tests were also performed. The loading procedure was the same as that of batch loading, i.e., 0.24 g SIR-600 per 120 mL of EIMWW contacted for 24 hours. The regeneration test procedure was the same as that followed

by the batch tests described in Section 3.3.2 except for their duration which was one week. The regeneration cycle also acted as a week-long high chlorine concentration contact period. In total, the full cycles (i.e., 1 loading phase + 1 regeneration/chlorine exposure phase) was repeated 5 times. 100 ppm and 1000 ppm as free Cl_2 were chosen as two hypochlorite concentration levels of the regenerants/exposure solutions. These free chlorine concentrations (i.e., HOCl plus OCl^- concentrations) were quantified by the unit ppm as free Cl_2 since the concentration of HOCl and OCl can be described by the concentration of Cl_2 with the equivalent oxidizing performance. The higher concentration was chosen based our estimates of the ppm Cl_2-hour exposure that could be expected by IE media over a one-year period of column operation. Before conducting the long-term loading-regeneration tests, the zeolites were preconditioned with three batch loading-regeneration cycles using 100 ppm as free Cl_2 hypochlorite solution as the regenerant.

3.3.4 Column Tests with NaCl Regeneration

Column studies were undertaken because column is the most common type of treatment scheme for IE systems, so this is a more realistic application. In addition, the loadings achieved in IE columns are somewhat different from that in batch tests, particularly because of the competition between ions with the constant influent composition in the column setup.

The column performance of SIR-600 with NaCl regeneration was evaluated in bench-scale continuous flow column tests. These tests were conducted using a clear glass column with 2.2 cm inner diameter (ID) and a 110 cm length. 96.1 g SIR-600 were added to the column. As a result, the bed volume and bed depth of the IE material were 116 cm^3 and 30.5 cm,

respectively. The IE materials were supported by a coarse sintered glass disk integrated in the column. The flow from the column can be shut down by a stopcock at the bottom of the column. The column setup is presented in Figure 3-5.

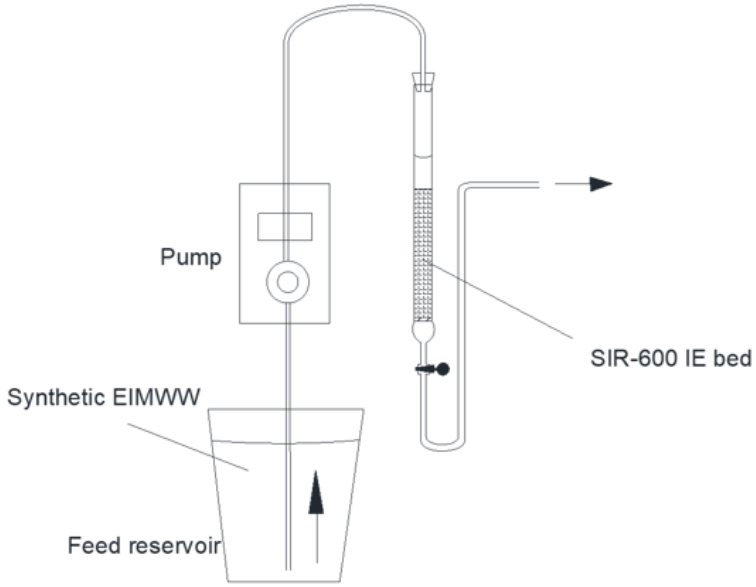

Figure 3-5 The schematic diagram of the column experimental setup.

Similar to the batch tests, one cycle of column test consisted of two phases: loading phase and regeneration phase. In the loading phase, the loading solution was identical to that used in batch tests. The flowrate of loading solution was controlled as approximately 50ml/min by a high-pressure liquid metering pump (Optos Model3, Eldex, Napa, CA). This flowrate was chosen from the range suggested by the supplier of SIR-600. The effluent flowrate was checked periodically by weighing the mass of the collected effluent in one

minute. Two main sets of tests were conducted. The first series of test was named as salt-long-loading (SLL) cycle tests consisting of a 23-hour loading phase. The second set, named as salt-short-loading (SSL) cycle, had a 6-hour loading phase. The latter are more representative of expected field operation conditions in that the effluent TAN concentration will need to be in the order of 10 mg N/L (0.71 meq/L) and the SLL runs cannot achieve this level of removal all the time. In both these cases, the same synthetic EIMWW was used as the influent and the effluent TAN, Ca and K concentrations were monitored at regular intervals.

The ion uptake performance of the SIR-600 column in the loading phase was calculated using the following mass balance equation:

$$q = \frac{\int_{V=0}^{V=loading\ phase\ end} (C_{inf} - C_{eff})dV}{M} \qquad \text{(eq. 3.3)}$$

$$q = \frac{\Sigma (C_{inf} - C_{eff})\Delta V}{M}$$

Where q is the ion uptake of the SIR-600 (meq/g), V is the volume of liquid treated (L) up to time t; C_{inf} is the influent concentration (meq/L); C_{eff} is the effluent concentration (meq/L) which changes with V (and time); and M is the mass of SIR-600 (g).

This part of the study used a 5% NaCl solution for the regeneration, because these tests with this standard regeneration solution were conducted to develop a baseline for later

comparison with column runs using chlorine solutions as the regenerant. The regenerant flowrate was set as approximately 16 ml/min which was regulated by a peristaltic pump (Masterflex L/S variable-speed economy drive, Cole-Parmer, Vernon Hills, IL). This flowrate was chosen from the range suggested by the supplier of SIR-600. A different pump was used to avoid potential corrosion problems. The effluent of regenerant was also sampled periodically. For the SPS cycle tests, there were two 23-hour loading phases + a 3-hour regeneration phase between the two loading phases, and for the SBT the 6-hour loading phase was followed by 1-hour regeneration phase. Before each series column test, the zeolite was preconditioned with 5% NaCl solution.

3.3.5 Column Test with Hypochlorite Regeneration

As discussed earlier, hypochlorite regeneration is part of the novelty of this thesis. The column performance of SIR-600 with hypochlorite regeneration was also evaluated in continuous flow column studies. The tests were accomplished with the same column and same IE material bed described in the last section. The loading phase of column tests with hypochlorite regeneration is the same as that of column tests with NaCl regeneration, i.e., they lasted 6 hours and used a flowrate of approximately 50 mL/min. The subsequent regeneration process used 1000 ppm (as free Cl_2) hypochlorite solution which was prepared with the same commercial bleach used in batch tests. Initially the regeneration flowrate was set at 50 ml per min, however this led to the formation of many bubbles within the column. They in turn constrained the flow and made the flowrate unstable. Accordingly, the average regenerant flowrate was reduced to 20 mL/min, monitored regularly, and adjusted if necessary.

Two series of tests were designed and conducted as well. The first series of test was named as chlorine-long-loading (CLL) cycle tests which includes two 23-hour loading phases plus one 3.4-hour regeneration phase between the two loading phases. The intent was to be able to compare directly with the pseudo-saturation runs conducted with 5% NaCl regeneration. The second set of tests was named as chlorine-short-loading (CSL) cycle included 3 cycles of 6-hour loading phases followed by 4-hour regeneration phases. Again, the objective was to be able to compare the performance with that of the similarly loaded column that used 5% NaCl regeneration. Before each series of column test, the zeolite was preconditioned with 5% NaCl solution to ensure the loading performances in the first loading phases of chlorine cycles was comparable to those of corresponding salt cycles. Loading effluent samples were analyzed for TAN, K, and Ca concentration. The ion uptake performance of the SIR-600 column in the loading phase was calculated using the equation (eq. 3.3).

References

American Public Health Association. (1992). *Standard methods for the examination of water and wastewater.* 18th ed. American Public Health Association, Washington, D.C.

American Public Health Association. (2017). *Standard methods for the examination of water and wastewater.* 23rd ed. American Public Health Association, Washington, D.C.

ASTM D6913 / D6913M-17. (2017) Standard Test Methods for Particle-Size Distribution (Gradation) of Soils Using Sieve Analysis, ASTM International, West Conshohocken, PA, www.astm.org

Chartrand, Z. (2018). The Selective Ion-Exchange Removal of Ammonia from Mining Wastewater. [MASc dissertation]. Department of Civil Engineering, University of Ottawa, Ottawa, Canada.

Chartrand, Z.G., Narbaitz, R.M., Sartaj, M., Downey J. (2020). "Ammonia-Ca-K competitive ion-exchange on zeolites in mining wastewater treatment: batch regeneration and column performance." *Journal of Sustainable Mining*, 19, 59-71.

Downey, J. (2018). Personal communication.

Hach. "Method 8021." Retrieved on September 17, 2021, from https://www.hach.com.

Hach. "Method 8167." Retrieved on September 17, 2021, from https://www.hach.com.

Koon, J. H., and Kaufman, W. J. (1975). "Ammonia removal from municipal wastewaters by ion exchange." *Journal-Water Pollution Control Federation*, 47, 448–465.

ResinTech Inc. (2020). “Resintech SIR-600.” Retrieved on May 15, 2021, from https://www.resintech.com/rks_images/shopcart/pdf_specs_90253.pdf

Schoeman, J.J. (1986). “Evaluation of a South African clinoptilolite for ammonia-nitrogen removal from an underground mine water.” *Water SA*, 12, 73-82.

Zhang, W., Zhou, Z., An, Y., Du, S., Ruan, D., Zhao, C., Ren, N., and Tian, X. (2017). “Optimization for zeolite regeneration and nitrogen removal performance of a hypochlorite-chloride regenerant.” *Chemosphere*, 178, 565–572.

Chapter 4 Batch Application of Ion-Exchange and Chlorine Regeneration Process for Ammonia Removal in Mining Wastewater

Abstract

Multi-cycle batch loading-regeneration tests were performed to evaluate the feasibility of ammonia removal using a commercial zeolite (SIR-600) for the treatment of a synthetic explosives impacted mining wastewater (EIMWW) and to investigate the performances of several different ion-exchange regeneration solutions. The long-term TAN (total ammonia nitrogen) uptake of SIR-600 regenerated with a NaOCl (100 mg free Cl_2/L) was 0.24 meq/g, which was approximately 80% of that achieved using a 5% NaCl regenerant which is the standard regeneration solution for this purpose. The chlorine regeneration increased the selectivity of SIR-600 for TAN compared with Ca and K. The application of NaOCl regenerant solution containing K and Ca did not significantly impact SIR-600's subsequent ion uptake. The five-week long chlorine batch exposure experiment using solutions of up to 1000 mg free Cl_2/L showed that such an exposure did not significantly impact SIR-600's particle size distribution, surface area, FTIR spectra and ion uptake.

Key words: ion-exchange, ammonia, regeneration, chlorine, competitive ion uptake, NaCl regeneration, NaOCl regeneration

4.1 Introduction

Mining wastewaters significantly contribute to aquatic ammonia pollution due to the extensive use of ammonia nitrate explosives in mining operation (Forsyth et al., 1995; Chartrand et al., 2020). It is reported that the ammonia nitrogen (NH_3-N) concentrations in some explosives-impacted-mining wastewaters (EIMWW) range from 0.3 to 80 mg as N/L (Pommen, 1983). Ammonia can be found as either ammonium ions (NH_4^+) or unionized ammonia (NH_3), the proportion of each of them is pH dependent (Emerson et al.,1975). Because of the analytical difficulties differentiating between the two species, the ammonia concentrations are expressed in terms of total ammonia nitrogen (TAN). While at near neutral pH ammonia is primarily present as ammonium ions, the principal concern is with the other TAN fraction, unionized ammonia, which is highly toxic to fish. The Canadian Council of Ministers of Environment (CCME) suggests that 0.019 mg as N/L unionized ammonia is the upper unionized ammonia concentration limit for freshwater bodies (Canadian Council of Ministers of the Environment, 2010). The threshold acute lethal concentration that causes the death of 50% of the rainbow trout in a period of 96-hour of ammonia in the wastewater effluent are 1 to 188 mg TAN as N /L depending on pH (Environment Canada, 2004). In Canada, mining site wastewater effluents are required to be below the acute lethality level according to Metal and Diamond Mining Effluent Regulations (SOR/2002-222) under the Fisheries Act (Minister of Fisheries and Oceans of Canada, 2012). This requirement objectively limits the ammonia levels in mining wastewater effluents. In addition to the NH_3 toxicity, biological nitrification in waters can consume dissolved oxygen and produce an anoxic aquatic environment, which is also

harmful to various aquatic species (Halling-Sørensen and Jørgensen, 1993; Suter et al., 2021).

Biological nitrification/denitrification, breakpoint chlorination, air stripping, and ion-exchange (IE) are some of methods available for TAN removal from wastewaters (Stone, 1978; Halling-Sørensen and Jørgensen, 1993; United States Environmental Protection Agency, 2000; Rahmani et al., 2004; Ding and Sartaj, 2015; Chartrand, 2018). Among these treatment methods, biological nitrification/denitrification is the most wildly applied ammonia removal method in full-scale municipal and industrial wastewater treatment. However, biological treatment may not be the best alternative for Canadian mining wastewaters due to biological nitrification's high sensitivity to low temperatures, heavy metals, toxic organic compound and high concentrations of ammonia (Loveless and Painter, 1968; Stensel et al., 1976; Luther et al., 2015; Jorgensen and Weatherley, 2003). Thus, biological nitrification of EIMWW requires careful operational supervision. In contrast, ion-exchange is not impacted by temperature and toxicity. In addition, it is simple in operation and requires minimal supervision, which is advantageous for most mining sites located in remote locations.

Ion-exchange processes are commonly applied in water softening (Clifford et al., 2012). Synthetic IE resin is more widely used which are more durable and have higher uptake capacities (Harland, 1994; Clifford et al., 2012). Cationic IE materials can also remove the ionized form of ammonia (NH_4^+) which accounts for virtually all of the ammonia at near neutral pH. Chartrand (2018) showed that the two zeolites tested performed better for the removal of ammonia from a multi-ion EIMWW than the three synthetic resins tested.

Zeolites, a type of inorganic IE materials, have been widely studied for TAN removal due to their excellent ion-exchanging properties, relatively low cost, and high availability in nature. However, most of the research studies investigated the removal of ammonia from synthetic solutions that did not contain other cations, while wastewaters, like EIMWW, contains other cations that may compete with TAN and decrease the removal of ammonia. Ames (1960) reported that clinoptilolite, which is the most used natural zeolite, has a higher preference for ammonia than many other cations (Hedström, 2001; Sarioglu, 2005). The general cation preference sequence of clinoptilolite is (Ames, 1960; Hedström, 2001; Sarioglu, 2005):

$$Cs^{+}>Rb^{+}>K^{+}>NH_4^{+}>Ba^{2+}>Na^{+}>Ca^{2+}>Fe^{2+}>Al^{3+}>Mg^{2+}>Li^{+} \quad \text{(eq. 4.1)}$$

Similar position of NH_4^+ in the preference sequence has been also reported by other studies (Jama and Yücel, 1989; Rahmani et al., 2004; Leyva-Ramos et al., 2004; Guo et al., 2008). Based on this sequence, potassium is somewhat preferred over ammonium which in turn is more preferred than calcium. The competition between these cations, especially between ammonium and potassium, is a challenge to apply clinoptilolite for ammonia removal in wastewater with potassium (Chartrand, 2018).

Because of the limited capacity of ion exchange materials, they must be regenerated and re-used in order for this technology to be economical and sustainable. Zeolites are generally regenerated using 2 to 10 % NaCl solutions (Dryden and Weatherley, 1989; Rahmani et al., 2004; Chartrand, 2018; ResinTech Inc, 2020). However, once used for the regeneration of ammonia laden IE, the regeneration solution contains high concentrations of NaCl and significant amount of NH_4-N. Thus, the regeneration solution

cannot be discharged directly into the environment, nor can it be recycled for the next regeneration cycle without first eliminating the NH_3-N. Therefore, the remediation of the used regeneration solution is regarded as another environmental problem, and it is desirable to find alternative regeneration methods.

The regeneration using a hypochlorite solution as the regenerant seems a promising method, the chlorine oxidizes the ammonia into nitrogen gas without generating serious secondary pollution (Huang et al., 2015; Zhang et al., 2017). Huang et al. (2015) reported on the successful application of this approach using in batch experiments, however their work didn't sufficiently quantify the competitive ion uptake nor evaluate the zeolite's preference on TAN over other competing ions after NaOCl regeneration. Zhang et al. (2017), also studied the performance of hypochlorite in zeolite regeneration and found that the use of a combined NaClO-NaCl regeneration solution performed better than a NaOCl solution alone. This NaOCl-NaCl regeneration approach may not be practical because the eventual discharge of the used high salt content regeneration solution could be problematic. Zhang et al. (2017) only focused on the performance of regenerated zeolite in the ammonium-solution without other competing counterions which is not representative of real applications.

The objective of this study was to assess the performance of NaOCl regeneration of a commercial zeolite (SIR-600) that was loaded with a synthetic EIMWW containing TAN, calcium and potassium. To assess the merits of this approach, multiple loading-regeneration cycles were performed using three major types of regenerants (NaCl, NaOCl, and their combination). In the application of IE system, the regeneration solutions are

prepared with the cleanest available water. However, in remote locations, tap water may not be readily available, so one would prepare the regeneration solution using the loading effluent or recycled regenerant which may contain competitive ions (e.g., Ca and K). To investigate the sustainability of this process, loading-regeneration experiments were performed using the regeneration solutions with competitive ions. Additionally, the long-term impact of exposure to high Cl_2 concentration solutions on the integrity of the zeolite and its ion uptake were also examined.

4.2 Experimental Materials and Methods

4.2.1 Experimental Materials

This study was undertaken using a commercial zeolite (SIR-600, ResinTech Inc., Candem, NJ) since the information from the manufacturer state SIR-600 has a relatively high selectivity for ammonium. SIR-600 is considered as clinoptilolite since the reported cation selectivity order of SIR-600 is similar to that of clinoptilolite (Ames, 1960; ResinTech Inc., 2020). A previous study showed good performance of this material in terms of TAN uptake (Chartrand et al., 2020) and a slightly higher selectivity for ammonia over potassium. Based on this selectivity SIR-600 is a particularly good IE material for ammonia removal in EIMWW which contains TAN, Ca, and K.

This research evaluated the effectiveness of SIR-600 to treat a synthetic EIMWW because an actual EIMWW was not accessible. The synthetic EIMWW wastewater was prepared using ammonium chloride, potassium chloride and calcium chloride hexahydrate (ACS grade, Fisher Scientific, Waltham, MA). Suggested by the research partner from Dowclear

Inc, the synthetic wastewater contained approximately 21 mg TAN as N/L, 30 mg K/L, and 80 mg Ca/L (1.5 meq/L, 0.77meq/L, and 4 meq/L) respectively (Downey, 2018).

Three main regenerant solutions were used in this study: a 5% NaCl solution, a 100 mg Cl_2/L solution and a combination of the two. The 5% NaCl solution was chosen because a previous study showed this regenerant was effective for SIR-600 regeneration (Chartrand et al., 2020). The 100 mg free Cl_2/L solution was chosen because it provides an amount of chlorine that is in excess of the quantity required to oxidize TAN on the zeolite (i.e., Cl_2:N mass ratio >8). The salt solutions were prepared using distilled water and ACS grade NaCl (Fisher Scientific, Waltham, MA). This solution was used to demonstrate the conventional regeneration approach. The 100 mg free Cl_2/L and 1000 mg free Cl_2/L regeneration solutions were prepared for the exposure tests by the dilution of a commercial bleach (NaOCl) and they also contained small concentrations of combined chlorine. To assess the impact of competitive ion in the recycled regenerants or the regenerants prepared with the loading effluent, some regeneration/loading cycles were performed using regeneration solutions containing potassium and calcium. These solutions were prepared by adding 80 mg/L Ca and 30 mg/L K to the 100 mg Cl_2/L regenerant and 5% NaCl regenerant. The Ca and K additions were accomplished by adding calcium chloride and potassium chloride. These solutions were denoted as NaOCl+Ca+K and NaCl+Ca+K.

4.2.2 Analytical Methods

The total ammonia nitrogen (TAN) concentration was measured using the Nessler method which was adapted from Standard Method 4500-NH_3 C (American Public Health Association, 1992). The Ca and K ion concentrations were measured using a flame atomic absorption spectrometer (AAS) (PinAAcle 500, PerkinElmer, Waltham, MA, United States) The analytical method was adapted from the Standard Method 3111B (American Public Health Association, 2017).

Free and total chlorine levels were determined using Hach method 8021 and 8167, respectively. They are equivalent to Standard Method 4500-Cl G for drinking water (American Public Health Association, 2017). The pH values were measured with a pH meter (VER Symphony B10P, VWR, Radnor, PA) and a pH probe (VWR 89231-580, VWR, Radnor, PA).

The long-term impact of chlorine exposure tests assessed the impact on the SIR-600 media in terms of the BET surface area, pore size distribution, Fourier Transfer Infrared (FTIR) absorbance, scanning electron microscope (SEM) images, and particle grain size analysis. The BET surface area and pore size distribution quantifications were performed using N_2 adsorption-based surface area analyzer (ASAP 2020, Micromeritics, Norcross, GA). The samples were analyzed at 77 K. The FTIR tests were performed using a FT-IR spectrometer (Nicolet 6700FT-IR, Thermo Electron Corporation, Massachusetts). The SEM images of the SIR-600 were captured with a field emission SEM (JMS7500F, JEOL Ltd, Tokyo). The particle size distribution tests were conducted following a sieve test procedure adapted from ASTM method D6913/D6913M – 17 (ASTM, 2017).

Approximately 50 g dried SIR-600 was placed on the top sieve of a stacked series of pre-weighed sieves (12, 16, 20, 30, 40, 45, and 50 US mesh). The sieves were shaken for approximately 10 minutes with a sieve shaker (SS-8R, Gilson Co., Lewis Center, OH). Each sieve was re-weighed to determine the mass of SIR-600 retained on each sieve. The sieve analysis was performed on the IE material before and after a 5-week chlorine exposure period.

4.2.3 Batch Loading Experiments

The batch experiments were performed to compare the multiple-cycle performance of different regenerant solutions on the ion uptake of SIR-600. The equilibrium ion uptake of zeolite in the next cycle was calculated to assess the efficiency of the regenerants. Furthermore, additional batch loading tests were also performed as part of the impact of long-term chlorine exposure tests.

A loading-regeneration batch cycle includes a batch loading phase followed by a batch regeneration phase. 0.24 g of SIR-600 was placed in a 120 ml glass bottle and filled with the synthetic EIMWW in the loading phase. The bottles were filled with the solution to the top, without headspace, to prevent the loss of ammonia due to its volatility. The Teflon tape was entwined on the threaded neck of the bottles to ensure the screw-on cap provided a good seal. The sealed bottles are spun in an end-over-end tumbler at a speed of approximately 10 rpm for 24 hrs to make sure that solid and liquid contact efficiently and finally reach equilibrium. Then, the bottles were taken out from the tumbler, and the liquid was separated by vacuum filtration through a 0.45 µm membrane filter (GN-6, Pall, New York). The NH_3-N, K^+ and Ca^{2+} concentrations of the liquid were then analyzed. The

SIR-600 particles were kept for the following regeneration experiments. The experiments were conducted in duplicate at room temperature (~22 ^{o}C), and the average results were reported.

The filtrate concentrations of one ion are the equilibrium liquid phase concentrations (C_{eq}). The equilibrium solid phase concentration (Q_{eq}) of the ions can be obtained using the following mass balance equation (eq. 4.2) based on the initial and final solid-phase and liquid-phase concentrations of the particular ion. That is:

$$M * Q_i + V * C_i \leftrightarrow M * Q_{eq} + V * C_{eq} \qquad \text{(eq. 4.2)}$$

Where, M represents the mass of the IE material (g); Q_i represents the initial solid concentration of this target ion (mg/g or meq/g); V represents the volume of the liquid (L); C_i represents the initial liquid-phase concentration of the target ion (mg/L or meq/L); C_{eq} represents the equilibrium liquid-phase concentration of the target ion (mg/L or meq/L); Q_{eq} represents the solid-phase concentration of the target ion at the equilibrium state (mg/g or meq/g).

Due to the reason that Q_i is not known, one generally uses the ion uptake by each gram of IE material (Q_{uptake}) in each cycle. It is calculated by assuming Q_i is equal to 0. Q_{uptake} can be found by eq. 4.3:

$$Q_{uptake} = \left(C_{eq} - C_i\right) * \frac{V}{M} \qquad \text{(eq. 4.3)}$$

4.2.4 Batch Regeneration Tests

Three major regenerants were used during the regeneration phases of 5 loading-regeneration cycles: i) 100 mg free Cl_2/L hypochlorite solutions; ii) 5% NaCl solutions; and iii) their combination. pH values of regenerants were increased to pH 10 by 4 M NaOH solution additions.

If the regenerant were to be recycled or prepared with loading-phase effluent, some Ca and K would exist within the regenerant. To test the impact of competitive ions present in the regeneration solutions, regenerations were also conducted using synthetic regeneration solutions containing Ca and K. They were prepared by adding 80 ppm Ca and 30 ppm K were added to the above-mentioned regeneration solutions. Their impact was studied over three loading/regeneration cycles.

In the regeneration phase, the loaded SIR-600 collected from the previous loading phase was used. During the regeneration phase the loaded SIR-600 was placed in a clean 120 ml clear glass bottle, then filled with the regeneration solution with no headspace and sealed as in the loading phase. Then, the bottle was secured in the end-over-end tumbler and rotated for 48 hours. Afterwards, the liquid was vacuum filtered through a 0.45 µm membrane filter (GN-6, Pall, New York) to collect all the regenerated SIR-600. The regenerated SIR-600 granules were then rinsed with deionized water and kept for the loading phase of the next cycle. To better demonstrate the long-term performance of the three main regeneration solutions, five cycles (i.e., batch loading + batch regeneration) were performed in this current study considering the previous study operated four cycles for the similar purposes (Chartrand, 2018).

4.2.5 IE Material Durability Tests with Chlorine Exposure

Resintech suggests that SIR-600 can withstand a cumulative free chlorine exposure of at least 106 ppm·hr (ResinTech Inc, 2020), however this is much lower than can be expected in the long-term operation using chlorine regeneration. Due to concerns regarding the impact of the exposure to high chlorine concentrations on the long-term durability of SIR-600, it was characterized before and after a five-week chlorine exposure period. The characterization was performed using SEM surface images, surface area analysis, particle size distribution, FTIR spectra, ion uptake ability tests. The 5-week duration was selected to evaluate a "long-term" exposure period representing the approximate ppm Cl_2 contact hour levels that may be expected in IE column operating over a period of one year. Two concentration levels (100 ppm and 1000 ppm as free Cl_2) of hypochlorite solution were selected to conduct the batch chlorine exposure tests. The SIR-600's ion uptake was monitored before, during and after the chlorine exposure period.

Loading-regeneration tests were performed on the samples exposed to chlorine to evaluate the impact of long-term chlorine exposure on ion exchange uptake ability of SIR-600. The loading procedure was the same as that of the batch loading. The regenerations were performed using the same procedure as that used for the batch regeneration except for their duration, which in this case was one week. The regeneration cycle also acted as a week-long high-chlorine-concentration contact period. The full cycles (i.e., 1 loading phase + 1 regeneration/chlorine exposure phase) were repeated five times. Prior to the long-term loading-regeneration tests, the zeolite samples were preconditioned with

three batch loading-regeneration cycles, the regeneration phases were performed using 100 ppm (as free Cl_2) hypochlorite solutions as the regenerant.

4.3 Results and Discussion

4.3.1 Batch Regeneration Studies

The impact of the regenerant composition was studied by multiple loading-regeneration cycles. The three types of regenerants, including NaCl (5% NaCl), NaOCl (100 ppm as free Cl_2) and their combination (5% NaCl +100 ppm as free Cl_2), were freshly prepared in each cycle. The average TAN, K and Ca uptake reached in 5 cycles regenerated by 5%NaCl are shown in Figure 4-1.

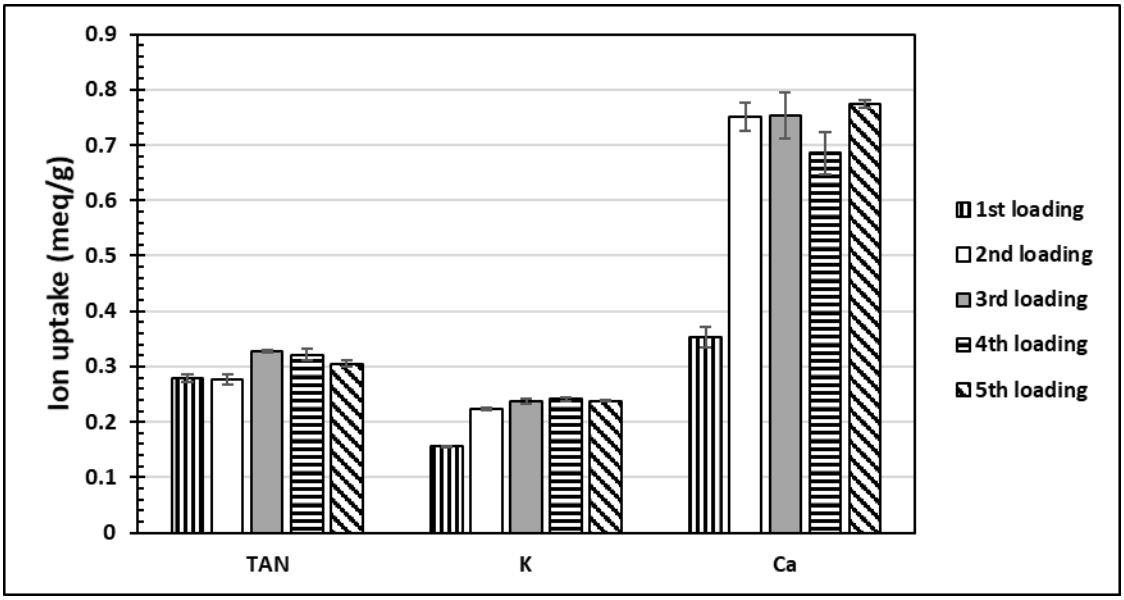

Figure 4-1 Multiple cycles performance using fresh 5% NaCl regenerant (average value of two replicates ± standard error).

It is worth nothing that the "uptake" in each cycle presented in the figure refer to the ion exchanged during the loading phase of the that specific cycle. This "uptake" should not be confused with the absolute capacity of the IE material in each cycle. In fact, the actual

capacity of the studied ion on the IE media may be higher due to potential residual ions from the last cycle.

The 5% NaCl regeneration resulted in several patterns in the loading phase's ion uptakes (Figure 4-1). First, there seems to be a general slightly increasing trend (~9% increase) in the TAN uptake from 1st to 5th loading phase. Second, Ca and K uptakes after the 1st loading increased significantly presumably due to the release of preloaded ions in the first cycle. The first loading was conducted with unconditioned SIR-600, that was preloaded with certain ions e.g., Ca and K, so during the initial cycle with NaCl regeneration, there likely was some Ca and K leaching. This in turn could had freed up sites for TAN leading to an increased TAN uptake (Milan et al., 1997; Hankins et al., 2004;). This pattern has been previously reported by different researchers (Sprynskyy et al., 2005; Chartrand et al., 2020). Third, the long-term uptake of TAN, K, and Ca followed the pattern of ion uptakes in the second loading phase, which is: TAN uptake was higher than that of K but almost half of Ca uptake. The higher Ca uptake may be attributed to its higher Ca concentration in the synthetic EIMWW (4 meq Ca/L versus 1.5 meq TAN/L and 0.7 meq K/L). The α_K^{TAN} and α_{Ca}^{TAN} separation factors in the fifth loading phase were equal to 0.46 and 3.15 respectively, the first indicate TAN is less preferred than K while the second shows TAN outcompetes Ca in this system. The separation factor of α_{Ca}^{TAN} of 3.15 was close to the 3.54 observed Chartrand (2018) in the study with the same IE material. Although the calculated α_K^{TAN} in the current study was less than α_K^{TAN} (2.95) reported by the study of Chartrand (2018), however, the 0.46 α_K^{TAN} separation factor is consistent with the order of selectivity reported by SIR-600 manufacturer (ResinTech Inc, 2020). The differences

with Chartrand (2018) values are possibly due to the significantly higher K to TAN ratios in their EIMWW. It should also be noted that if the TAN selectivity is expressed in terms of the ratio of the uptakes it may yield somewhat different conclusions. For the fifth cycle, one obtains a q_{TAN}/q_K value of approximately 1.3, which is somewhat more in line with the 0.96 value reported by Chartrand (2018). Again, it is speculated, that difference is due to the higher K to TAN ratios in the two EIMWWs, that is the lower K to TAN ratio in the solution in this study (0.51versus 0.74 meq TAN/meq K) resulted in the higher q_{TAN}/q_K ratio (1.3 versus 0.96).

The five cycles with NaOCl regeneration (100 ppm as free Cl_2) led to gradual decreasing ion uptakes (Figure 4-2). After 5 cycles, the SIR-600 TAN uptake decreased by approximately 18%. Using the multi-component loading solution, the reduction of zeolite's TAN uptake after multi-cycle NaOCl regenerations was also found in the study of Huang et al. (2015). The SIR-600 long-term TAN uptakes (Figure 4-2) were approximately 20% lower than the TAN uptakes achieved with 5% NaCl regeneration (0.239 ± 0.001 meq TAN/g vs. 0.305 ± 0.006 meq TAN/g, the ± is the standard error). On the other hand, the K uptakes of NaOCl regenerated SIR-600 decreased to 0.076 ± 0.004 meq/g, about 66% of those observed when using 5% NaCl regenerated SIR-600. The NaOCl regeneration decreased the Ca uptakes to 0.018± 0.007 meq/g, or about 2.5% of that achieved with 5% NaCl regeneration.

In the case of the post NaOCl regeneration loading phases, the ion uptakes are lower than those for NaCl regeneration. However, a TAN uptake represents approximately 70% of

the total ion uptake while for the NaCl regeneration it was only 25%. This is a significant improvement in the selectivity of TAN over K.

This could be explained by the following mechanisms. First, the oxidation of the desorbed ammonia by NaOCl, which is described in the following equation (Zhang et al. 2017):

$$2NH_4^+ + 3ClO^- + 2OH^- \rightarrow N_2 \uparrow + 3Cl^- + 5H_2O \qquad \text{(eq. 4.4)}$$

Thus, the destruction of the NH_4^+ leads to the formation of nitrogen gas which could leave the system and leads to the further release of TAN from the zeolite. This suggests the chlorine only regenerated sites containing TAN and it did not regenerate sites contacting Ca and K. Second, the NaOCl (100 ppm as free Cl_2) solution contains relatively low concentrations of Na assuming NaOCl is the only source of Na in the original bleach (i.e., 32 mg/L in NaOCl regenerant versus 19658 mg/l for the 5% NaCl regenerant) so the regeneration could only free Ca and K from a limited number of sites, thus there are a smaller number of sites available for the next loading step, and the regenerated TAN-occupied sites appears to be TAN-selectiveThis is evident from the decrease in the sum of the TAN, K and Ca uptakes from 0.82 in the first cycle to 0.33 meq/g in the last cycle, and TAN accounted for approximately 70% of the total ion uptake in the last cycle. Third, due to the higher selectivity of K over Ca and the large quantities of Ca remaining on the zeolite, the Ca uptake decreases significantly in subsequent cycles. Huang et al, (2015) also observed this phenomenon in terms of zeolite regeneration using chlorination.

As is discussed, NaOCl regenerant should majorly regenerate the sites previously occupied by TAN. On the subsequent loading phase, it is expected that these sites would be accessible to K, Ca as wells as TAN. Due to competition among the ions, one would expect the decrease of TAN uptake. However, as shown in Figure 4-2, there was no significant change of the TAN uptakes. This seems to indicate the existence of some TAN specific sites. It is unclear why this would be the case as it contradicts the general principle of ion exchange.

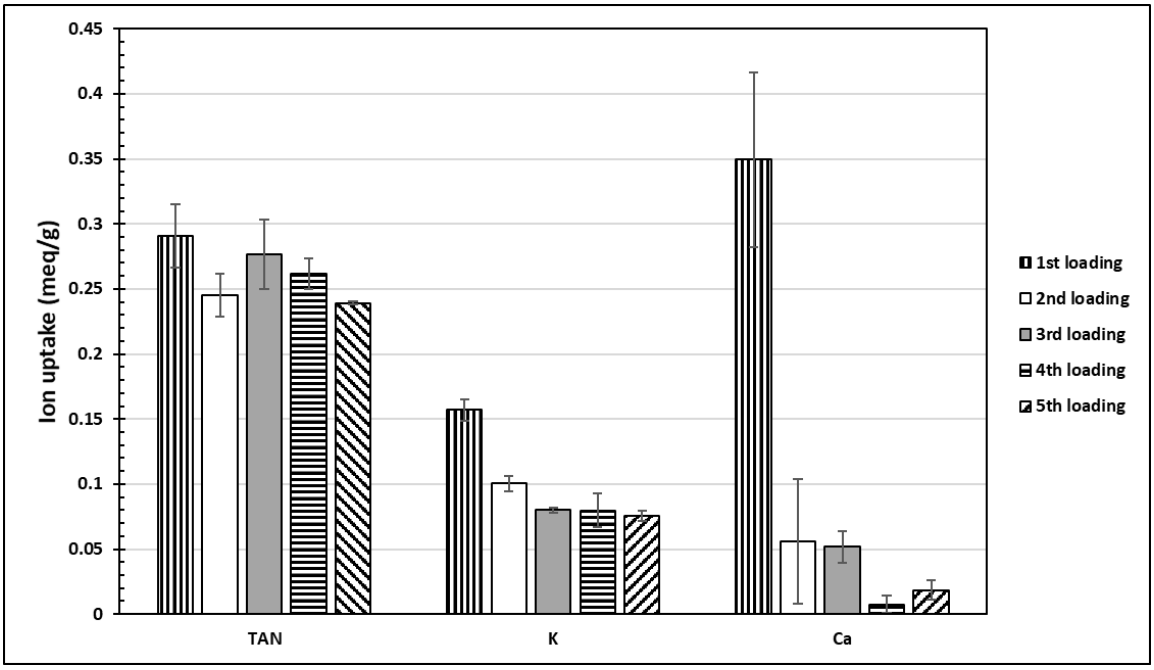

Figure 4-2 Multiple cycles performance using NaOCl (100 ppm as Cl_2) regenerant (average value of two replicates ± standard error).

To evaluate if there is an additive regenerating effect by using the combination of NaCl and NaOCl, five loading-regeneration cycles were performed using a 5% NaCl + NaOCl (100 ppm as free Cl_2) regeneration solution. The key results from these experiments are

shown in Figure 4-3. First, the TAN, K, and Ca mass uptakes were similar to those for the NaCl regenerated SIR-600 (0.31 meq TAN/g vs. 0.30 meq TAN/g, 0.24 meq K/g vs. 0.24 meq K/g, 0.76 meq Ca/g vs. 0.77 meq Ca/g) suggesting no additive effect was found. Second, as with the NaCl regeneration cycles there were increments in the TAN, K and Ca uptakes after the first cycle. Thus, it seems that the 5% NaCl played a dominant role in this NaCl+NaOCl regeneration due to the high Na concentrations caused the elution of the preloaded counterions and released more sites for K and Ca uptake in the following cycles. This TAN uptake of SIR-600 increased slightly (14%) after 5-cycle NaCl+NaOCl regenerations in this study. However, the increment differs from the result of Zhang et al (2017) which claimed that NH_4^+-N removal capacity of the zeolite decreased 18.2% after five times NaOCl-NaCl regeneration. The difference may be due to the differences in the IE media, which are discussed in section 4.3.2.1, and due to difference in the loading solutions (for example, Zhang's solution did not contain competing cations).

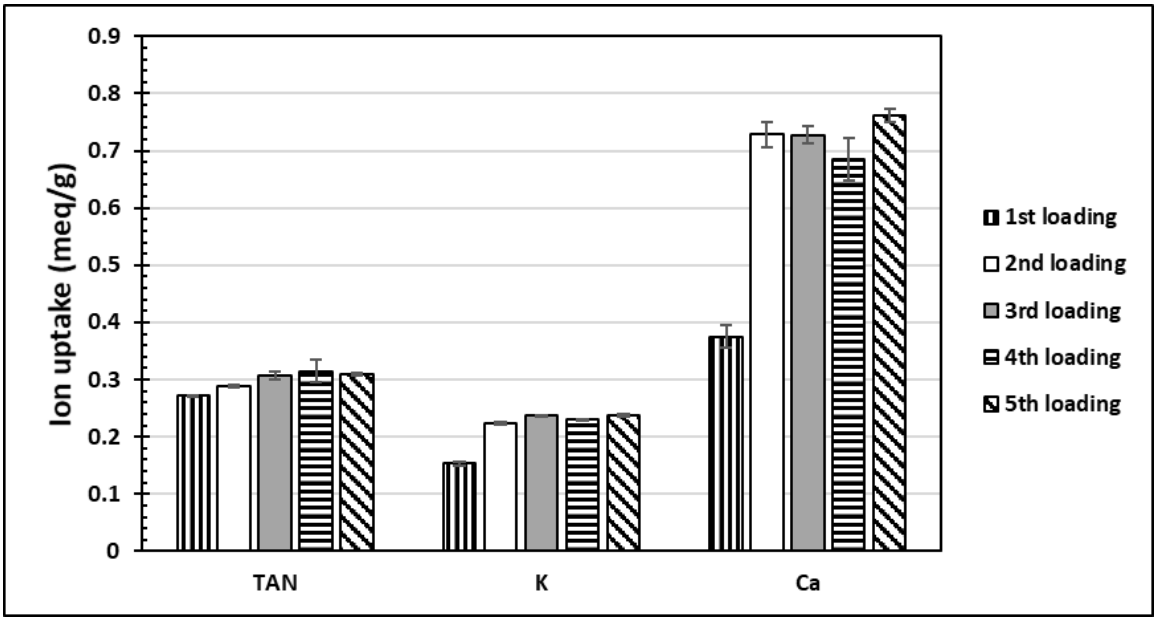

Figure 4-3 Multiple regeneration cycles using fresh 5% NaCl+ NaOCl 100 ppm as Cl_2 regenerant (average value of two replicates ± standard error).

A comparison of the fifth-cycle ion uptakes for the three different regeneration solutions (Figure 4-4) illustrates more clearly the points raised earlier. The key observations were as follows: First, the TAN uptake of SIR-600 with NaOCl regeneration was approximately 80% of that with NaCl or combined regeneration. Second, the K and Ca uptakes of SIR-600 with NaOCl regeneration were significantly lower than those with NaCl or combined regeneration. Third, the 5^{th} cycle TAN, K, and Ca uptakes of SIR-600 with NaCl are similar to those with combined regeneration due to the dominant role of high-level sodium in the regeneration when 5% NaCl only regenerant has much higher sodium concentration than NaOCl only regenerant (100 ppm as Cl_2) does. Fourth, the 5^{th} cycle total ion uptake of NaOCl regenerated SIR-600 is much smaller than that with NaCl or combined regenerant because of the significantly lower Ca and K uptakes following NaOCl

regeneration compared to those following the NaCl and the NaCl+NaOCl regenerations. Fifth, it should also be noted that the total ion uptake after the fifth NaOCl cycle was approximately 0.33 meq/g which is very close to the 0.3 meqTAN/g uptake during the final loading achieved using 5%NaCl regeneration. This suggests that the NaOCl essentially only regenerates the sites occupied by TAN.

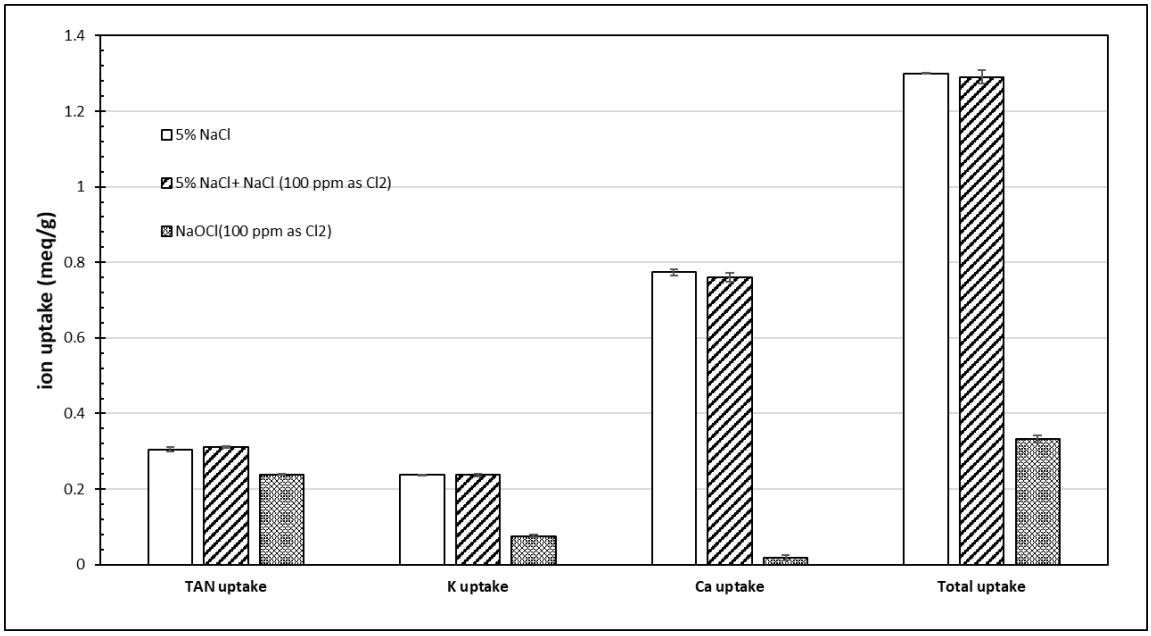

Figure 4-4 Fifth cycle ion uptakes comparisons of the NaCl, NaOCl, and combined regeneration. (average value of two replicates ± standard error).

In practical applications, which generally use column ion exchange units, the NaOCl regeneration solutions would be recycled or prepared using the IE column's effluent, so the regenerant contains K and Ca on some levels after certain cycles. To evaluate the impact of competitive ions in these regenerant, a regenerant was prepared adding 80 ppm Ca and 30 ppm K to a 100 ppm as free Cl_2 NaOCl solution. Two loading-regeneration

cycles were performed using the two types of regeneration solutions: i) 100 ppm as free Cl_2 solution prepared in distilled water, which is the same as in previous experiments; and ii) a mixture of 80 ppm Ca, 30 ppm K, and 100 ppm as free Cl_2 also prepared using distilled water (Ca+K+NaOCl).

Figure 4-5 compares the ion uptakes of the third loading phases for the above regeneration solutions. The third cycle results are presented because during the earlier cycles the ion uptakes change as the IE material was readjusting to this different regeneration solutions. The uptake of the NaOCl regenerated SIR-600 was the same as presented earlier. The Ca+K+NaOCl regenerant led to calcium desorption in the loading phase. Given that the regeneration solution contains the same concentrations of Ca and K as the loading solution, during this regeneration phase there should be both Ca and K uptake. Thus, in the subsequent loading phase one would expect a lower total TAN+K+Ca uptake and possibly some Ca and/or K desorption. Given the IE materials greater affinity for K than Ca, it seems logical that there was greater Ca desorption.

The SIR-600 regenerated by NaOCl had the highest TAN uptake in the 3rd loading phase. This was presumably due to the fact that NaOCl regenerant without extra competitive ions (Ca and K) removed and oxidized ammonia on the IE material and left some vacant IE sites for the next loading phase. However, the difference between the TAN uptake of NaOCl regenerated SIR-600 and that of Ca+K+NaOCl regenerated SIR-600 was not very significant (0.277 ± 0.027meq/g Vs. 0.245 ± 0.007 meq/g).

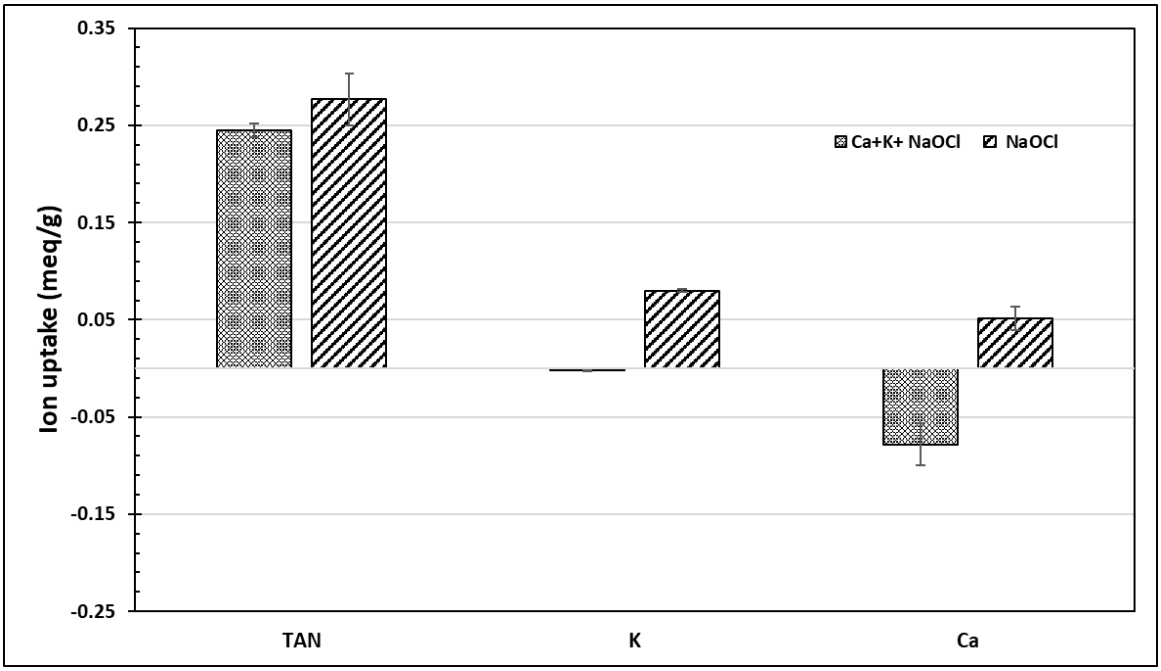

Figure 4-5 Comparison of third loading phases SIR-600 ion uptakes between using a 100 ppm NaOCl solution and the Ca+K+NaOCl regeneration solution. (Average value of two replicates ± standard error).

For comparison with the Ca+K+NaOCl regeneration, a similar set of experiments was performed with NaCl regeneration solutions prepared with water containing Ca and K. The regeneration solutions were 5% NaCl prepared in distilled water (NaCl) and 80 ppm Ca, 30 ppm K, and 5% NaCl mixture (Ca+K+NaCl). Three loading-regeneration cycles were performed with each of the regeneration solutions, only the more re-equilibrated third cycles results are presented (Figure 4-6). The ion uptake in the 3rd cycle after the regeneration with the NaCl solution containing 80 ppm Ca+ 30 ppm K was very close to that with NaCl regeneration. It is inferred that high level of NaCl was dominating the regeneration effect of Ca+K+NaCl as regenerant, while the competitive ions (e.g., K) in the

regenerant was adsorbed during the regeneration phase and led the lower TAN and K uptake in the following loading phase.

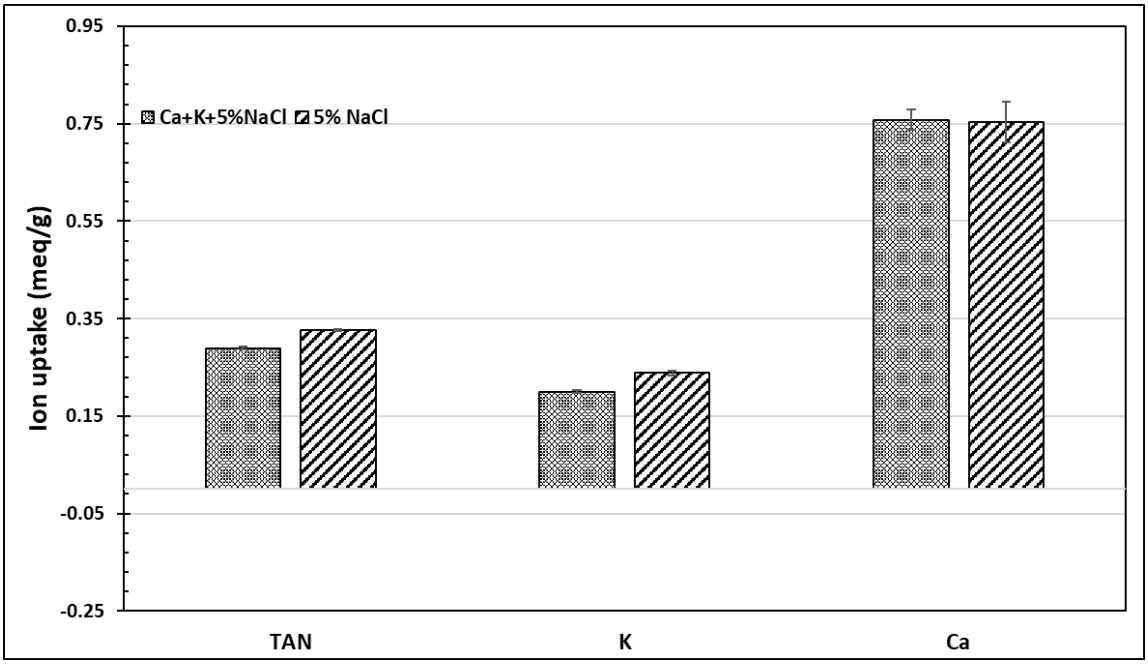

Figure 4-6 Comparison of the third loading phase SIR-600 ion uptakes achieved using a 5% NaCl regeneration and a 5% NaCl regeneration containing 80 ppm Ca and 30 ppm K. (average value of two replicates ± standard error).

4.3.2 Longevity Studies of Chlorine Exposed SIR-600

The following subsections present the results of the BET surface area, pore size analysis, the FTIR spectra, the particle size distribution, the SEM images, and the ions uptake tests of SIR-600 materials before and after the 5-week long 1000 and 100 mg/L free chlorine exposure.

4.3.2.1 BET surface area

For all of the materials tested the N_2 gas adsorption tests yielded the same pattern, the adsorbed N_2 versus relative pressure graphs can be described as BET type II isotherms

with a slight hysteresis (Thommes et al., 2015). For type II isotherms, the BET method provides a more accurate estimation of the surface area for this type of zeolite compared to the Langmuir method (Thommes et al., 2015).

The major observations from Figure 4-7 are that the BET surface area of SIR-600 is approximately 16 m^2/g and there is no significant difference in terms of BET surface area among SIR-600 before exposure and the ones exposed to the two levels of chlorine. Other studies reported similar levels of BET surface areas (~20 m^2/g) of their tested zeolites (Huang et al., 2015; Ghasemian and Falamaki, 2017). In addition, Figure 4-8 shows that the pore volume of macropores and mesopores take the most proportion of total pore volume of this material. This finding is basically consistent with the feature of type II isotherm where most the pore volume is associated with macropores (Thommes et al., 2015). The BJH average pore widths of the 3 samples (fresh, 100 ppm, and 1000ppam) are 204.4 Å, 155.3 Å, and 167.8 Å, respectively, which are close to average pore widths (approximately 150 Å -250 Å) reported by other studies (Huang et al., 2015; Dosa et al., 2018).

Compared to the SIR-600 used in this study, the zeolite material used by Zhang et al. (2017) has a significantly larger surface area (67.9 versus 16 m^2/g) and an average smaller pore size (31.6 Å versus 204 Å). The stable surface area of the IE material under chlorine exposure is contrary to the findings of Zhang et al. (2017) who reported that after 10 NaClO-NaCl regeneration cycles the BET surface area of their zeolite material increased from 67.9 to 81.4 m^2/g. Zhang et al. (2017) claimed the micropore volume of their material increased by 27.3% and 31.8% after 10 and 20 cycles of NaClO-NaCl

regenerations. However, as is shown in Figure 4-9, there was no significant change observed in terms of SIR-600 micropore (<20 Å) volume after 5-week chlorine exposure.

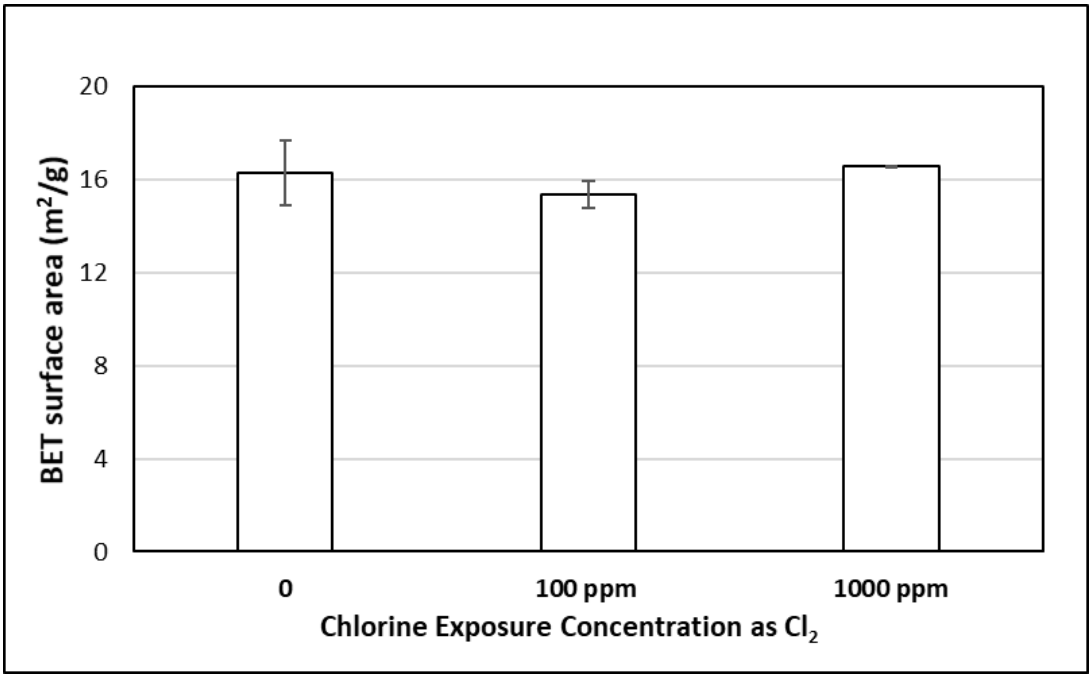

Figure 4-7 BET Surface area after 5-week different levels chlorine exposure (average value of two replicates ± standard error)

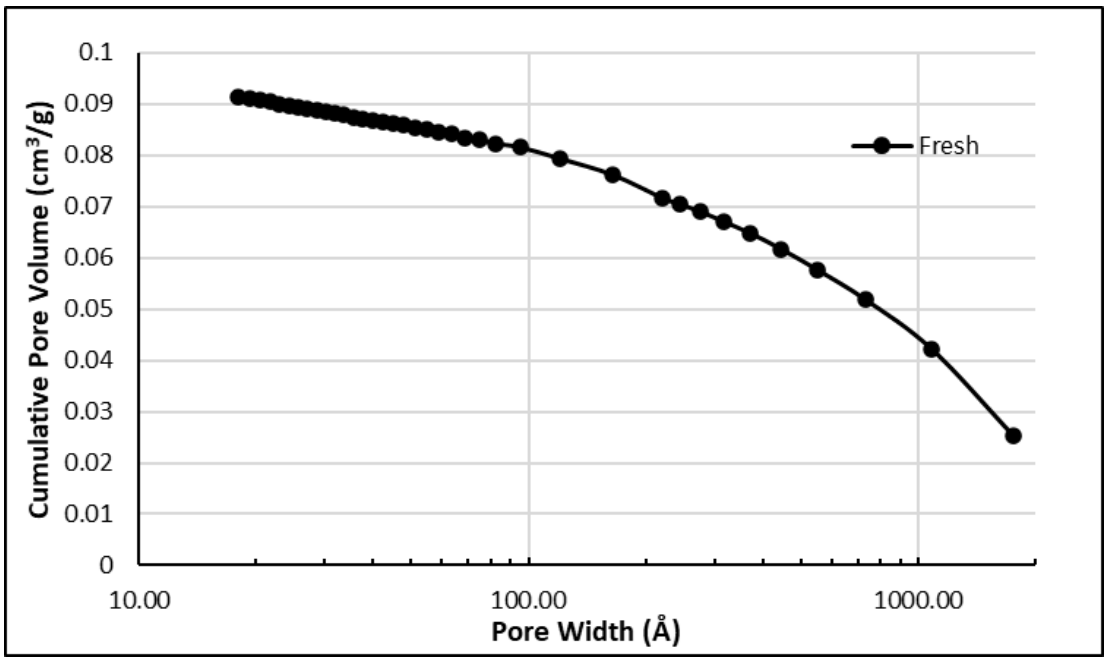

Figure 4-8 BJH pore volume of untreated fresh SIR-600

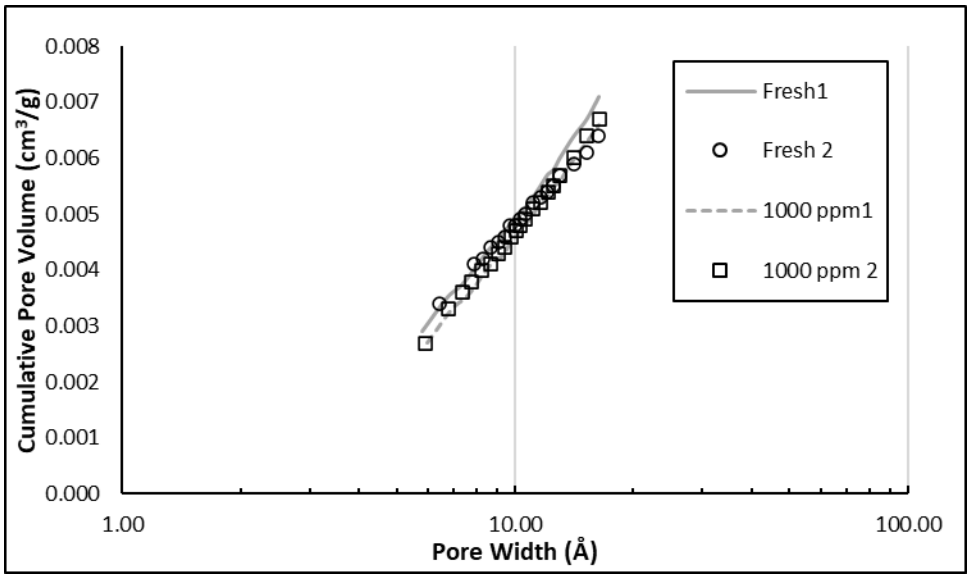

Figure 4-9 Horvath-Kawazoe pore volume of untreated fresh SIR-600 and SIR-600 treated with 1000 ppm as Cl_2.

4.3.2.2 FTIR spectra

Zeolites are aluminosilicate minerals. The key results pertaining to the FTIR spectra of zeolites are the types of bonds on the zeolite, and the location of the most important lattice vibrations associated with these bonds are presented in Table 4-1 (Lercher and Jentys, 2007). Figure 4-10 shows the existence of the O-T-O bending (439-449 cm^{-}), which represented the TO_4 tetrahedra basic building unit of zeolite framework, where T (such as Al^{3+} and Si^{4+}) is any cation can have tetrahedral coordination (McCusker and Baerlocher, 2007). This peak is evident in all the sets of samples (unexposed, exposed with 100 ppm free Cl_2 solution and exposed to 1000 ppm as free Cl_2 solution) (Lercher and Jentys, 2007; McCusker and Baerlocher, 2007; Mintova, and Čejka, 2007). By replacing Si^{3+} with Al^{3+} in silica framework, the aluminosilicate framework consisting of SIO_4 and AlO_4 has negative charges showing affinity to cations (McCusker and Baerlocher, 2007; MIntova, and Čejka, 2007). Besides the O-T-O bending, some other lattice vibration bands, including asymmetrical stretch and pore opening, were also observed in the spectra. The similar IR spectra bands were also reported in other articles about zeolite characterization (Mozgawa, 2000). FTIR is a qualitative analysis tool rather than quantitative analysis tool, it helps identify the existence of particular bonds but the height of the peaks is not significant. By comparing the IR spectra of samples shown in Figure 4-10, it can be found the patterns and location of bonds were similar which indicates the chlorine exposure did not alter the zeolite structure significantly.

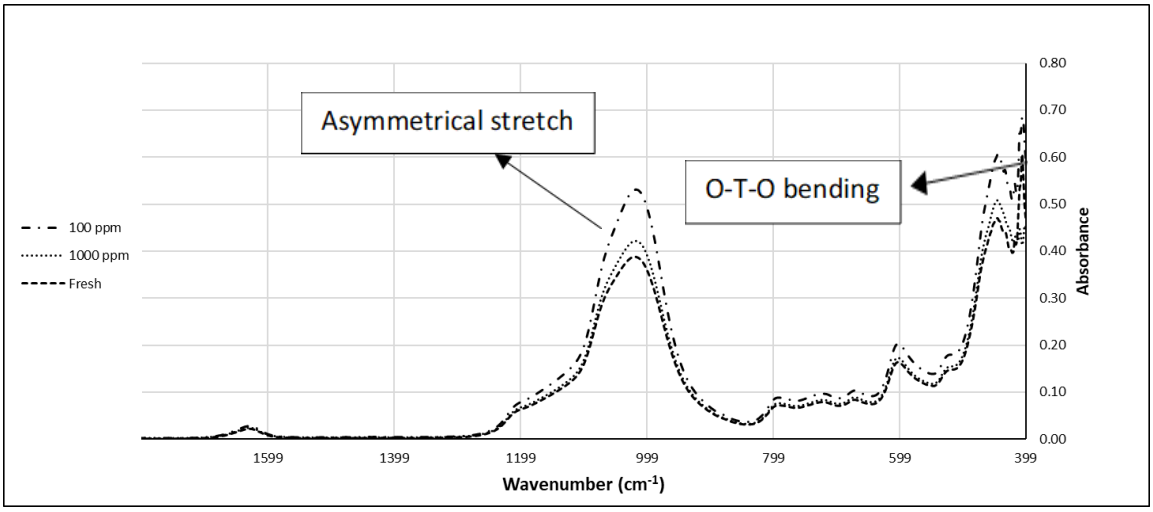

Figure 4-10. FTIR spectra of SIR-600 with and without 5-week chlorine (100 and 1000 ppm as free Cl_2) exposures.

Table 4-1 Zeolite lattice vibration and the corresponding wavelength range. (Source: Lercher and Jentys, 2007)

Intra-tetrahedral bands (structure insensitive)	
Asymmetrical Stretch	950-1250 cm^{-1}
Symmetrical Stretch	650-720 cm^{-1}
O-T-O bending	420-500 cm^{-1}

4.3.2.3 Particle size distribution

To evaluate the impacts of chlorine exposures on the particle size distribution of the material sieve analyses were conducted on chlorine exposed SIR-600 and fresh SIR-600. The major results of this particle size analysis (Figure 4-11) are as follows: First, there was no significant change in the particle size distribution among the three groups (fresh, 100ppm, and 1000 ppm). It can be inferred that the five-week chlorine (up to 1000 ppm

as free Cl_2) exposures did not break down the SIR-600 particles into smaller particles. Second, the particle size of SIR-600 mainly fell into the range between 400 microns to 1680 microns, this is consistent with the manufacturer's specification (ResinTech Inc, 2020).

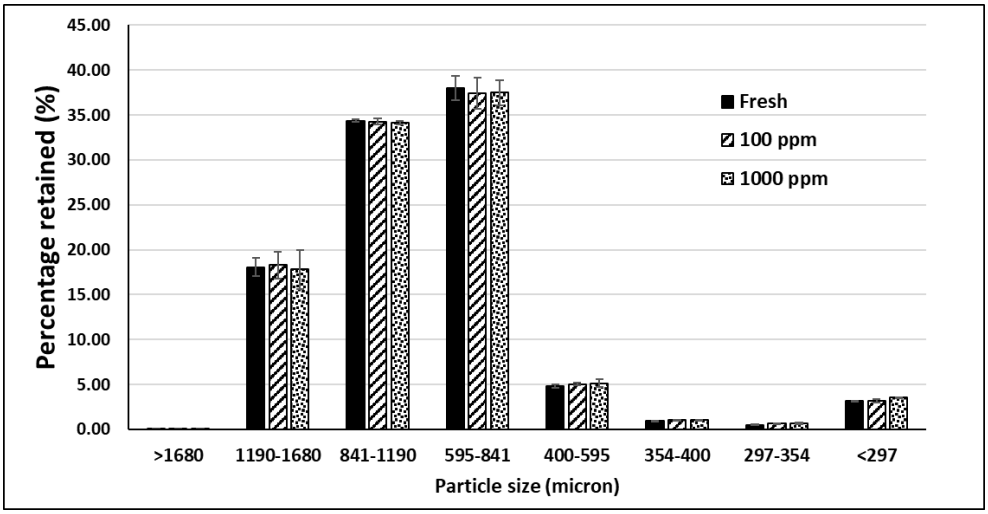

Figure 4-11 Particle size distributions of SIR-600 with and without 5-week chlorine (100 and 1000 ppm as free Cl_2) exposure (average value of two replicates ± standard error).

4.3.2.4 SEM analysis

The SEM images (Figure 4-12) show that the SIR-600 is in the form of stratified plates or sheets which is a typical feature of clinoptilolite. The similar SEM images were also reported by other studies (Ghasemian and Falamaki, 2017, Chen et al., 2018). Comparing the morphology of two samples, no significant differences were found between the unexposed SIR-600 and that exposed to chlorine for 5-weeks.

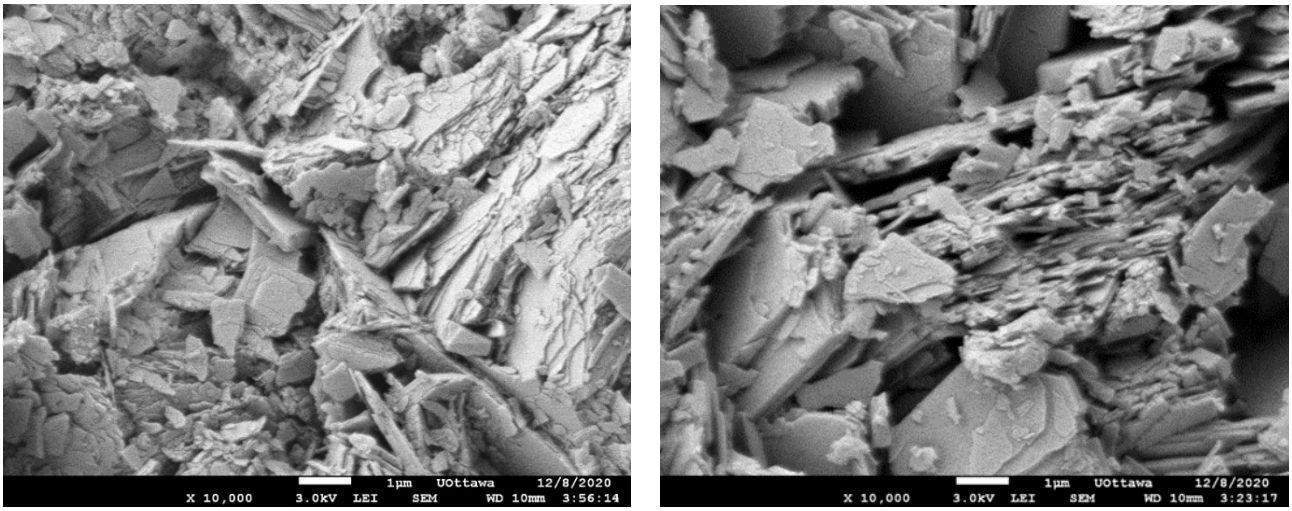

Figure 4-12 SEM image of SIR-600 after 5-week 1000 ppm as free Cl_2/L exposure (left); SEM image of fresh SIR-600 without chlorine exposure.

4.3.2.5 Ions uptake ability tests.

The impact of chlorine exposure on ion uptake capability of the IE material was measured by loading SIR-600 with synthetic EIMWW during the 5-week chlorine exposure tests. After the preconditioning, 5 cycles of regeneration-loading cycles were conducted during these experiments. Each week-long regeneration phase (exposure phase) was also regarded as a chlorine exposure phase. It should be noted that due to the reduction of chlorine level caused by the ammonia oxidization, the chlorine level in each exposure phase was not strictly the nominal 100 or 1000 mg free Cl_2/L for the entire period. However, for the convenience of expression, "5-week 100 ppm free Cl_2 or 1000 ppm free Cl_2" were still used to describe the exposure level in the following text.

Figure 4-13 shows that during the 5-week exposure with 1000 ppm as free Cl_2, the ion uptake of all ion species finally stabilized from that after the pre-conditioning (chlorine exposure time = 0 hr) which used 100 mg free Cl_2/L regenerant solutions. It is observed that the total ion uptake increased after the 1st week 1000 mg free Cl_2/L exposure. It could be explained by the fact that the more abundant Na^+ ions in the 1000 ppm Cl_2 solution (prepared using NaOCl) released some ion-exchange sites which were pre-occupied by other cations in the 5-week exposure. The ion uptake after the 5th week did not change significantly from that of the cycles after the pre-conditioning.

The ion uptakes in the 100 mg free Cl_2/L exposure experiments (Figure 4-14) were somewhat different. First, the uptakes of the three species and their summation increased slightly over the exposure cycles. The lack of uptake changes over the first cycle is reasonable as the pre-conditioning also used a 100 mg free Cl_2/l solution. Second, the TAN uptakes were slightly lower than those of the 1000 mg free Cl_2/L exposure experiments. However, the 100 mg free Cl_2/L solutions contain more than the stoichiometric requirements to oxidize all the TAN. Thus, it is hypothesized that the change was caused by the additional sodium present, as the chlorine solution was prepared using NaOCl.

The results shown in Figure 4-13 and Figure 4-14 all implied that 5-week 100 and 1000 ppm as Cl_2 exposure is not detrimental to the ion uptake capability of SIR-600. Thus, these results are consistent with the results of FTIR, BET and particle size distribution tests.

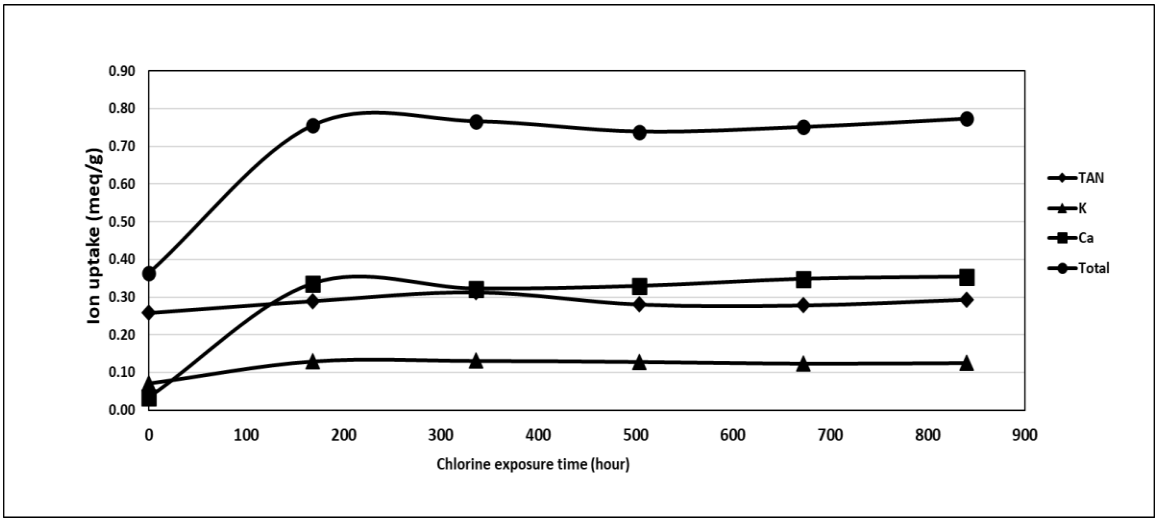

Figure 4-13 The variation of ion uptake with chlorine exposure time using initial chlorine level of 1000 ppm as free Cl_2 in each exposure cycle

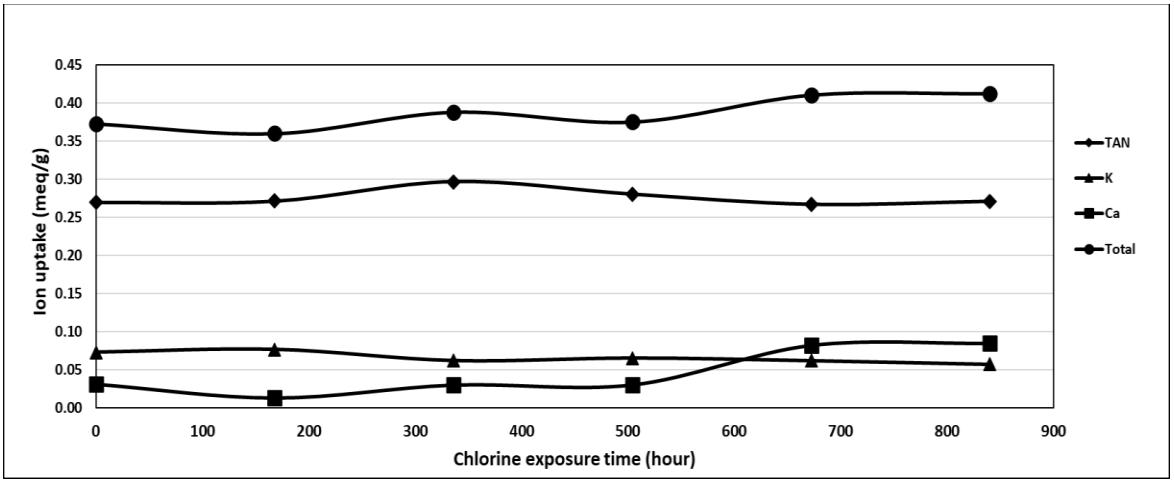

Figure 4-14 The variation of ion uptake with chlorine exposure time using initial chlorine level of 100 ppm as free Cl_2 in each exposure cycle

4.4 Conclusion

The long-term ion-uptake of SIR-600 for removing ammonia from EIMWW and the effectiveness of different regenerants were tested using multi-cycle batch loading-regeneration experiments. These experiments with a multi-solute EIMWW initiative represents a significant contribution since the earlier studies into chlorine regeneration did not investigate the impact of competing ions. The results showed that three to five cycles were required to obtain consistent uptake results. After 5 cycles of regeneration using 100 mg free Cl_2/L solution, the IE material's TAN uptake was quite significant (0.24 meq/g), and it was approximately 80% of that obtained using a 5% NaCl solution, a standard regeneration solution. However, due to calcium and potassium uptake of the chlorine regenerated SIR-600, chlorine regeneration resulted in a much greater TAN selectivity. It is also found that 80ppm Ca and 30 ppm K in NaOCl or NaCl regeneration solution did not significantly hinder SIR-600's TAN uptake.

The five-week-long chlorine exposure did not have a significant impact on SIR-600's grain size distribution, surface area, appearance, internal bonding (FTIR) and the ion uptake. Accordingly, chlorine regeneration does not appear to have a detrimental impact on the performance of the commercial zeolite studied and SIR-600 has the potential for use long-term use in field applications.

Acknowledgements

The authors acknowledge this research was funded by the Natural Sciences and Engineering Research Council of Canada's Engage program (grant 535910-18), Ontario Centre of Innovation's VIP program (grant #33021) and our industrial partners (Milestone Environmental Inc. and Dowclear Inc.).

References

American Public Health Association. (1992). *Standard methods for the examination of water and wastewater.* 18th ed. American Public Health Association, Washington, D.C.

American Public Health Association. (2017). *Standard methods for the examination of water and wastewater.* 23rd ed. American Public Health Association, Washington, D.C.

Ames, L. L. (1960). "The cation sieve properties of clinoptilolite." *The American Mineralogist*, 45, 689–700.

ASTM D6913 / D6913M-17. (2017). *Standard Test Methods for Particle-Size Distribution (Gradation) of Soils Using Sieve Analysis*. ASTM International, West Conshohocken, PA, www.astm.org

Canadian Council of Ministers of the Environment. (2010). "Canadian water quality guidelines for the protection of aquatic life: Ammonia." In *Canadian environmental quality guidelines, 1999*. Canadian Council of Ministers of the Environment, Winnipeg, MB, Canada.

Chartrand, Z. (2018). *The Selective Ion-Exchange Removal of Ammonia from Mining Wastewater.* [MASc dissertation]. Department of Civil Engineering, University of Ottawa, Ottawa, Canada.

Chartrand, Z.G., Narbaitz, R.M., Sartaj, M., and Downey J. (2020). "Ammonia-Ca-K competitive ion-exchange on zeolites in mining wastewater treatment: batch regeneration and column performance". *Journal of Sustainable Mining*, 19, 59-71.

Chen, H., Lin, Y., Chen, B., Yoshiyuki, I., Liou, S. Y., and Huang, R. (2018). "A further investigation of $NH4^+$ removal mechanisms by using natural and synthetic zeolites in different concentrations and temperatures." *Minerals*, 8, 499.

Clifford, D., Sorg, T. J., and Ghurye, G.L. (2012). "Ion exchange and adsorption of inorganic contaminants." Chapter 12 in J. K. Edzwald (Ed.), *Water quality & treatment: a handbook on drinking* water (6th ed., pp. 12.1-12.97). McGraw-Hill, New York, NY.

Ding, Y., and Sartaj, M. (2015). "Statistical analysis and optimization of ammonia removal from aqueous solution by zeolite using factorial design and response surface methodology." *Journal of Environmental Chemical Engineering*, 3, 807–814.

Dosa, M., Piumetti, M., Bensaid, S., Russo, N., Baglieri, O., Miglietta, F., and Fino, D. (2018). "Properties of the clinoptilolite: characterization and adsorption tests with methylene blue." *Journal of Advanced Catalysis Science and Technology*, 5, 1-10.

Downey, J. (2018). Personal communication.

Dryden, H.T., and Weatherley, L.R. (1989). "Aquaculture water treatment by ion exchange: continuous ammonium ion removal with clinoptilolite." *Aquacultural Engineering*. 8, 109-126.

Emerson, K., R. Lund, R. Thurston and R. Russo. (1975). "Aqueous ammonia equilibrium calculations: effect of pH and temperature." *Journal of the Fisheries Research Board of Canada,* 32, 2379–2383.

Environment Canada. (2004). *Guideline for the Release of Ammonia Dissolved in Water Found in Wastewater Effluents. Canada Gazette, December 4th, Part I.*

Forsyth, B., Cameron A. and Miller, S. (1995). "Explosives and water quality". In T.P. Hynes, and M.C. Blanchette (Ed.), *Proceedings of Sudbury '95: Mining and the Environment, Volume II, Ground and Surface water (pp. 795-803)*. CANMET, Ottawa.

Ghasemian, N. and Falamaki, C. (2017). "Zn^{2+}, Fe^{2+}, Cu^{2+}, Mn^{2+}, H^{+} Ion-exchanged and raw clinoptilolite zeolite catalytic performance in the Propane-SCR-NOx process: A comparative study." *International Journal of Chemical Reactor Engineering*, 16, 20160192.

Guo, X., Zeng, L., Li, X., and Park, H.-S. (2008). "Ammonium and potassium removal for anaerobically digested wastewater using natural clinoptilolite followed by membrane pretreatment." *Journal of Hazardous Materials*, 151, 125–133.

Hach. "Method 8021." Retrieved on September 17, 2021, from https://www.hach.com.

Hach. "Method 8167." Retrieved on September 17, 2021, from https://www.hach.com.

Halling-Sørensen, B., and Jørgensen, S. E. (1993). The *Removal of Nitrogen Compounds from Wastewater*. Elsevier, Amsterdam, Netherlands.

Hankins, N. P., Pliankarom, S., and Hilal, N. (2004). An equilibrium ion-exchange study on the removal of NH_4^+ ion from aqueous effluent using clinoptilolite. *Separation Science and Technology*, 39, 3639–3663.

Harland, C. E. (1994). Ion Exchange: Theory and Practice. 2nd ed. Royal Society of Chemistry, Cambridge, UK.

Hedström, A. (2001). "Ion exchange of ammonium in zeolites: a literature review." *Journal of Environmental Engineering*, 127, 673–681.

Huang, H., Yang, L., Xue, Q., Liu, J., Hou, L., and Ding, L. (2015). "Removal of ammonium from swine wastewater by zeolite combined with chlorination for regeneration." *Journal of Environmental Management*, 160, 333–341.

Jama, M. A., and Yücel, H. (1989). "Equilibrium studies of sodium-ammonium, potassium-ammonium, and calcium-ammonium exchanges on clinoptilolite zeolite." *Separation Science and Technology*, 24, 1393–1416.

Jorgensen, T. C., and Weatherley, L. R. (2003). "Ammonia removal from wastewater by ion exchange in the presence of organic contaminants." *Water Research*, 37, 1723–1728.

Lercher, J. A., and Jentys, A. (2007). "Infrared and Raman spectroscopy for characterizing zeolites." Chapter 13 in J. Čejka (Ed.), *Introduction to zeolite science and practice* (3rd rev. ed., pp. 13-38). Elsevier, Amsterdam, Netherlands.

Leyva-Ramos, R., Aguilar-Armenta, G., Gonzalez-Gutierrez, L. V., Guerrero-Coronado, R. M., and Mendoza-Barron, J. (2004). "Ammonia exchange on clinoptilolite from mineral deposits located in Mexico." *Journal of Chemical Technology and Biotechnology*, 79, 651–657.

Loveless, J. E., and Painter, H. A. (1968). “The influence of metal ion concentrations and pH value on the growth of a Nitrosomonas strain isolated from activated sludge.” *The Journal of General Microbiology,* 52, 1-14

Luther, A. K. (2015). *Ammonia Toxicity in Bacteria and Its Implications for Treatment of and Resource Recovery from Highly Nitrogenous Organic Wastes* (Order No. 10019315). [Doctoral dissertation, The State University of New Jersey]. ProQuest Dissertations and Theses Global.

McCusker, L. B., and Baerlocher, C. (2007). “Zeolite structure.” Chapter 2 in J. Čejka (Ed.), *Introduction to zeolite science and practice* (3rd rev. ed., pp. 13-38). Elsevier, Amsterdam.

Milan, Z., Sánchez, E., Weiland, P., de Las Pozas, C., Borja, R., Mayari, R., and Rovirosa, N. (1997). “Ammonia removal from anaerobically treated piggery manure by ion exchange in columns packed with homoionic zeolite.” *Chemical Engineering Journal*, 66, 65–71.

Minister of Fisheries and Oceans of Canada. (2012). *Metal and Diamond Mining Effluent Regulations (SOR/2002-222)*. https://laws-lois.justice.gc.ca/eng/Regulations/SOR-2002-222/index.html

Mintova, S., and Čejka, J. (2007). “Micro/mesoporous composites.” Chapter 9 in J. Čejka (Ed.), *Introduction to zeolite science and practice* (3rd rev. ed., pp. 301-326). Elsevier, Amsterdam, Netherlands.

Mozgawa, W. (2000). “The influence of some heavy metals cations on the FTIR spectra of zeolites.” *Journal of Molecular Structure*, 555, 299–304.

Pommen, L.W. (1983). *The Effect on Water Quality of Explosives Use in Surface Mining. Volume 1: Nitrogen Sources, Water Quality, and Prediction and Management of Impacts.* Ministry of Environment Technical Report 4, Ministry of Environment, Water Management Branch, Victoria: B.C..

Rahmani, A., Mahvi, A., Mesdaghinia, A., and Nasseri, S. (2004). “Investigation of ammonia removal from polluted waters by Clinoptilolite zeolite.” *International Journal of Environmental Science and Technology (Tehran)*, *1,* 125–133.

ResinTech Inc. (2020). “Resintech SIR-600.” Retrieved on May 15, 2021, from https://www.resintech.com/rks_images/shopcart/pdf_specs_90253.pdf

Sarioglu, M. (2005). “Removal of ammonium from municipal wastewater using natural Turkish (Dogantepe) zeolite.” *Separation and Purification Technology*, 41, 1–11.

Sprynskyy, M., Lebedynets, M., Terzyk, A. P., Kowalczyk, P., Namieśnik, J., and Buszewski, B. (2005). “Ammonium sorption from aqueous solutions by the natural zeolite Transcarpathian clinoptilolite studied under dynamic conditions.” Journal of Colloid and Interface Science, 284, 408–415.

Stensel, H., McDowell, C., and Ritter, E. (1976). “An automated biological nitrification toxicity test.” *Journal of Water Pollution Control Federation*, 48, 2343-2350.

Stone, R. W. (1978). *Full-Scale Demonstration of Nitrogen Removal by Breakpoint Chlorination*. Environmental Protection Agency, Office of Research and Development, Municipal Environmental Research Laboratory, Ohio. Access by the National Technical Information Service. https://nepis.epa.gov/Exe/ZyPURL.cgi?Dockey=9101XG1X.txt.

Suter, G., II, Latimer, H., Bowersox, M., Schofield, K., and Cormier, S. (2021). *Ammonia.* Retrieved on April 13, 2021, from https://www.epa.gov/caddis-vol2/ammonia#:~:text=Ammonia%20also%20exerts%20a%20biochemical,ammonia%20into%20nitrite%20and%20nitrate.

Thommes, M., Kaneko, K., Neimark, A.V., Olivier, J.P., Rodriguez-Reinoso, F., Rouquerol, J., and Sing, K.S.W. (2015). "Physisorption of gases, with special reference to the evaluation of surface area and pore size distribution (IUPAC Technical Report)." *Pure and Applied Chemistry*, 87, 1051-1069.

United States Environmental Protection Agency. (2000). *Wastewater Technology Fact Sheet Ammonia Stripping, USEPA 832-F-00-019*. Washington, D.C.

Zhang, W., Zhou, Z., An, Y., Du, S., Ruan, D., Zhao, C., Ren, N., and Tian, X. (2017). "Optimization for zeolite regeneration and nitrogen removal performance of a hypochlorite-chloride regenerant." *Chemosphere*, 178, 565–572.

Chapter 5 Assessing the Feasibility and Performance of Chlorine Regeneration of Bench-scale Zeolite Column for Ammonia Removal from Explosives Impacted Mining Wastewater

Abstract

There has only been limited research on ammonia removal by zeolites followed by chlorine regeneration; these used batch tests. To better simulate full-scale applications, this study used a continuous flow through ion exchange column system to assess the feasibility of chlorine regeneration of a zeolite for the removal of ammonia from a synthetic explosives impacted mining wastewater (EIMWW). Multi-cycle column loading-regeneration tests were used to evaluate and compare the performance using a NaOCl (1000 ppm as free Cl_2) solution with that using a standard salt regeneration. In addition, the impact of two loading cycle durations were evaluated. The 23-hr loading cycles yielded higher total ammonia nitrogen (TAN) uptakes (0.38 meq/g) per cycle, however the 6-hour loading duration experiments had a higher cumulative TAN uptake (~0.8 meq/g) per 23 hr. After three operational cycles, the TAN uptake after NaOCl regeneration were almost the same as those obtained with salt regeneration (0.21 meq/g Vs. 0.21 meq/g). Compared to NaCl regenerated SIR-600, NaOCl regenerated SIR-600 showed a higher preference for TAN (total ammonia nitrogen) over Ca and K, however the NaOCl regeneration took longer to complete. It is also found that effluent pH, total chlorine level, and free chlorine level during the chlorine regeneration were positively

related, seemingly confirming that the ammonia is oxidized to nitrogen gas and producing hydrogen ions.

Key words: column, zeolite, ammonia removal, chlorine regeneration

5.1 Introduction

Due to the extensive use of ammonia nitrate explosives in the mining industry, mining wastewaters are a significant source of ammonia pollution in aquatic environments (Forsyth et al., 1995; Chartrand et al., 2020). Pommen (1983) reported that explosive impacted mining wastewater (EIMWW) had total ammonia nitrogen (TAN) concentrations in the 0.3 to 80 mg as N/L range. NH_3 is highly toxic to aquatic organisms (Randall and Tsui, 2002; Canadian Council of Ministers of the Environment, 2010; Souza-Bastos et al., 2017; Kleinhenz et al., 2018). To avoid such toxicity, Canadian Council of Ministers of the Environment. (2010) advises the NH_3 levels in freshwater bodies should be below 0.019 mg N/L. This upper ammonia level is used to determine the maximum wastewater effluent ammonia concentrations to avoid toxic effects. In Canada, the wastewater effluents from mining sites should not be acutely lethal corresponding to Metal and Diamond Mining Effluent Regulations (SOR/2002-222) under Fisheries Act (Minister of Fisheries and Oceans of Canada, 2012). In addition, the threshold acute lethal (i.e., 50% rainbow trout lethality in 96 hours tested with Reference Method EPS 1/RM/13) for wastewater effluents was reached when ammonia concentrations were as low as 2 mg TAN as N /L (Environment Canada, 2004; Environmental Technology Center of Canada and Environmental Canada, 2000).

The potential approaches for ammonia removal from aqueous phase include biological nitrification/denitrification, breakpoint chlorination, air stripping, and ion-exchange (Stone, 1978; Halling-Sørensen and Jørgensen, 1993; United States Environmental Protection Agency, 2000; Rahmani et al., 2004; Ding and Sartaj, 2015; Chartrand, 2018). Biological nitrification/denitrification is the most broadly applied ammonia removal method in municipal and industrial wastewater treatment. Nevertheless, biological treatment is not particularly suitable in the treatment of mining wastewaters in some situations because of its low-temperature sensitivity, operational complexity, the toxicity of heavy metals, the toxicity of some organic substance, and the toxicity of high concentration of ammonia (Loveless and Painter, 1968; Stensel et al., 1976, Luther et al., 2015; Jorgensen and Weatherley, 2003). In comparison, ion-exchange is a promising method for the treatment of mining wastewater considering its simplicity of in-site operation without those shortcomings mentioned above for biological treatment systems.

Cationic ion-exchangers are able to practically adsorb ammonium (NH_4^+) which is the major form of the ammonia at near neutral pH levels. Zeolite, as a cationic ion exchanger, has been widely researched for TAN removal because of its good TAN removal capacity, low price, and high availability in nature. However, many of these studies used single-solute ammonia solutions, while practical application involve wastewater with many ions that compete for ion exchange sites. Clinoptilolite, a common type of zeolite, was studied by Ames (1960) who found through multiple column tests that ammonia is somewhat preferred over some major exchanged cations including some divalent ions (Hedström,

2001; Sarioglu, 2005). The cation preference order of clinoptilolite is presented below (Ames, 1960; Hedström, 2001; Sarioglu, 2005):

$$Cs^{+}>Rb^{+}>K^{+}>NH_4^{+}>Ba^{2+}>Na^{+}>Ca^{2+}>Fe^{2+}>Al^{3+}>Mg^{2+}>Li^{+} \quad \text{(eq. 5.1)}$$

Other studies also verified the ammonium's position in preference sequence (Jama and Yücel, 1989; Rahmani et al., 2004; Leyva-Ramos et al., 2004; Guo et al., 2008). Based on the preference sequence, this potassium outcompetes ammonia which is preferred over calcium. Hence, it may be less effective to utilize clinoptilolite for ammonia removal in wastewater than when treating single-solute ammonia solutions because of competition with potassium (Chartrand, 2018).

To restore the uptake capacity of ion exchanger, the zeolite should be regenerated frequently. 2 to 10% NaCl solutions are usually the standard regenerant for zeolites (Dryden and Weatherley, 1989; Rahmani et al., 2004; Chartrand, 2018, ResinTech Inc, 2020). The used regeneration solution will contain highly concentrated TAN and NaCl so it cannot be released without treatment. However, it is not practical to recycle the regeneration solution for the next regeneration without eliminating a significant portion of the NH_4-N from it. Therefore, the treatment of used regeneration solutions becomes an environmental challenge. Thus, a different regeneration method is needed.

The regeneration using hypochlorite solution to chlorinate the ammonia-loaded zeolite is one such approach. This method which has been studied by Huang et al. (2015) and Zhang et al. (2017). These authors claimed that the ammonia nitrogen could be converted to N_2 through chlorination, thus the ammonia is removed from the regeneration solution and

thus prevents the above-mentioned secondary pollution. And they suggested it occurred by the following chemical reaction (Huang et al., 2015; Zhang et al., 2017):

$$2NH_4^+ + 3ClO^- + 2OH^- \rightarrow N_2 \uparrow + 3Cl^- + 5H_2O \qquad \text{(eq. 5.2)}$$

Huang et al. (2015) reported that this approach was successful in regenerating a zeolite using batch mode operation. Zhang et al. (2017) also evaluated the effectiveness of hypochlorite application in zeolite regeneration and suggested that the use of a combined NaClO-NaCl regeneration could reach the optimal regeneration effect. However, a combined NaOCl and NaCl regenerant is not so practical because eventually the used regenerant will have to be disposed, whose high salt concentration is a trouble. Zhang et al. (2017) only studied the regeneration of a zeolite loaded with a single-solute ammonia solution. Huang et al. (2015) used a multi-ion synthetic swine wastewater; however, they did not thoroughly study the removal of the other ions. In addition, the standard ion-exchange systems consist of continuous flow column systems and both these studies evaluated the regeneration efficiency in batch mode. Due to competitive ion uptake effects, limited flow contact time with the media, and possibly different ion diffusion rates, the ion preference for column systems may be different from that for batch (equilibrium) systems (Chartrand et al. 2020). A potential difficulty of the NaOCl regeneration method is that the regeneration of ion exchange sites containing other ions, such as calcium and potassium, is likely going to be limited, as shown in Chapter 4. This may reduce the number of sites available for TAN resulting in a reduction in the TAN uptake.

In this study, the feasibility of NaOCl regeneration of a zeolite was assessed for more realistic conditions, that is by conducting multiple loading and regeneration cycles using a continuous flow column to treat a multi-ion solution (TAN, calcium, and potassium). For comparison experiments were also performed using a 5% NaCl regeneration solution, which is a standard regenerant.

5.2 Experimental Materials and Methods

A commercial zeolite (SIR-600, ResinTech Inc, Candem, NJ) was used for this study because it performed well for TAN uptake in an earlier study (Chartrand et al., 2020). SIR-600 is regarded as clinoptilolite due to its order of selectivity is almost identical to that of clinoptilolite (Ames, 1960; ResinTech Inc., 2020).

The loading experiments were conducted using a synthetic EIMWW wastewater. It was prepared with ammonium chloride, potassium chloride and calcium chloride hexahydrate (ACS grade, Fisher Scientific, Waltham, MA). The synthetic wastewater had approximately 21 mg TAN as N/L, 30 mg K/L, and 80 mg Ca/L (1.5 meq/L, 0.77meq/L, and 4 meq/L, respectively) according to the recommendation of the research partner from Dowclear Inc. (Downey, 2018).

Two main regenerant solutions were used in this study, a NaCl solution and a NaOCl solution. The 5% NaCl regenerant was prepared by dissolving solid NaCl (ACS grade, Fisher Scientific, Waltham, MA) in distilled water. The 5% NaCl solution was selected due to the recommendation of the zeolite supplier and the fact that a previous study indicated this regenerant was efficient for SIR-600 regeneration (Chartrand et al., 2020). The NaOCl

regeneration solution was obtained by the dilution of a commercial bleach. The 1000 mg free Cl_2/L solution was chosen because it provides a sufficient quantity of chlorine required to oxidize TAN on the zeolite (i.e., Cl_2:N mass ratio >8).

The column experiments were primarily intended to compare the multiple-cycle performance of the two regenerants. The ion uptake of zeolite in the next cycle was calculated to evaluate the effectiveness of the regenerant.

5.2.1 Analytical Methods

Total ammonia nitrogen (TAN) concentration was quantified using Nessler method which was adapted from Standard Method 4500-NH_3 C (American Public Health Association, 1992). The Ca and K ion concentrations were quantified using a procedure adapted from Standard Method 3111B (American Public Health Association, 2017). The Ca and K ion concentrations were both analyzed using a flame atomic absorption spectrometer (AAS) (PinAAcle 500, PerkinElmer, Waltham, MA, United States). Free and total chlorine concentrations were measured using Hach method 8021 and 8167 (equivalent to Standard Method 4500-Cl G for drinking water) (American Public Health Association, 2017). pH values were analyzed with a pH meter (VER Symphony B10P, VWR, Radnor, PA) with a pH probe (VWR 89231-580, VWR, Radnor, PA)

5.2.2 Experimental Methods

5.2.2.1 Column tests with NaCl regeneration

Column studies were conducted since continuous column operation is the most common type of treatment scheme for IE systems. In addition, the loadings achieved in IE columns

are somewhat different from that in batch tests, particularly because of the competition between ions, the flow-IE bed contact time, and the column dynamics (Chartrand et al., 2020). The loadings are also impacted by the breakthrough level to which the column is operated (Chartrand et al., 2020). This part of the study uses a 5% NaCl solution for the regeneration because this is standard regeneration method, these tests were conducted to develop a baseline for comparison with regeneration using chlorine solutions.

Bench-scale continuous flow column studies were conducted to assess SIR-600's performance in the column. A clear glass column with 2.2 cm inner diameter (ID) and 110 cm length was used for these tests. 96.1 g SIR-600 were loaded into the column which resulted in an IE bed depth of 30.5 cm and a bed volume of 116 cm^3. A coarse sintered glass disc integrated into the column supported the IE materials. A stopcock at the bottom of the column was used to stop the flow from the column when needed.

The performance of the IE system was evaluated using multiple-cycles to approximate the long term performance of the system. Each cycle of column test is divided into two parts: a loading phase and a regeneration phase. In the loading phase, the applied EIMWW solution was passed through the SIR-600 bed in the down-flow direction. The flowrate of loading solution was maintained at approximately 50ml/min by a high-pressure liquid metering pump (Optos Model3, Eldex, Napa, CA). The effluent flowrate was occasionally monitored by weighing the mass of effluent collected over one minute, and the pump setting was adjusted if it was necessary. Two main sets of tests were performed to study the feasibility of the loading-regeneration cycles with different durations. The first set of tests, called salt-long-loading (SLL) cycle tests, had 23-hour long loading phases. They are

denoted as SLL#, where # denotes the number of the cycle. The second set, named as salt-short-loading (SSL) cycles, had 6-hour long loading phases. They are denoted as SSL#, where # denotes the number of the cycle. Two SLL cycles were performed followed by three SSL cycles. In both these cases, the same synthetic EIMWW was used as the influent and the effluent TAN, Ca and K concentrations were monitored at regular intervals.

The ion uptake of the SIR-600 column in the loading phase can be calculated using an integral mass balance of the ion, the resulting equation is:

$$q = \frac{\int_{V=0}^{V=loading\ phase\ end} (C_{inf} - C_{eff}) dV}{M} \qquad \text{(eq. 5.3)}$$

Where q is the ion uptake of the SIR-600 (meq/g), V is the volume of liquid treated (L) which changes with time; C_{inf} is the influent ion concentration (meq/L); C_{eff} is the effluent ion concentration (meq/L) which changes with volume (V) and time; M is the mass of SIR-600 (g) in the column.

During the regeneration phases the regeneration solution was also circulated in the down-flow mode. During the 5% NaCl regeneration phases, the regenerant flowrate was maintained at approximately 16 ml/min using a peristaltic pump (Masterflex L/S variable-speed economy drive, Cole-Parmer, Vernon Hills, IL). A different pump was used for the regeneration phase to prevent potential corrosion of the expensive high pressure liquid metering pump used for the loading phase. For the SLL cycle tests, the 23-hour loading

phases plus a 3-hour regeneration phase was performed between two loading phases; And for the SSL, the three 6-hour loading phase were followed by 1-hour regeneration phases.

5.2.2.2 Column test with hypochlorite regeneration

As mentioned earlier, hypochlorite regeneration in a continuous-flow column system is part of the novelty of this thesis. The same column and same IE material bed as described in the last section were used in this set of experiments. The loading phase of column tests with hypochlorite regeneration was the same as that of column tests with NaCl regeneration, i.e., they lasted 6 hours or 23 hours and used a flowrate of approximately 50 mL/min. The subsequent regeneration process used 1000 ppm (as free Cl_2) hypochlorite solution which was prepared using commercial bleach. After the 23-hour load phase, the regeneration flowrate was initially selected at 50 ml per min, however this led to the formation of many bubbles within the column, they in turn, constrained the flow and made the flowrate unstable. Accordingly, the average regenerant flowrate was reduced to 20 mL/min, monitored regularly, and adjusted if necessary. After the 6-hour loading phase, the average regenerant flowrate was approximately 16 ml/min.

The experiments were divided into two groups based on the loading-regeneration cycle durations. The first series of tests was called chlorine-long-loading (CLL) cycle tests; they consisted of two 23-hour loading phases plus one 3.4-hour regeneration phase between the two loading phases. They are denoted as CLL#, where # denotes the number of the cycle. The purpose of the CLL runs was to compare directly with the same duration loading phases that were followed by a 5% NaCl regeneration (SLL). The second set of tests was

named chlorine-short-loading (CSL) cycle tests, they included three cycles of 6-hour loading phases followed by 4-hour regeneration phases. They are denoted as CSL#, where # denotes the number of the cycle. Again, the goal was to be able to compare the performance of the column to that of a similarly loaded column that used 5% NaCl regeneration (SSL). Before each series of column tests (i.e., CLL and CSL), the zeolite was preconditioned with 5% NaCl solution to ensure the loading performances in the first loading phases of chlorine cycles was equivalent to those of corresponding to those using salt regeneration. The TAN, K, and Ca effluent concentrations were measured afterwards. The ion uptake performance of the SIR-600 column in the loading phase was calculated using eq. 5.3.

5.3 Results and Discussions

5.3.1 Loading Phases of the Cycles with 5% NaCl Regeneration

The impact of using a 5% NaCl regenerant was investigated by multiple column loading-regeneration cycles to establish what TAN uptakes could be expected using a standard regeneration approach.

The ion loading breakthrough curves of two SLL cycles are presented in Figure 5-1. The most important observations from the Figure 5-1 are as follows. First, the loading breakthrough curves of two cycles almost coincided with each other. This implies that ion uptakes for the same ion species were almost identical in the two loading phases. Thus, the 3hr-long 5% NaCl regeneration was effective in restoring the ion exchange capacity of the zeolite. At the end point of the column runs, the effluent Ca and TAN concentrations

approached those in the influent but that was not the case for the K concentrations. That was why this series of tests was also referred to as “pseudo-saturation” runs. The ion uptakes calculated by eq.5.3 are presented in Figure 5-2, as expected from the very similar breakthrough curve, the ion uptakes achieved in both cycles were very similar as well. The order of the ion uptakes (meq/g) in one loading phase was Ca >TAN> K. This order is the same as that of the ion concentrations in the loading solution. Thus, as expected, the ion concentrations (in meq/L) in the feed solution can positively impact the ion uptake in the column loading process when 5% NaCl was applied.

Figure 5-3 illustrates the impact of the column kinetics on the cumulative ion uptake ratio in loading phase of the second SLL cycle. As is observed, the Ca:TAN ion uptake ratio decreased from 2.7:1 at 51 BVs to 1.8:1 at 586 BVs, which means Ca became less and less preferable to be absorbed over TAN in IE column during the loading phase. The same trend is also observed for TAN:K uptake ratio which decreased from 2.0:1 at 51 BVs to 1.3:1 at 586 BVs. This TAN:K uptake ratio change marks the preference on the uptake of TAN over K was gradually reduced during the 23-hour loading phase. Thus, shorter loading phases should be more favorable for TAN removal. Furthermore, the column run duration or breakthrough concentration selected are critical to column performance in terms of the q_{TAN}/q_K ratios achieved. This is consistent with the findings of Chartrand et al (2020).

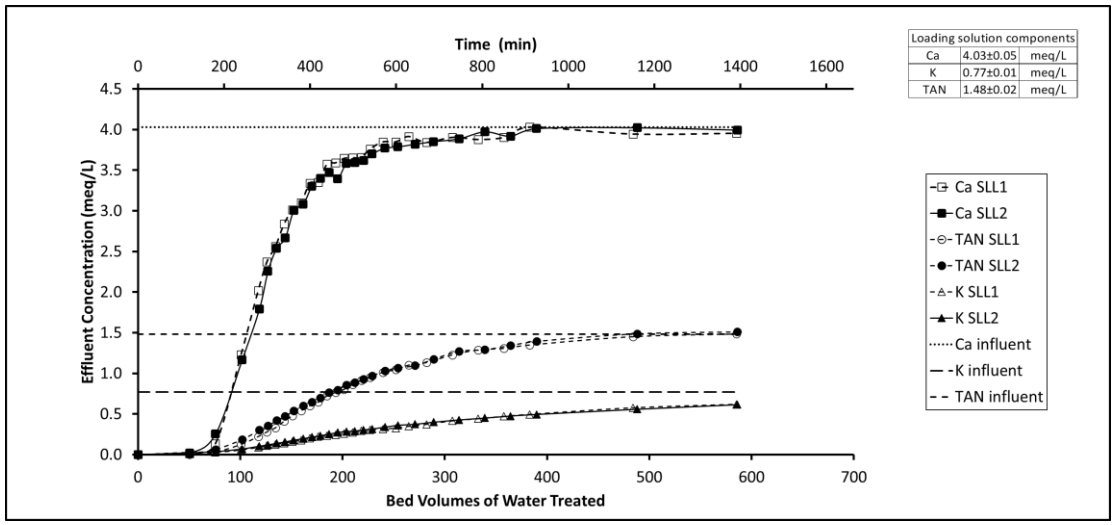

Figure 5-1 Ion breakthrough curves for the SIR-600 column's SLL cycles

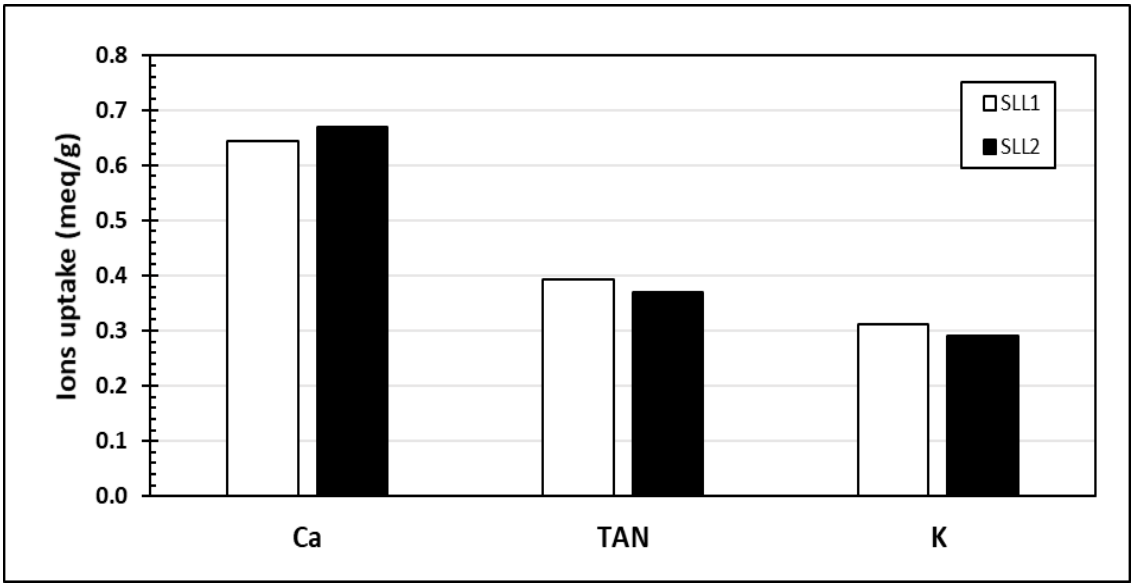

Figure 5-2 Ion uptakes for the SIR-600 column's SLL loading phases

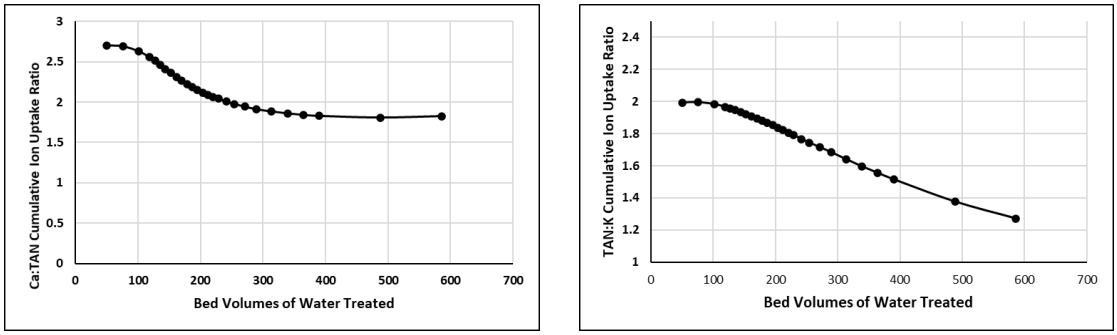

Figure 5-3 cumulative Ca:TAN uptake ratio in the loading phase of the SLL2 cycle (left); cumulative TAN:K uptake ratio in the loading phase of the SLL2 cycle (right)

Chapter 4 conducted batch (equilibrium) tests with 120 ml of the same EIMWW solution and 0.24 g SIR-600 using 5% NaCl regeneration. The ion uptake was relatively stable by the final cycle (5^{th} cycle) of the batch test is selected for comparison. As evident from Figure 5-2 the total TAN uptake of SIR-600 in the loading phase of the 2^{nd} SLL cycle is 0.37 meq/g which is approximately 20% higher than that in the 5^{th} cycle in the batch tests. Higher Ca and K uptakes were also detected in the loading phase of the 2^{nd} SLL cycle compared to those in the 5^{th} cycle of the batch test. This can be explained by the fact that the equilibrium liquid phase concentrations during the batch tests are lower than those in the EIMWW, while the loadings in the column tend towards to saturation (i.e., the loadings that are in equilibrium with the EIMWW).

Chartrand et al. (2020) conducted bench-scale column loading tests using SIR-600 with 10% NaCl for the treatment of a different multi-component EIMWW. Their EIMWW had higher TAN concentrations (3.87meq/L). After treating 2305 ml (50 bed volumes) EIMWW, the column's TAN uptake was 0.24 meq/g when the effluent concentration reached 0.55 meq TAN/L ($C_{effluent}/C_{influent}$=0.14). In the loading phase of the SLL2 cycle, the SIR-600

column reached the same level of TAN uptake after treating 16566 ml (143 bed volumes) feeding solution; and the SIR-600 reached the same TAN $C_{effluent}/C_{influent}$ ratio after treating approximately 11722 - 13660 ml (102 -119 bed volumes) feeding solution resulting in a TAN uptake in the range of 0.18-0.20 meq/g. To reach the same level of total TAN uptake, the IE column required 2.8 times the bed volumes of feeding water that required in the study of Chartrand (2020). To reach the same TAN $C_{effluent}/C_{influent}$ ratio, the IE column required 2.04-2.38 times the bed volumes of feeding water that required in the study of Chartrand (2020). This differences in the bed volumes treated between two studies may be due to that fact that the EIMWW used by Chartrand et al (2020) contained 2.6 times as much TAN as the feeding waster contained in this study. So, it seems that the TAN-loading performances of the IE columns were very close in both studies.

However, the Ca:TAN:K concentration (in meq/L) ratio in the loading solution was 5.2:2.0:1 which differed with that of ions uptakes (in meq/g) at the end of SLL1 loading phase (2.1:1.3:1) or SLL2 loading phase (2.3:1.3:1).The difference between uptake ratios can be explained by the fact that the ion preference order is $K>NH_4^+>Ca$ (Ames, 1960). This preference may render the relatively higher proportion of K uptake in the total uptake compared to the proportion of K in the constituents of feeding water.

SSL cycles (6h loading + 1 hour regeneration) were conducted to assess the performance of the SIR-600 column with shorter loading and regeneration time. Figure 5-4 shows the TAN breakthrough curves of the three loading SSL cycles; the breakthroughs of the succeeding cycles occur progressively earlier. Thus, there was a decreasing trend of TAN uptake throughout the loading phases of three cycles with 5% NaCl regeneration.

However, the difference in the TAN breakthroughs of the second and third SSL cycle are relatively small. This could be the result of insufficient regeneration during the one-hour regeneration phase duration. However, this SSL duration was selected to exceed the regeneration phase duration to loading phase duration ratio of the earlier 23hr loading phase in a SLL cycle tests that yielded a very efficient regeneration. Based on the TAN breakthrough trend with subsequent cycles the third SSL cycle should be the most representative of the long-term performance.

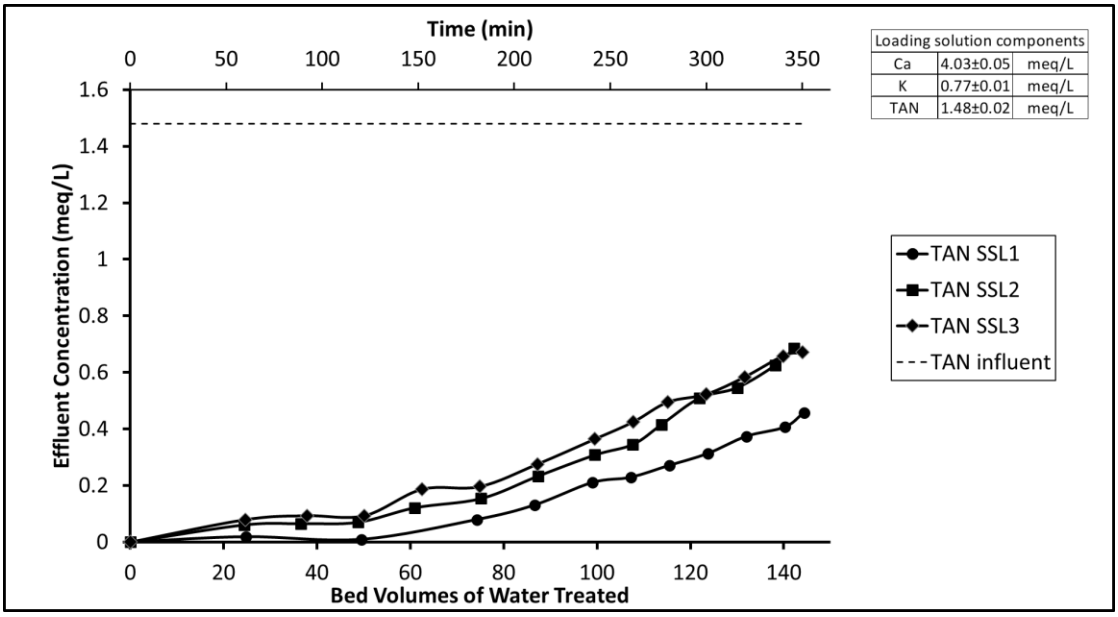

Figure 5-4 TAN breakthrough curves for the SIR-600 column's loading phases of 3 SSL cycles.

The SSL3 cycle's loading-phase breakthrough curves of the three ions were plotted in Figure 5-5. At the end point of the third loading phase, the effluent concentrations of Ca, TAN, and K were respectively 75%, 46% and 34% of the influent concentration of those three types of ions. Thus, it shows none of the three types of ions reached the saturation

state in SIR-600 column at the end of the loading phase, this is due to the short loading duration.

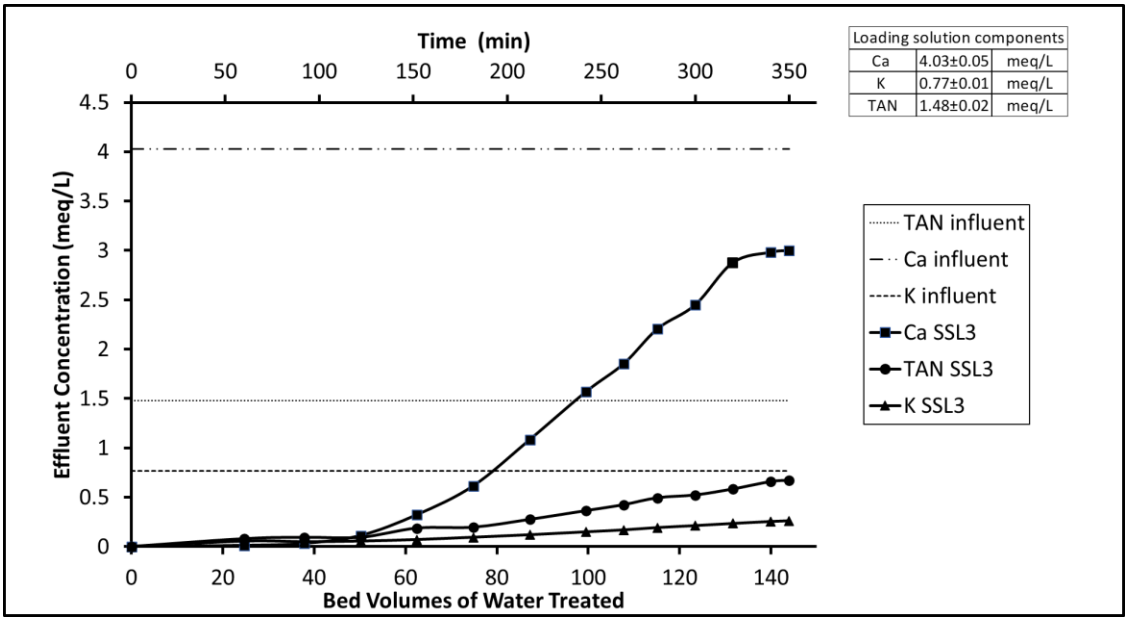

Figure 5-5 Ion breakthrough curves for the SIR-600 column's SSL3 loading phase

The uptakes of TAN, K, and Ca during the three SSL cycles are presented in Figure 5-6. It can be observed that the uptake of three ions declined over the three cycles. The most significant uptake reduction was for Ca^{2+}, which decreased from 0.60 meq/g in SSL1 to 0.52 meq/g in SSL3 (~13% reduction). K^{+} and TAN uptake decreased by approximately 4% and 10%, respectively. These changes were attributed to the re-equilibration of the system to the shorter duration loading phases. As mentioned above, the declines of ion uptake through cycles could be owing to insufficient regeneration duration in each cycle.

Similar to the result in SLL cycles, the ion uptake order (from high to low) in terms of meq/g was Ca>TAN>K. This order was the same as the ion concentration order in the loading solution. The ratio of Ca:TAN:K uptake (meq/g) in the SSL3 loading phase is 4.5:1.8:1, which is close to the Ca:TAN:K concentration (in meq/L) ratio in the loading solution (5.2:1.9:1). Comparing the result of loadings in SLL cycles, the ion uptake ratios in SSL loadings were presumably more related to the ion concentration ratio in the loading solution.

The variation of cumulative ions uptake ratios with time in the loading phase of the third SSL cycle is presented in Figure 5-7. It should be noted that the Ca:TAN and TAN:K cumulative uptake ratio decreased with bed volumes of treated water. Ca:TAN ratio decreased from 2.8:1 at 25 BVs to 2.5:1 at 144 BVs; TAN:K ratio decreased from 1.9:1 at 25 BVs to 1.8:1 at 144 BVs. Comparing to the ion uptake ratio change in the SLL cycle, the ion uptake ratios (Ca:TAN and TAN:K) didn't decrease significantly during the 6-hour loading phase of the third SSL cycle. This can be explained by the fact that the IE material didn't reach or nearly reach the saturation state for any of the three types of ions in SSL loading phases and the uptake of K was lower and it led to less competition for exchange sites. As the column becomes more saturated, the K exerts more competition on the other ions. It should also be noted that there are different ways of quantifying selectivity. In the above experiments, column yielded larger uptakes for TAN than K, which suggest SIR-600 has a greater preference on TAN with this applied EIMWW. The greater TAN to K uptake ratio for the shorter loading phases indicates that dynamics of the column system impact the preference of TAN over K. This is not consistent with preference order

observed by Ames, however, it should be noted that Ames' work was based on equal meq concentration of the different ions. In addition, the q_{TAN}/q_K ratio greater than one is consistent with the results of Chartrand et al (2020) for their shorter column run (50BV, $C_{TAN\ eff}$ / $C_{TAN\ inf}$ =0.14). They reported a q_{TAN}/q_K ratio of 1.14, which is significantly smaller than the 1.8 observed in this study. The differences are likely linked to the lower K to TAN ratios in the two EIMWWs. Chartrand et al (2020) claimed that the preference was related to the feed concentration.

In the SSL3 loading phase, Ca, TAN and K uptakes are lower than those obtained using the 23 hr loading cycle (SLL2) (22%, 43% and 60% lower, respectively). This is due to the shorter loading duration of SSL3 loading phase compared to that of SLL2 loading phase.

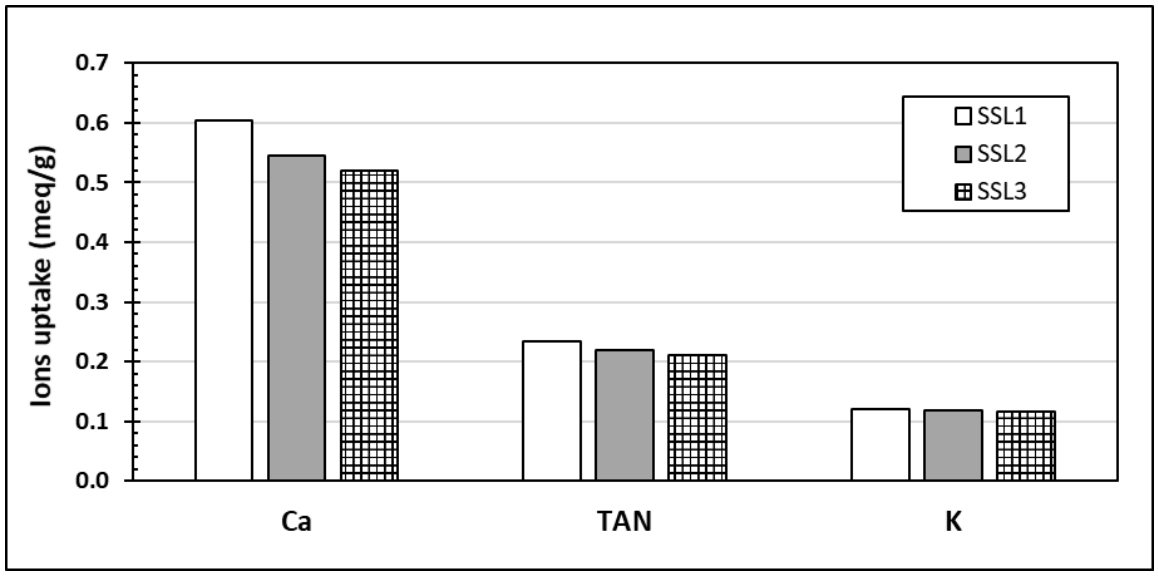

Figure 5-6 Ion uptakes for the SIR-600 column's SSL phases

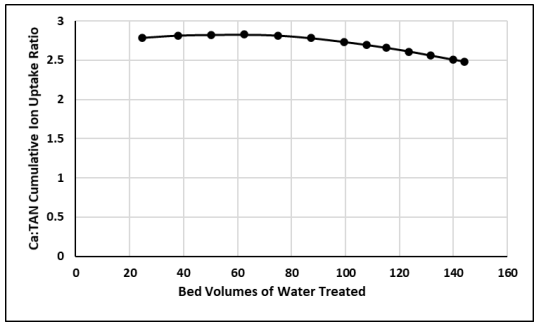

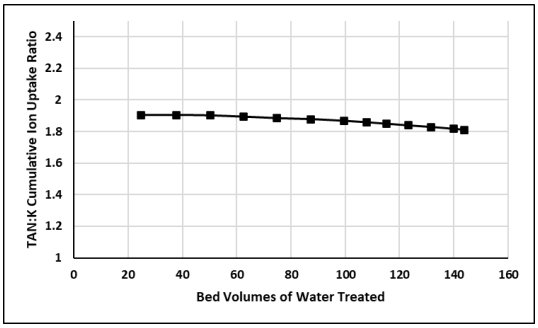

Figure 5-7 Cumulative Ca:TAN uptake ratio in the loading phase of the SSL3 cycle (left); cumulative TAN:K uptake ratio in the loading phase of the SSL3 cycle (right)

As is expected, the 6-hr loading phases accomplished lower ion uptakes than the 23-hr loading phases (i.e., 0.21 me/g TAN versus 0.38 meq TAN/g). However, over a 23-hr period, one could perform 3.83 of the 6 hr loading phases, so over that a 23-hr period of time, the same media would have a total TAN uptake of 0.8 meq TAN/g (i.e., 3.83 x 0.21 meq TAN/g). Accordingly, the short loading phases the SIR-600 would be twice as productive, while using only a slightly larger volume of NaCl regenerant. In addition, in the shorter cycles the TAN uptakes are less impacted by competition with K, as the TAN:K ratio increased from 1.3 to 1.8. Thus, the shorter loading phases seem much more efficient and practical. Considering the ions uptake ratios of 23-hr loading for the purpose of TAN removal, 6-hour loading phase didn't have as a significant decreasing Ca:TAN uptake ratio which marks the lowering preference of Ca over TAN; however, 6-hour loading phase greatly avoid the decreasing TAN:K uptake ratio which occurred in the 23-hour loading.

5.3.2 Loading Phases of the Cycles with Chlorine Regeneration.

To test the feasibility of chlorine (1000 ppm as free Cl_2) regeneration to restore the TAN uptake capacity of a SIR-600 packed column, two series of column tests (CLL and CSL) were performed as with the NaCl regeneration experiments. They were different in loading time and regeneration time (23h loading + 3.4h regeneration and 6h loading+ 4h regeneration). The CLL cycles were conducted first, the duration of the chlorine regeneration phase after CLL1 was approximately the same duration as that used for the SLL tests. The proportionally longer regeneration phases for the CSL cycles of test were chosen to try to have higher regeneration efficiencies than observed during the CLL experiments.

The breakthrough curves of two 23-h loading CLL phases were presented in Figure 5-8. It should be noted that prior to first cycle the column's SIR was regenerated/pre-conditioned with 5% NaCl to verify that the SIR-600 in the column was still performing similarly as it did in earlier experiments. Thus, CLL1 is a run using NaCl regenerated SIR-600, while only CLL2 used chlorine regenerated media. A comparison of the breakthroughs for CLL1 (Figure 5-8) and for SLL1 (Figure 5-1) show that these breakthroughs are similar. For instance, the C_{eff}/C_{in}=0.5 levels for Ca, TAN and K occurred at approximately 122, 193 and 290 bed volumes of water in both CLL1 and SLL1 loading phase. The "rapid increase" in effluent concentrations of the three ions occurred earlier in CLL2 loading curve compared to that in CLL1 loading curve. It may be due to the fact that that prior to CLL1 the SIR-600 was regenerated with 5% NaCl and the insufficient regeneration with NaOCl solution between two CLL cycles. It is also observed that at the

end of the CLL1 run, Ca and TAN reached saturation and K almost reached saturation levels. And during the CLL2 cycle, the column actually reached saturation levels.

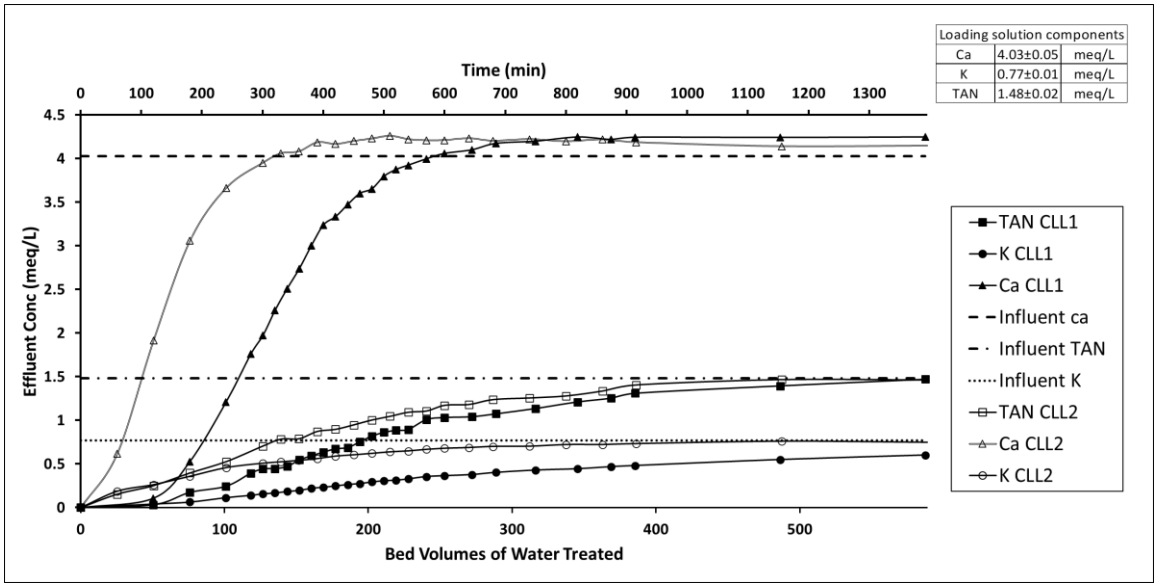

Figure 5-8 Ion breakthrough curves for the SIR-600 column's CLL cycles.

Figure 5-9 summarizes and compares the ion uptake of Ca, K, and TAN in the loading phases of CLL1 and CLL2. As expected from the breakthrough curves, there was a significant decline of uptake of the three key ions from the CLL1 loading phase to the CLL2 loading phase. The calcium uptake dropped by approximately 60% after the NaOCl regeneration, while the potassium and TAN uptakes decreased by 65% and 23%, respectively. Among the three types of ions, TAN had the lowest uptake decline. The declines could be explained by the fact that the chlorine regeneration primarily targets the regeneration of the TAN occupied sites as shown in Chapter 4. The loaded TAN was eluted and oxidized freeing up the ion exchange sites originally loaded with ammonium,

while the regeneration of the Ca and K occupied sites occurred by ion exchange with the limited quantities of Na introduced through the NaOCl solution. It is limited in that the hypochlorite solution introduces approximately 324 mg Na/L (assuming NaOCl is the only Na source in the original bleach) while the salt regeneration solution contains 19,658 mg Na/L. Thus, the much lower Ca and K uptakes in the CLL2 loading phase. Consequently, the chlorine regenerated SIR-600 preferred to uptake TAN over Ca and K in the following loading phase.

As expected since they are essentially repeat experiments, the ion uptake ratio (Ca:TAN:K) in the loading phase of CLL1 (1.8:1.3:1) was very similar to that in the loading phase of SLL1 or SLL2. However, the ion uptake ratio was altered significantly after the 3.4h chlorine regeneration between two loading phases (i.e., CLL2) and came to a new ratio (2.1:2.7:1). It is worth nothing that the TAN accounted for a much higher proportion in the total ion uptake of CLL2 loading phase. This result is consistent with the previous observed result in the batch test with chlorine regeneration in Chapter 4. The batch tests in chapter 4 suggest that during the subsequent loading phase the Ca and K uptake is expected to be achieved by competitive ion exchange onto the site occupied by TAN at the end of the first loading phase. Given that for CLL2 $q_{Ca}+q_{TAN}+q_{K}$ equals approximately 0.64 meq/g and in CLL1 q_{TAN} was approximately 0.39 meq TAN/ g suggests that the sodium in the NaOCl solution had a fairly significant role in the column regeneration.

It could be the result of the reaction occurred between OCl^- in the regenerant and the adsorbed ammonia on the column during the regeneration phase following the CLL1 loading phase. The reaction is described as follows (Zhang et al. 2017):

$$2NH_4^+ + 3ClO^- + 2OH^- \rightarrow N_2 \uparrow + 3Cl^- + 5H_2O \qquad \text{(eq. 5.4)}$$

The equation above (eq.5.4) is equivalent to the overall reaction of breakpoint chlorination (Black and Veatch Corporation, 2010):

$$2NH_4^+ + 3ClO^- \rightarrow N_2 \uparrow + 3Cl^- + 3H_2O + 2H^+ \qquad \text{(eq. 5.5)}$$

The ammonia was oxidized into the nitrogen gas which left the system. The bubbles generated during the regeneration of the SIR-600 bed suggest that this reaction was taking place.

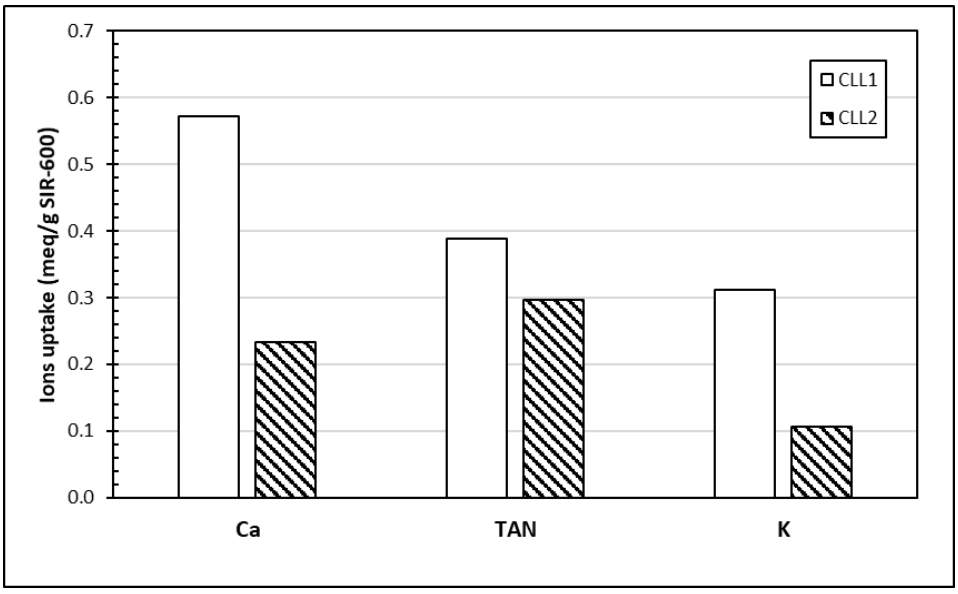

Figure 5-9 Ion uptakes for the SIR-600 column's CLL loading phases

To evaluate the SIR-600 column performance cycles with a shorter loading time and chlorine regeneration time, referred to as CSL cycles, were performed. The 6h loading phases were chosen to be the same as that of the SSL cycles, and the 4 h regeneration phases were chosen because the 3.4 h regeneration phases were not so effective, so proportionally longer regeneration phases were necessary. The three loading-regeneration cycles were performed. To verify the performance of the SIR-600 was unchanged, the SIR-600 was pre-conditioned with 5%NaCl prior to the CSL1 loading phase. At approximately 144 bed volumes of water, the C_{eff}/C_{in} levels for Ca, TAN and K approximately reached 0.49, 0.30, and 0.23 respectively in both CSL1, which are consistent with the values achieved during SSL1. This demonstrates that the performance of the SIR-600 remained essentially the same. The similarity between CSL1 and SSL1 was also confirmed by the uptake and the ion distribution, the Ca:TAN:K ion uptakes (in meq/g) ratios were 4.9:2.0:1 and 5.0:1.9:1 for the CSL1 and SSL1 runs, respectively, and the TAN uptake in SSL1 loading phase is close to that in CSL1 loading phase (0.23 meq/L Vs. 0.24 meq/L). To better approximate field applications, the SIR-600 loaded during second and third CSL cycles (CSL2 and CSL3) the 1000 ppm as free Cl_2 regeneration solution was prepared with the used regeneration solution from the previous regeneration cycle. As there was no used regenerant at that time, during the first the CLL regeneration phase was conducted with freshly prepared NaOCl regenerant (1000 ppm as free Cl_2) in distilled water.

Figure 5-10 shows the loading curves of TAN in three CSL cycles. It can be observed that: first, there was a considerable gap between CSL1 loading curve and CSL2 and CSL3 loading

curves. The breakthrough curves for the CSL2 and CSL3 occurred significantly earlier than that of the CSL1 presumably because of the re-equilibration from the 5% NaCl pre-conditioning to the NaOCl regeneration. However, there was no significant gap between the loading curve of CSL2 and that of CSL3. It shows that the TAN uptake decreased from CSL1 cycle and stabilized in CSL2 and the following CSL3 cycle.

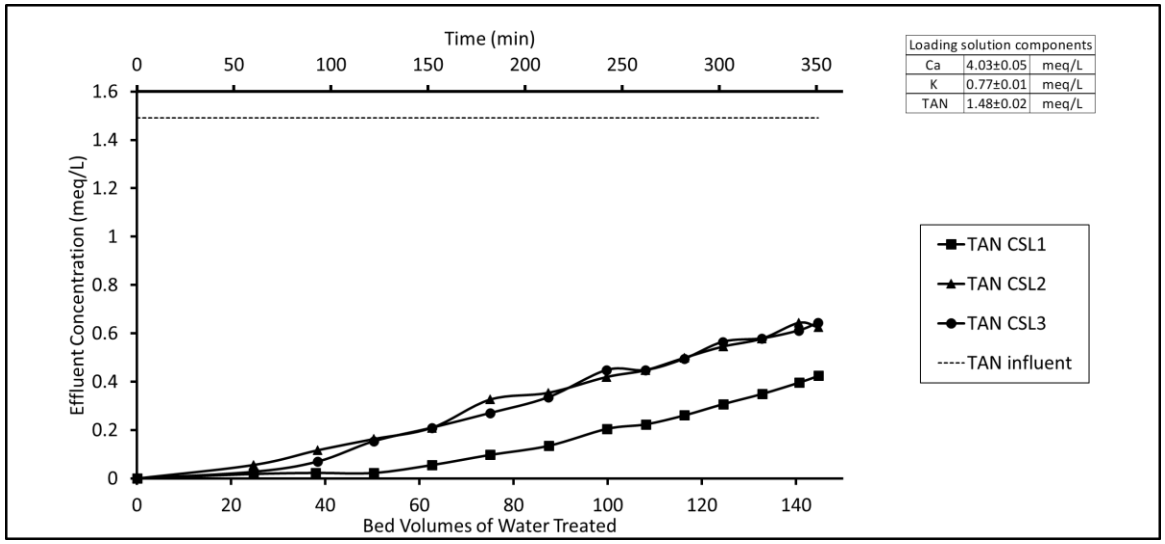

Figure 5-10 TAN breakthrough curves for the three CSL loading phases

Because of this re-equilibration the following discussion will focus on the performance during the third cycle which should be more representative of long-term performance. The Ca, TAN, and K breakthrough curves of cycle CSL3 are presented in Figure 5-11, its main characteristics are as follows. Only Ca concentration of effluent approached that of feed solution by the end of the CSL3 loading phase; the K and TAN concentrations in effluent reached approximately 54% and 43% of the influent concentrations by the end of the CSL3 loading phase. With the comparable total bed volumes at the end of the CSL3 and SSL3 loading phases (145 BV Vs. 144 BV), the ratio between the TAN effluent

concentration and the TAN influent concentration at the end point of the CSL3 loading phase was very close to that of SSL3 loading phase (43% Vs. 45%). This implies that 1000 ppm as Cl_2 regenerations in the CSL cycles performed as well as 5% NaCl did in SSL cycle. However, 1000 ppm as free Cl_2 regenerant did not perform as well as 5% NaCl did in terms of Ca and K uptake regeneration, given Ca and K effluent concentration at the end of the CSL3 loading phase were significantly higher than those at the SSL3 loading phase respectively. This could be explained by the fact that NaOCl regeneration primarily releases the ion-exchange sites occupied by ammonium ions and there was a very low level of cations in chlorine regenerant.

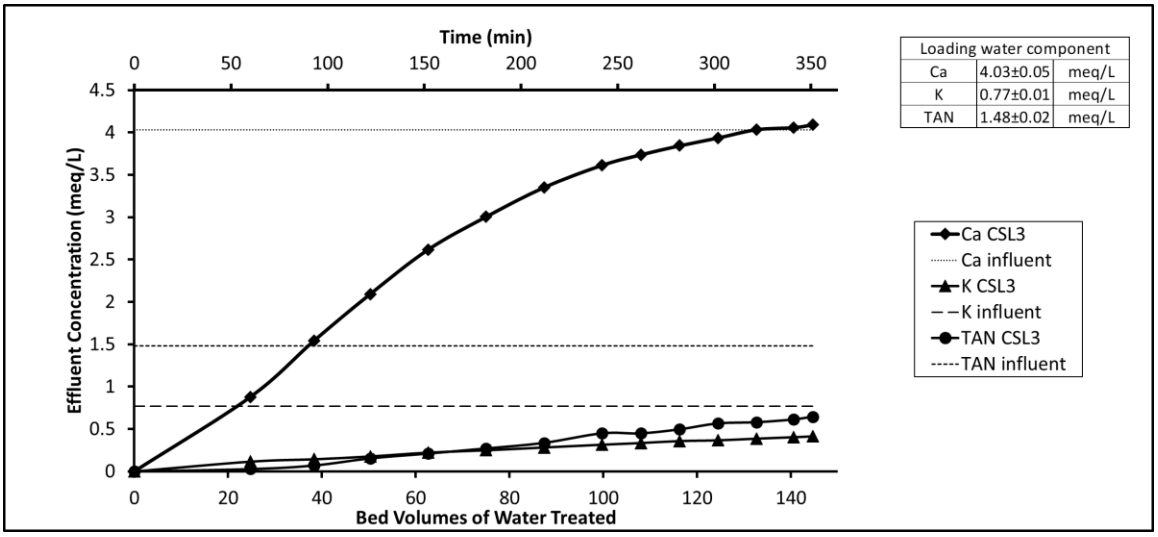

Figure 5-11 Ion breakthrough curves for the loading phase of CSL3 cycle

Figure 5-12 presents the Ca, K, and TAN uptakes of three CSL cycles for comparison. As expected from the K and Ca breakthrough curves discussed above, the K and Ca uptake decreased throughout the three CSL cycles. The TAN uptake decreased by 12% from CSL1 loading phase to CSL3 loading phase. On the other hand, the Ca and K uptakes decreased

by 57% and 24%, respectively. This confirms that the 1000 ppm NaOCl regenerant was only able to efficiently release the IE site occupied by ammonium. The TAN uptake stabilized in CSL2 and CSL3 cycles. Also, The TAN uptake in CSL3 is approximately the same as that in SSL3 (0.21 meq/g Vs. 0.21 meq/g). This is contrast to the 20% reduction observed in the batch tests presented in chapter 4, thus confirming that the results in batch tests are not always transferable to the more practical continuous flow column operation.

As for ion uptake ratio, Ca:TAN:K ion uptake (in meq/g) ratio changed from 4.9:2.0:1 in CSL1 to 2.8:2.3:1 in CSL3, due to the NaOCl's high regeneration effectiveness on TAN uptake over Ca and K uptake. It should be noted that the Ca:TAN:K uptake ratio by the end of the CSL3 loading phase reached 2.8:2.3:1 which is significantly different from that of SSL3 (4.5:1.8:1). In the CSL3 loading phase, the TAN uptake represented a much higher proportion in the total ion uptake. This could be due to a process that NaOCl regeneration primarily regenerates the ion-exchange sites occupied by ammonium ions. However, for CSL3 $q_{Ca}+q_{TAN}+q_{K}$ is approximately 0.56 meq/g which is much larger than original (CSL1) loading (i.e., 0.24 meq/g). This implies that the Na in the NaOCl has a significant role in the column regeneration. In addition, it indicates that this role is much greater in the IE column than in the batch tests presented in chapter.

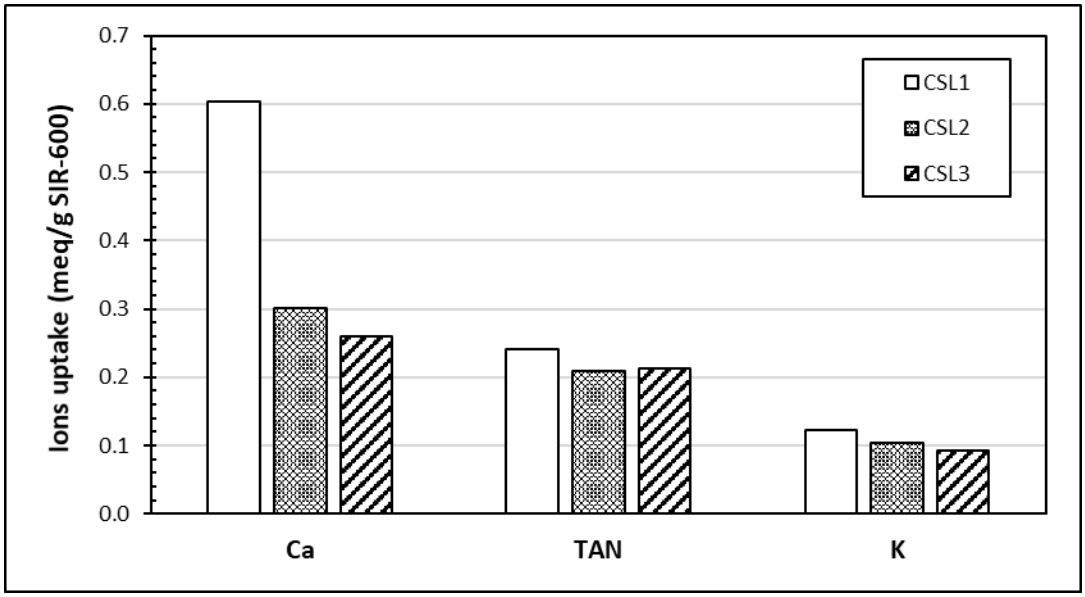

Figure 5-12 Ion uptakes for the SIR-600 column's CSL loading phases

Figure 5-13 presents the variation of cumulative ions uptake ratios with bed volumes of water treated (i.e., time) in the loading phase of the third CSL cycle. As is observed, Ca:TAN cumulative uptake ratio consistently decreased with bed volumes of treated water (e.g., 2.4:1 at 25 BV to 1.2:1 at 144 BV), and the TAN:K ratio increased from 2.1:1 at 25 BV to 2.3:1 at 144 BV. Thus, the relative TAN uptake in CSL3 increased with increasing number of bed volumes treated. It is noted that this is contrast to a decreasing TAN:K ratio in the loading after the 6-hour salt regeneration (i.e., SSL3 in Figure 5-7). Thus, the NaOCl regeneration are more selective of TAN uptake as mentioned above.

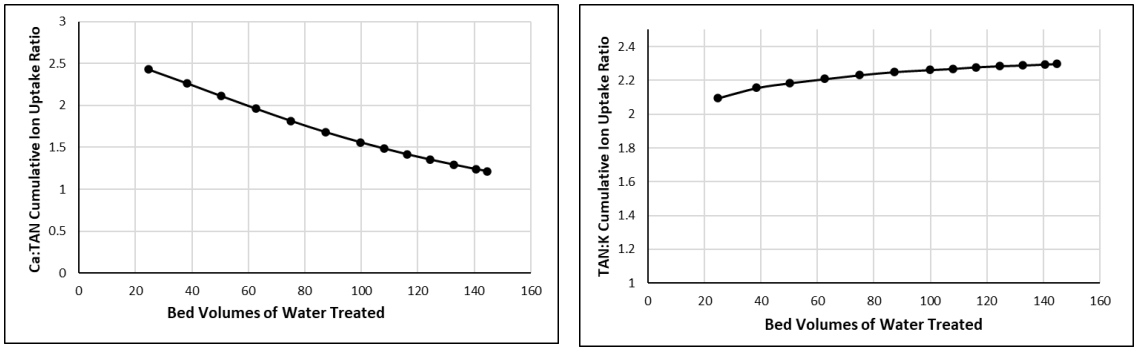

Figure 5-13 Cumulative Ca:TAN uptake ratio in the loading phase of cycle CSL3 (left); cumulative TAN:K uptake ratio in the loading phase of the CSL3 cycle (right)

5.3.3 Chlorine Reactions within the Hypochlorite Regeneration of the Column

The chlorine-ammonia reactions are complex and involve multiple steps and multiple species and is greatly impacted by pH and the Cl_2:N ratio (Black and Veatch Corporation, 2010). The classical reactions state that NH_3 is oxidized to NH_2Cl, $NHCl_2$, and NCl_3, these products are also referred to as combined chlorine. The combined chlorine equals the total chlorine minus the free chlorine. It should be noted that preponderance of the various chloramines is pH and Cl_2:N ratio dependent (Black and Veatch Corporation, 2010). To investigate the mechanisms of the chlorine regeneration process, the pH, the free chlorine, and total chlorine concentrations were measured in the regeneration effluent samples taken at different times during the regeneration phase.

The CSL2 and CSL3 regeneration phases were chosen for study due to the close TAN uptakes in CSL2 and CSL3 loading phases. Figure 5-14 shows the pH values, combined and free chlorine concentrations Vs. bed volumes in the regeneration phases of CSL2 and CSL3 following their loading phases. The major features of Figure 5-14 are as follows. First, the free chlorine levels in both CSL2 and CSL3 cycles followed the same trend, for the initial

16 bed volumes the free chlorine concentrations were much lower (below 20 ppm) than the feed concentration and then increased until they reached approximately 800 ppm at the end of the regeneration process. Thus, at the end of this regeneration phase some of the SIR-600 is still being regenerated as still approximately 20% of the free chlorine is being consumed. Given the effluent free chlorine profile is similar to a breakthrough curve it seems the pattern seems to be due to diffusional limitations. Second, the pH variation Vs. bed volumes of regenerant processed also had the same general trends in the two regeneration phases. The pH dropped to approximately 3 as the regenerant gradually replaced the distilled water present within the column's voids prior to introduction of the NaOCl solution. After that, the pH remained at approximately 3 till about 16 BV of water treated, and increased after that reaching approximately a pH of 8. The trend of pH change with BV increased with the growing free chlorine level. It suggests that the pH is related to the free chlorine level during the chlorine regeneration phase in the column. This pattern is further supported by the occurrence of the above mentioned reaction (eq. 5.5) which generated the H^+ ions and led to the decreased the pH in the solution. In the reaction of eq. 5.5, oxidization of one mole of ammonia into nitrogen gas consumes 1.5 mole ClO^- and generates 1 mole H^+ ion (or consumes 1 mole OH^- equivalently). During the beginning 14 BV of the regeneration process, the free chlorine level remained low (approximately 10 mg free Cl_2/L) which was negligible compared to 1000 mg free Cl_2/L in NaOCl regenerant influent. The fact that not all of the free chlorine reacts (i.e., the effluent concentrations are not zero) indicates that there are mass transfer resistances due to the hydraulics within the column. For the 1000 mg free Cl_2/L NaOCl solution (14.1

mmol OCl^-/L), eq. 5.5 predicts it would generate 9.4 mmol/L H^+. Given the influent regenerant pH was equal to ~9, the 9.4 mmol/L H^+ would be expected to lower the effluent pH to ~2. However, the measurements indicate the actual regeneration effluent pH was generally remained at ~3. The higher actual pH than the theoretical pH was possibly due to the reaction between monochloramine and acid, the reaction of hypochlorite ion and the acid, or even the reaction between the IE material and the acid.

The amount of free chlorine consumed and the amount of oxidized ammonia in CSL3 regeneration phase were compared to further verify the reaction occurred during the chlorine regeneration phase. The CSL3 cycle were chosen due to the fact that the TAN uptake in the loading phase of this cycle were stabilized as observed in Figure 5-12. This implies that the 4-hour chlorine regeneration phase should be effective to remove the TAN uptake in the column during loading phase of the same cycle. It should be noted that the quantity of oxidized ammonia was estimated to be the difference between TAN uptake in the loading phase and the eluted TAN in the following regeneration phase. The free chlorine consumption was approximately 39 mol during the CSL3 regeneration phase, while the amount of the oxidized ammonia was approximately 19 mol in the same regeneration phase. However, according to the stoichiometry of eq. 5.5, the computed free chlorine consumption was expected to be approximately 29 mol which is 26% lower than the measured value. The higher than stoichiometric Cl_2:N ratio may indicate there are other reactions taking place (Black and Veatch, 2010).

It is observed in Figure 5-14 that the combined chlorine curves in the two cycles have the small spike at the beginning of the regeneration phase and then stay relatively constant

at approximately 40-70 mg /L as Cl_2. In contrast, the free chlorine curves were relatively flat up approximately 16 BV. The difference between free chlorine and total chlorine curves, which is small, suggests the formation of some chloramines at the beginning stage during the regeneration process. However, given the fact that the regenerant influent contained certain level of combined chlorine approximately 40 mg/L as Cl_2, the generation of the combined chlorine was inferred to be very limited during the most time of chlorine regeneration phase.

Figure 5-14 also compares effluent regenerant's pH, free chlorine, and total chlorine concentration during the regeneration phase of CSL3. In general, the pH, free chlorine, and total chlorine follow the same trend: relatively low at the start and gradually increasing during the middle of the regeneration phase. It is hypothesized that this is due to the following process: As the hypochlorite solution gradually entered the SIR-600 bed, it is hypothesized that the abundant ammonium absorbed by the IE material in the loading phase was rapidly oxidized into nitrogen gas or other species (e.g., NO_3^-) with limited "nuisance residual" (NH_2Cl, NCl_3, organic chloramines) generated (Black and Veatch Corporation, 2010). H^+ ion generated as a by-product of this reaction, lowered the pH of the effluent. With no doubt, the free chlorine and total chlorine level were at a low level while almost all of the free chlorine was consumed. Then the pH progressively increased as less chlorine was consumed so presumably less remaining TAN was being oxidized with time. Meanwhile, the total chlorine mounted with the increased free chlorine which was indicating it was the main constituent of the total chlorine at this stage.

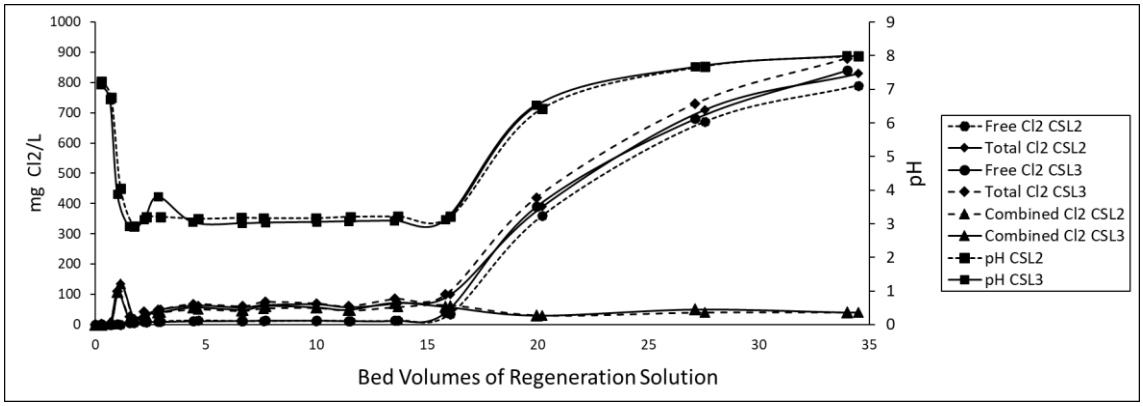

Figure 5-14 Effluent regenerant water quality during the 4h-regeneration in CSL2 and CSL3: pH, Combined chlorine, Total chlorine and Free Chlorine.

5.4 Conclusion

The SIR-600 performance in TAN removal from EMIWW and the effectiveness of different regenerants were tested using multi-cycle bench-scale column loading-regeneration experiments. The major findings were as follows:

- After operating the column for several operational cycles, the TAN loadings achieved using NaOCl regeneration were almost the same as those achieved with salt regeneration, although NaOCl regeneration required a longer duration. This is contrast to the 20% reduction observed in the batch tests presented in chapter 4, thus confirming that the results in batch tests are not always transferable to the more practical continuous flow column operation.

- In the column cycles, the NaOCl regeneration increased SIR-600's TAN preference over K and Ca in the synthetic EIMWW compared to that of NaCl regenerated SIR-600.

- By analyzing the regenerant effluent samples during the chlorine regeneration, it was found that the total chlorine level, pH, and free chlorine level were somewhat positively related during the regeneration process with limited combined chlorine generation. This may illustrate that the oxidization of ammonia into nitrogen gas is the major mechanism behind chlorine regeneration of TAN loaded zeolite.
- Comparing the Ca, TAN plus K uptakes after NaOCl regeneration with the TAN uptake achieved by salt regeneration suggests that the Na in the NaOCl regeneration solution had a smaller but significant role in the regeneration.
- Due to the higher TAN mass removal per 23 hours, the short duration loading cycles were preferred over the long duration loading cycles.

References

American Public Health Association. (1992). *Standard methods for the examination of water and wastewater.* 18th ed. American Public Health Association, Washington, D.C.

American Public Health Association. (2017). *Standard methods for the examination of water and wastewater.* 23rd ed. American Public Health Association, Washington, D.C.

Ames, L. L. (1960). "The cation sieve properties of clinoptilolite." *The American Mineralogist*, 45, 689–700.

Black and Veatch Corporation. (2010). *White's handbook of chlorination and alternative disinfectants.* 5th ed. John Wiley & Sons, Inc., Hoboken, New Jersey.

Canadian Council of Ministers of the Environment. (2010). "Canadian water quality guidelines for the protection of aquatic life: Ammonia." In *Canadian environmental quality guidelines, 1999*. Canadian Council of Ministers of the Environment, Winnipeg, MB, Canada.

Chartrand, Z. (2018). The Selective Ion-Exchange Removal of Ammonia from Mining Wastewater. [MASc dissertation]. Department of Civil engineering, University of Ottawa, Ottawa, ON.

Chartrand, Z.G., Narbaitz, R.M., Sartaj, M., and Downey J. (2020). "Ammonia-Ca-K competitive ion-exchange on zeolites in mining wastewater treatment: batch regeneration and column performance." *J. of Sustainable Mining, 19, 59-71.*

Ding, Y., and Sartaj, M. (2015). “Statistical analysis and optimization of ammonia removal from aqueous solution by zeolite using factorial design and response surface methodology.” *Journal of Environmental Chemical Engineering*, 3, 807–814.

Downey, J. (2018). Personal communication.

Dryden, H.T., and Weatherley, L.R. (1989). “Aquaculture water treatment by ion exchange: continuous ammonium ion removal with clinoptilolite.” *Aquacultural Engineering*. 8, 109-126.

Environment Canada. (2004). *Guideline for the Release of Ammonia Dissolved in Water Found in Wastewater Effluents. Canada Gazette, December 4th, Part I.*

Environmental Technology Center of Canada and Environmental Canada. (2000). *Biological test method: Reference method for determining acute lethality of effluents to rainbow trout (2nd ed.). Environmental Canada, Ottawa.*

Forsyth, B., Cameron A. and Miller, S. (1995). “Explosives and Water Quality”. In *Proceedings of Sudbury ’95: Mining and the Environment, Volume II, Ground and Surface water,* T.P. Hynes, and M.C. Blanchette (Ed.), CANMET, Ottawa *(pp. 795-803)*.

Guo, X., Zeng, L., Li, X., and Park, H.-S. (2008). “Ammonium and potassium removal for anaerobically digested wastewater using natural clinoptilolite followed by membrane pretreatment.” *Journal of Hazardous Materials*, 151, 125–133.

Hach. “Method 8021.” Retrieved on September 17, 2021, from https://www.hach.com.

Hach. “Method 8167.” Retrieved on September 17, 2021, from https://www.hach.com.

Halling-Sørensen, B., and Jørgensen, S. E. (1993). The *Removal of Nitrogen Compounds from Wastewater*. Elsevier, Amsterdam.

Hedström, A. (2001). "Ion exchange of ammonium in zeolites: a literature review." *Journal of Environmental Engineering*, 127, 673–681.

Huang, H., Yang, L., Xue, Q., Liu, J., Hou, L., and Ding, L. (2015). "Removal of ammonium from swine wastewater by zeolite combined with chlorination for regeneration." *Journal of Environmental Management*, 160, 333–341.

Jama, M. A., and Yücel, H. (1989). "Equilibrium studies of sodium-ammonium, potassium-ammonium, and calcium-ammonium exchanges on clinoptilolite zeolite." *Separation Science and Technology*, 24, 1393–1416.

Jorgensen, T. C., and Weatherley, L. R. (2003). "Ammonia removal from wastewater by ion exchange in the presence of organic contaminants." *Water Research*, 37, 1723–1728.

Leyva-Ramos, R., Aguilar-Armenta, G., Gonzalez-Gutierrez, L. V., Guerrero-Coronado, R. M., and Mendoza-Barron, J. (2004). "Ammonia exchange on clinoptilolite from mineral deposits located in Mexico." *Journal of Chemical Technology and Biotechnology, 79, 651–657.*

Loveless, J. E., and Painter, H. A. (1968). "The influence of metal ion concentrations and pH value on the growth of a Nitrosomonas strain isolated from activated sludge." *The Journal of General Microbiology,* 52, 1-14

Luther, A. K. (2015). *Ammonia toxicity in bacteria and its implications for treatment of and resource recovery from highly nitrogenous organic wastes* (Order No. 10019315). [Doctoral dissertation, The State University of New Jersey]. ProQuest Dissertations and Theses Global.

Minister of Fisheries and Oceans of Canada. (2012). *Metal and Diamond Mining Effluent Regulations (SOR/2002-222)*. https://laws-lois.justice.gc.ca/eng/Regulations/SOR-2002-222/index.html

Pommen, L.W. (1983). *The Effect on Water Quality of Explosives Use in Surface Mining. Volume 1: Nitrogen Sources, Water Quality, and Prediction and Management of Impacts.* Ministry of Environment Technical Report 4. Victoria: B.C. Ministry of Environment, Water Management Branch.

Rahmani, A., Mahvi, A., Mesdaghinia, A., and Nasseri, S. (2004). "Investigation of ammonia removal from polluted waters by Clinoptilolite zeolite." *International Journal of Environmental Science and Technology (Tehran)*, *1,* 125–133.

Randall, D. J., and Tsui, T. K. N. (2002). "Ammonia toxicity in fish." *Marine Pollution Bulletin*, 45, 17–23.

ResinTech Inc. (2020). "Resintech SIR-600." Retrieved on May 15, 2021, from https://www.resintech.com/rks_images/shopcart/pdf_specs_90253.pdf

Sarioglu, M. (2005). "Removal of ammonium from municipal wastewater using natural Turkish (Dogantepe) zeolite." Separation and Purification Technology, 41, 1–11.

Souza-Bastos, L. R., Val, A. L., and Wood, C. M. (2017). “Are Amazonian fish more sensitive to ammonia? Toxicity of ammonia to eleven native species.” *Hydrobiologia*, 789, 143– 155.

Stensel, H., McDowell, C., and Ritter, E. (1976). “An automated biological nitrification toxicity test.” *Journal of Water Pollution Control Federation*, 48,2343-2350.

Stone, R. W. (1978). *Full-Scale Demonstration of Nitrogen Removal by Breakpoint Chlorination*. Environmental Protection Agency, Office of Research and Development, Municipal Environmental Research Laboratory, Ohio. Access by the National Technical Information Service. https://nepis.epa.gov/Exe/ZyPURL.cgi?Dockey=9101XG1X.txt.

Kleinhenz, L. S., Trenfield, M. A., Mooney, T. J., Humphrey, C. L., van Dam, R. A., Nugegoda, D., and Harford, A. J. (2018). “Acute ammonia toxicity to the larvae (glochidia) of the tropical Australian freshwater mussel Velesunio spp. Using a modified toxicity test protocol.” *Environmental Toxicology and Chemistry*, 37, 2175–2187.

United States Environmental Protection Agency. (2000). *Wastewater Technology Fact Sheet Ammonia Stripping, USEPA 832-F-00-019*. Washington, D.C.

Zhang, W., Zhou, Z., An, Y., Du, S., Ruan, D., Zhao, C., Ren, N., and Tian, X. (2017). “Optimization for zeolite regeneration and nitrogen removal performance of a hypochlorite-chloride regenerant.” *Chemosphere*, 178, 565–572.

Chapter 6 Conclusions

This thesis studied the ion-exchange removal of ammonia from a synthetic explosives impacted mining wastewater (EIMWW) using a commercial zeolite (ResinTech SIR-600). The focus of the thesis was comparing the performance of the IE systems regenerated with NaCl with those that uses a chlorine regeneration solution. This study quantified the impact of the competing ions within the EIMWW, this is a significant contribution because earlier studies using chlorine regeneration did not investigate the role of competing ions. The main conclusions of the two results chapters will be discussed separately, they are as follows:

6.1 Batch Application of Ion-exchange and Chlorine Regeneration Process for Ammonia Removal in Mining Wastewater

a) Batch tests showed that ResinTech SIR-600 effectively removed TAN from a synthetic EIMWW.

b) After 5 cycles of regeneration using 100 mg free Cl_2/L solution in the batch mode, the IE material's TAN uptake was 0.24 meq/g, and it was approximately 80% of that attained using 5% NaCl regeneration.

c) Compared to NaCl regeneration, chlorine regeneration led to a much greater TAN selectivity of SIR-600 with respect to Ca and K. This makes NaOCl regeneration very promising for EIMWW application as EIMWW also contains significant concentrations of K.

d) The NaOCl regeneration mechanism appears to primarily impact the sites that are occupied by ammonium.

e) SIR-600's TAN uptake was not significantly hindered by adding 80ppm Ca and 30 ppm K to NaOCl or NaCl regeneration solution.

f) The five-week-long chlorine exposure did not substantially impact SIR-600 in terms of grain size distribution, surface area, appearance, internal bonding (FTIR) and the ion uptake. Thus, SIR-600 has the potential for use long-term use in field applications.

6.2 Assessing the Feasibility and Performance of Chlorine Regeneration of Bench-scale Zeolite Column for Ammonia Removal from Explosives Impacted Mining Wastewater

a) In the column tests, the TAN loadings achieved using NaOCl regeneration were almost identical to those achieved with NaCl regeneration after multiple operational cycles, although NaOCl regeneration needed a longer duration. This in contrast with the 20% lower TAN uptakes for NaOCl regenerated via batch tests, this seems to indicate that the results in batch tests are not always transferable to the more practical continuous flow column operation.

b) In the column tests, the chlorine regenerated SIR-600 shows an increased TAN preference over K and Ca in the synthetic EIMWW compared to that of NaCl regenerated SIR-600. This makes NaOCl regeneration very promising for EIMWW treatment.

c) During the chlorine regeneration, the main regeneration mechanism appears to be the oxidation of ammonia into nitrogen gas. This was based on the small effluent combined chlorine concentrations and the positively relation between the effluent pH and free chlorine concentrations.

d) Due to the higher mass TAN removal per 23-hour period, the 6-hr duration loading cycles were favored over the 23-hr duration loading cycles.

6.3 Recommendations

a) The chlorine regeneration of the batch experiments should be repeated using a 1000 mg/L free chlorine solutions to facilitate the comparison with the column runs using the same chlorine concentrations.

b) The chlorine regeneration of the column runs be conducted using lower chlorine concentrations to evaluate if this eliminates the bubble generation and flow restrictions.

c) The gas collected from the column chlorine regeneration could be characterized to verify the reaction mechanism behind the chlorination

d) That in future experiments, the concentrations of Na be also monitored.